

Supporting information

Pictet–Spengler reaction based biosynthetic machinery in fungi

Wei Yan^{a,1}, Hui Ming Ge^{a,1}, Gang Wang^{a,b,1}, Nan Jiang^{c,1}, Ya Ning Mei^d, Rong Jiang^a, Sui Jun Li^a, Chao Jun Chen^a, Rui Hua Jiao^a, Qiang Xu^a, Seik Weng Ng^{e,f} and Ren Xiang Tan^{a,2}

^aInstitute of Functional Biomolecules, State Key Laboratory of Pharmaceutical Biotechnology, Nanjing University, Nanjing 210093, China.

^bState Key Laboratory of Elemento-organic Chemistry, Nankai University, Tianjin 300071, China.

^cSchool of Pharmacy, Nanjing Medical University, Nanjing 210029, China.

^dDepartment of Clinical Laboratory, the First Affiliated Hospital of Nanjing Medical University, Nanjing 210029, P. R. China.

^eDepartment of Chemistry, University of Malaya, 50603 Kuala Lumpur, Malaysia; and Chemistry

^fDepartment, Faculty of Science, King Abdulaziz University, Jeddah 80203, Saudi Arabia.

¹Authors contributed equally to the work.

²To whom correspondence should be addressed. E-mail: rxtan@nju.edu.cn.

Table of contents

General experimental procedure	5
1. Enzyme inhibition experiments	5
2. Extraction and isolation	5
3. ¹³ C-labeling experiments.....	6
4. Preparation of intra- and extracellular fungal proteins	6
5. Enzymatic transformation of chaetoglines.....	7
6. Physicochemical properties of 1–8	7
7. Antibacterial and AChE inhibitory assays	9
8. Computational details	9
References.....	9
Table S1. Tryptophan derivatives screened for the <i>FPS</i> gene up-regulator.	11
Table S2. ¹ H- and ¹³ C-NMR data for 1	12
Table S3. ¹ H- and ¹³ C-NMR data for 2 , 7 and 8	13
Table S4. ¹ H- and ¹³ C-NMR data for 3 , 4 and 5	15
Table S5. ¹ H- and ¹³ C-NMR data for 6	17
Table S6. Monooxygenase genes of <i>Chaetomium globosum</i> CBS 148.51.	18
Table S7. Incorporation of ¹³ C-labeled acetate and methionine into 1	19
Table S8. Incorporation of ¹³ C-labeled acetate and methionine into 2	20
Table S9. Incorporation of ¹³ C-labeled acetate and methionine into 5	21
Table S10. Incorporation of ¹³ C-labeled acetate and methionine into 6	22
Table S11. Primers used in the work.	23
Table S12. The Mulliken partial charges on carbon atoms of flavipin.....	23
Table S13. The optimized XYZ coordinates of 9 at B3LYP/6-31G(d,p) level.	24
Table S14. The optimized XYZ coordinates of 10 at B3LYP/6-31G(d,p) level.	25
Table S15. The optimized XYZ coordinates of 11 at B3LYP/6-31G(d,p) level.	27
Table S16. The optimized XYZ coordinates of 3 at B3LYP/6-31G(d,p) level.	28
Table S17. The optimized XYZ coordinates of 5 at B3LYP/6-31G(d,p) level.	30
Table S18. Genes around <i>FPS</i> in <i>Chaetomium globosum</i> CBS 148.51	32
Table S19. Antibacterial activity of 1–8	32
Figure S1. qPCR screening of tryptophan derivatives for <i>FPS</i> gene up-regulators. ..	33
Figure S2. 1-MT exposure afforded changes in the ¹ H-NMR of crude extracts from <i>C. globosum</i> cultures	35
Figure S3. Key ¹ H- ¹ H COSY, HMBC and ROESY correlations of 1	36
Figure S4. Single-crystal X-ray structure of 1	36
Figure S5. Key HMBC and ROESY correlations for 2	37
Figure S6. ¹³ C-labeling pattern for 2 ascertained by feeding sodium [1- ¹³ C]-, [2- ¹³ C]-, and [1,2- ¹³ C ₂]-acetates.	37
Figure S7. Comparison between experimental and calculated CD spectra of 2	38
Figure S8. CD spectra of 1 and 2	39
Figure S9. Key ¹ H- ¹ H COSY, HMBC and ROESY correlations of 3 and 4	39
Figure S10. Single-crystal X-ray structure of 4	40
Figure S11. CD spectra of 3 and 4	40
Figure S12. Key ¹ H- ¹ H COSY and HMBC correlations of 5	41

Figure S13. Comparison between experimental and calculated CD spectra of 5 .	42
Figure S14. Single-crystal X-ray structure of 6 .	43
Figure S15. Key ^1H - ^1H COSY, HMBC and ROESY correlations of 7 .	43
Figure S16. Key ^1H - ^1H COSY, HMBC and ROESY correlations of 8 .	44
Figure S17. Comparison between experimental and calculated CD spectra of 7 .	45
Figure S18. Comparison between experimental and calculated CD spectra of 8 .	46
Figure S19. ^1H -NMR spectrum of flavipin.	47
Figure S20. The free energy profile of the reaction pathway from 9 to 3 .	48
Figure S21. LC-MS profile for 1 , 4 and 6 in the culture with exposures to 3-(trifluoromethyl)-phenylacetone	49
Figure S22. LC-MS profile for 1–8 in the culture with exposures to NaN_3	50
Figure S23. Steady-state inhibition of AChE by 6 .	51
Figure S24. Isolated compounds derived from 1-MT.	52
Figure S25. Phylogenetic analysis of characterized PS reaction enzymes.	52
Figure S26. ^1H -NMR spectrum of 1	54
Figure S27. ^{13}C -NMR spectrum of 1 .	55
Figure S28. ^1H - ^1H COSY spectrum of 1 .	56
Figure S29. HSQC spectrum of 1 .	57
Figure S30. HMBC spectrum of 1 .	58
Figure S31. ROESY spectrum of 1 .	59
Figure S32. ^1H -NMR spectrum of 2 .	60
Figure S33. ^{13}C -NMR spectrum of 2 .	61
Figure S34. ^1H - ^1H COSY spectrum of 2 .	62
Figure S35. HSQC spectrum of 2 .	63
Figure S36. HMBC spectrum of 2 .	64
Figure S37. ROESY spectrum of 2 .	65
Figure S38. ^1H -NMR spectrum of 3 .	66
Figure S39. ^{13}C -NMR spectrum of 3 .	67
Figure S40. ^1H - ^1H COSY spectrum of 3 .	68
Figure S41. HSQC spectrum of 3	69
Figure S42. HMBC spectrum of 3	70
Figure S43. ROESY spectrum of 3 .	71
Figure S44. ^1H -NMR spectrum of 4 .	72
Figure S45. ^{13}C -NMR spectrum of 4 .	73
Figure S46. ^1H - ^1H COSY spectrum of 4 .	74
Figure S47. HSQC spectrum of 4 .	75
Figure S48. HMBC spectrum of 4 .	76
Figure S49. ROESY spectrum of 4 .	77
Figure S50. ^1H -NMR spectrum of 5 .	78
Figure S51. ^{13}C -NMR spectrum of 5 .	79
Figure S52. ^1H - ^1H COSY spectrum of 5 .	80
Figure S53. HSQC spectrum of 5 .	81
Figure S54. HMBC spectrum of 5 .	82
Figure S55. NOESY spectrum of 5 .	83

Figure S56. ^1H -NMR spectrum of 6	84
Figure S57. ^{13}C -NMR spectrum of 6	85
Figure S58. ^1H - ^1H COSY spectrum of 6	86
Figure S59. HSQC spectrum of 6	87
Figure S60. HMBC spectrum of 6	88
Figure S61. ROESY spectrum of 6	89
Figure S62. ^1H -NMR spectrum of 7	90
Figure S63. ^{13}C -NMR spectrum of 7	91
Figure S64. ^1H - ^1H COSY spectrum of 7	92
Figure S65. HSQC spectrum of 7	93
Figure S66. HMBC spectrum of 7	94
Figure S67 ROESY spectrum of 7	95
Figure S68. ^1H -NMR spectrum of 8	96
Figure S69. ^{13}C -NMR spectrum of 8	97
Figure S70. ^1H - ^1H COSY spectrum of 8	98
Figure S71. HSQC spectrum of 8	99
Figure S72. HMBC spectrum of 8	100
Figure S73. ROESY spectrum of 8	101
Figure S74. ^{13}C -NMR spectrum of 1a labeled by sodium $[1-^{13}\text{C}]$ acetate	102
Figure S75. ^{13}C -NMR spectrum of 1b labeled by sodium $[2-^{13}\text{C}]$ acetate	103
Figure S76. ^{13}C -NMR spectrum of 1c labeled by sodium $[1,2-^{13}\text{C}_2]$ acetate	104
Figure S77. ^1H -NMR spectrum of 1d labeled by $[\text{methyl-}^{13}\text{C}]$ -L-methionine	105
Figure S78. ^{13}C -NMR spectrum of 1d labeled by $[\text{methyl-}^{13}\text{C}]$ -L-methionine.....	106
Figure S79. ^{13}C -NMR spectrum of 2a labeled by sodium $[1-^{13}\text{C}]$ acetate	107
Figure S80. ^{13}C -NMR spectrum of 2b labeled by sodium $[2-^{13}\text{C}]$ acetate	108
Figure S81. ^{13}C -NMR spectrum of 2c labeled by sodium $[1,2-^{13}\text{C}_2]$ acetate.	109
Figure S82. INADEQUATE spectrum of 2c	110
Figure S83. ^1H -NMR spectrum of 2d labeled by $[\text{methyl-}^{13}\text{C}]$ -L-methionine.	111
Figure S84. ^{13}C -NMR spectrum of 2d labeled by $[\text{methyl-}^{13}\text{C}]$ -L-methionine.....	112
Figure S85. ^{13}C -NMR spectrum of 5a labeled by sodium $[1-^{13}\text{C}]$ acetate.	113
Figure S86. ^{13}C -NMR spectrum of 5b labeled by sodium $[2-^{13}\text{C}]$ acetate	114
Figure S87. ^{13}C -NMR spectrum of 5c labeled by sodium $[1,2-^{13}\text{C}_2]$ acetate.	115
Figure S88. ^1H -NMR spectrum of 5d labeled by $[\text{methyl-}^{13}\text{C}]$ -L-methionine.....	116
Figure S89. ^{13}C -NMR spectrum of 5d labeled by $[\text{methyl-}^{13}\text{C}]$ -L-methionine	117
Figure S90. ^{13}C -NMR spectrum of 6a labeled by sodium $[1-^{13}\text{C}]$ acetate	118
Figure S91. ^{13}C -NMR spectrum of 6b labeled by sodium $[2-^{13}\text{C}]$ acetate	119
Figure S92. ^{13}C -NMR spectrum of 6c labeled by sodium $[1,2-^{13}\text{C}_2]$ acetate.	120
Figure S93. ^1H -NMR spectrum of 6d labeled by $[\text{methyl-}^{13}\text{C}]$ -L-methionine.....	121
Figure S94. ^{13}C -NMR spectrum of 6d labeled by $[\text{methyl-}^{13}\text{C}]$ -L-methionine.....	122

General experimental procedure

Optical rotations were measured on a Rudolph Autopol III automatic polarimeter. Melting points (m.p.) were determined on a Boetius micromelting apparatus and are uncorrected. The UV spectra were recorded on a Hitachi U-3000 spectrophotometer, and IR spectra (KBr) on a Nexus 870 FT-IR spectrometer. 1D and 2D NMR spectra were acquired on either Bruker DRX-400 or DRX-600 spectrometers with TMS as an internal standard. HR-ESI-MS spectra were obtained from an Agilent 6210 TOF LC-MS spectrometer. Single-crystal X-ray diffractions were accomplished on an Agilent Technologies SuperNova Dual diffractometer with an Atlas detector (Cu K α radiation, $\lambda = 1.54184 \text{ \AA}$). Silica gel (200-300 mesh) for column chromatography (CC) was purchased from the Qingdao Marine Chemical Factory, Qingdao, China, and Sephadex LH-20 from the Pharmacia Biotech, Uppsala, Sweden. ODS-A GEL (AA12S50) was produced by the YMC Co., Ltd, Japan. Semi-preparative HPLC was performed on an Agilent 1260 Infinity HPLC system consisting of a G1312C pump and a G1315D UV detector equipped with a Hypersil ODS 5 μm column (250 x 10 mm) from Thermo Fisher Scientific, Inc., USA.

1. Enzyme inhibition experiments

At the 84th hour of the 1-MT exposed culture (see above), enzyme inhibitors in water or EtOH separately started to be added as specified below. Phenylbutazone and proadifen (two CYP450 monooxygenase inhibitors (1, 2)) and methimazole (an FMO monooxygenase inhibitor (2)) were tested at dosages of 0.1 and 1 mM, NaN₃ (peroxidase inhibitor) at 0.1, 0.5 and 1 mM, and 3-(trifluoromethyl)-phenylacetone (a carboxyl esterase inhibitor) at 0.5 mM. In each inhibition test, a 12 day cultivation was followed after the final addition of inhibitors. The culture was extracted twice with an equal volume of EtOAc, and the dryness afforded after *in vacuo* evaporation of solvent was dissolved in acetonitrile for the follow-up LC-MS analysis (Figure 2).

2. Extraction and isolation

2.1 Isolation of 1 and 2

The filtrate of the fungal culture (16 L) was extracted with EtOAc (20 L \times 3) at room temperature, and the removal of solvent under reduced pressure afforded a brown crude extract (20 g), which was separated by CC over silica gel with CHCl₃/MeOH (v/v 100:0, 100:1, 100:2, 100:4, 100:8, 100:16 0:100). Alkaloidal CC subfractions were subjected to the gel filtration over Sephadex LH-20 in MeOH, followed by semi-preparative HPLC (MeOH/H₂O, 70:30) to yield **1** (30 mg, $R_t = 17.8 \text{ min}$) and **2** (25 mg, $R_t = 44.5 \text{ min}$).

2.2 Isolation of 3–6

Methimazole, an FMO monooxygenase inhibitor (2), was supplemented at 1 mM in the 1-MT exposed culture (10 L), which, after a 12 day cultivation, was extracted with EtOAc (15 L \times 3). Evaporation of solvent from the extract under reduced pressure to afford a brown crude extract (15 g), which was fractionated by CC over silica gel with CHCl₃/MeOH (v/v 100:0, 100:1, 100:2, 100:4, 100:8, 100:16 0:100). The first

alkaloidal fraction was further separated by CCs successively over silica gel (CHCl₃/MeOH, 10:1) and a reversed-phase ODS (MeOH/H₂O, 20:80, 40:60, 60:40, 80:20, 100:0), followed by the semi-preparative HPLC (MeOH/H₂O, 65:35) to give **3** (16 mg, $R_t = 16.4$ min) and **4** (7 mg, $R_t = 23.7$ min). The second alkaloidal fraction was chromatographed over a Sephadex LH-20 column to afford **5** (15 mg) and **6** (8 mg).

2.3 Isolation of **7** and **8**

Proadifen, a CYP450 monooxygenase inhibitors (**2**), was added at 0.1 mM to the 1-MT exposed culture (16 L), which, after a 12 day cultivation, was extracted with EtOAc (16 L × 3). Removal of organic solvent from the extract under reduced pressure yielded a brown crude extract (18 g), which was separated by CC over silica gel with CH₃Cl/MeOH mixtures (v/v 100:0, 100:1, 100:2, 100:4, 100:8, 0:100). The alkaloidal CC fraction was filtered over a Sephadex LH-20 column, followed by semi-preparative HPLC (MeOH/H₂O, 70:30) to afford **7** (3.2 mg, $R_t = 25.6$ min) and **8** (3.0 mg, $R_t = 37.8$ min).

3. ¹³C-labeling experiments

At the 72nd, 84th, 96th and 108th hour of the 1-MT exposed culture (see **3.1**), sodium [1-¹³C]acetate in aqueous solution was fed to the cultivation by adjusting its concentration to 0.6, 1.2, 1.8 and 2.4 mM, respectively. After a 10 day culture, the culture was extracted with EtOAc, and the *in vacuo* evaporation of solvent from the extract gave a brown solid which was separated by CC using the CHCl₃/MeOH gradient of a growing polarity. The first alkaloid-containing fraction B was filtrated over Sephadex LH-20 in MeOH, followed by semi-preparative HPLC to afford **1a** (1.1 mg, $R_t = 17.8$ min) and **2a** (3.2 mg, $R_t = 44.5$ min). The second alkaloidal fraction C was separated by gel filtration over Sephadex LH-20 in MeOH to give **5a** (3.5 mg) and **6a** (3.8 mg). The sodium [2-¹³C]acetate feeding experiments and subsequent fractionation were accomplished identically, to give **1b** (3.1 mg, $R_t = 17.8$ min), **2b** (3.4 mg, $R_t = 44.5$ min), **5b** (2.7 mg) and **6b** (4.0 mg). The labeling attempt with sodium [1,2-¹³C₂]acetate was completed in the same manner to afford **1c** (3.1 mg, $R_t = 17.8$ min), **2c** (3.4 mg, $R_t = 44.5$ min), **5c** (2.7 mg) and **6c** (4.0 mg). Identical to the experimentation with the sodium acetates, the fungal culture exposed to [methyl-¹³C]-L-methionine produced **1d** (2.1 mg, $R_t = 17.8$ min), **2d** (1.4 mg, $R_t = 44.5$ min), **5d** (7.7 mg) and **6d** (5.2 mg).

4. Preparation of intra- and extracellular fungal proteins

4.1 Intracellular protein

After cultivated in Czapek's medium at 28 °C with orbital shaking at 120 rpm for 5 days, the fungal mycelium was collected by filtering the culture with a Buchner funnel, washed twice with distilled water, frozen in liquid nitrogen, and ground into fine powder, which was suspended in PBS buffer (pH = 7.0), applied to ultra-sonication for 30 min and then centrifuged at 10000 rpm for 20 min. The supernatant was collected and the protein concentration was assessed using the BCA

Protein Assay Kit.

4.2 Extracellular protein

After cultivated for 5 days as above, the fungal culture was filtrated in a Buchner funnel. The filtrate was centrifuged to get rid of the insoluble material, and the supernatant was precipitated with $(\text{NH}_4)_2\text{SO}_4$. The precipitated protein was collected by centrifugation at 10000 rpm for 30 min, and the resultant precipitate was dissolved in citric acid-disodium hydrogen phosphate buffer (pH = 5.0), followed by the protein quantification as mentioned above.

5. Enzymatic transformation of chaetoglines

Taking the transformation of chaetoglines C (**3**) and E (**5**) as an example: 1-MT and flavipin were dissolved in DMSO at 50 mg/mL, and 20 μL of the solution were added to each millilitre of reaction buffer containing 100 μL intra- or extra-cellular proteins solution and 880 μL of PBS buffer. The *in vitro* transformation was carried out in PBS buffers (pH = 7.0) at 28 $^\circ\text{C}$ for 10 h. The reactions were quenched by adding 10 μL HCl (1 mM) and extracted by equal volume of EtOAc. The organic phases were dried *in vacuo* and dissolved in acetonitrile followed by LC-MS analysis. Transformations of chaetogline A (**1**), D (**4**) and F (**6**) were performed by following the same procedure.

6. Physicochemical properties of 1–8

Chaetogline A (**1**), orange red monoclinic crystals; $[\alpha]_{\text{D}}^{20} -68.9^\circ$ (*c* 0.09, MeOH); UV (MeOH) λ_{max} (log ϵ) 325 (2.43), 228 (2.79), 211 (2.74), 207 (2.75) nm; IR (KBr) ν_{max} 3459.6, 3170.7, 3053.2, 2948.4, 2582.8, 1690.9, 1225.3, 740.8 cm^{-1} ; HR-ESI-MS m/z 367.1284 ($[\text{M} + \text{H}]^+$, calcd. for $\text{C}_{20}\text{H}_{19}\text{N}_2\text{O}_5$, 367.1289); ^1H and ^{13}C -NMR data assigned and listed in [Table S2](#).

Chaetogline B (**2**), red solid; $[\alpha]_{\text{D}}^{20} -128.0^\circ$ (*c* 0.09, MeOH); UV (MeOH) λ_{max} (log ϵ) 338 (2.41), 206 (2.77), 197 (2.55) nm; IR (KBr) ν_{max} 3418.5, 3057.1, 2922.5, 2851.4, 1696.3, 1623.8, 1613.4, 1351.6, 742.4 cm^{-1} ; HR-ESI-MS m/z 506.1715 ($[\text{M} + \text{H}]^+$, calcd for $\text{C}_{30}\text{H}_{24}\text{N}_3\text{O}_5$, 506.1711); ^1H and ^{13}C -NMR data assigned and listed in [Table S3](#).

Chaetogline C (**3**), light brown solid; $[\alpha]_{\text{D}}^{20} -24.0^\circ$ (*c* 0.21, MeOH); UV (MeOH) λ_{max} (log ϵ) 271 (2.61), 220 (2.42), 192.5 (1.71) nm; IR (KBr) ν_{max} 3526.3, 3311.1, 3076.5, 2925.6, 1719.8, 1635.1, 1602.6, 1315.2, 737.8 cm^{-1} ; HR-ESI-MS m/z 419.1210 ($[\text{M} + \text{Na}]^+$, calcd for $\text{C}_{21}\text{H}_{20}\text{N}_2\text{O}_6\text{Na}$, 419.1214); ^1H and ^{13}C -NMR data assigned and listed in [Table S4](#).

Chaetogline D (**4**), light brown crystals; $[\alpha]_{\text{D}}^{20} -32.9^\circ$ (*c* 0.17, MeOH); UV (MeOH) λ_{max} (log ϵ) 273 (2.27), 220 (2.84) nm; IR (KBr) ν_{max} 3389.2, 3183.8, 3054.6, 2949.1, 1726.5, 1662.1, 1613.8, 1274.2, 737.1 cm^{-1} ; HR-ESI-MS m/z 433.1375 ($[\text{M} + \text{Na}]^+$, calcd for $\text{C}_{22}\text{H}_{22}\text{N}_2\text{O}_6\text{Na}$, 433.1370); ^1H and ^{13}C -NMR data assigned and listed in [Table S4](#).

Chaetogline E (**5**), purple solid; $[\alpha]_D^{20} +25.5^\circ$ (*c* 0.13, MeOH); UV (MeOH) λ_{\max} (log ϵ) 272 (2.27), 221 (2.84) nm; IR (KBr) ν_{\max} 3353.4, 3056.8, 2924.3, 1663.6, 1613.3, 1469.8, 1279.2, 742.7 cm^{-1} ; HR-ESI-MS m/z 417.1059 ($[\text{M} + \text{Na}]^+$, calcd for $\text{C}_{21}\text{H}_{18}\text{N}_2\text{O}_6\text{Na}$, 419.1057); ^1H and ^{13}C -NMR data assigned and listed in Table S4.

Chaetogline F (**6**), dark green powder; UV (MeOH) λ_{\max} (log ϵ) 363.0 (2.14), 350.0 (2.13), 291.5 (2.56), 262.0 (2.72), 219.0 (2.90), 194.5 (2.44) nm; IR (KBr) ν_{\max} 3389.4, 3104.3, 3067.4, 2958.4, 1676.6, 1627.4, 1206.1, 1120.4, 753.3 cm^{-1} ; HR-ESI-MS m/z 379.1288 ($[\text{M} + \text{H}]^+$, calcd for $\text{C}_{21}\text{H}_{19}\text{N}_2\text{O}_5$, 379.1289); ^1H and ^{13}C -NMR data assigned and listed in Table S5.

Chaetogline G (**7**), yellow solid; $[\alpha]_D^{20} -66.6^\circ$ (*c* 0.18, MeOH); UV (MeOH) λ_{\max} (log ϵ) 389 (2.26), 384 (2.25), 313 (2.37), 207 (2.88), 202 (2.89) nm; IR (KBr) ν_{\max} 3408.6, 3057.3, 2923.7, 2853.4, 1697.3, 1625.9, 1613.5, 1351.6, 743.5 cm^{-1} ; HR-ESI-MS m/z 574.1585 ($[\text{M} + \text{Na}]^+$, calcd for $\text{C}_{31}\text{H}_{25}\text{N}_3\text{O}_7\text{Na}$, 574.1587); ^1H and ^{13}C -NMR data assigned and listed in Table S3.

Chaetogline H (**8**), yellow solid; $[\alpha]_D^{20} -18.5^\circ$ (*c* 0.18, MeOH); UV (MeOH) λ_{\max} (log ϵ) 396 (2.27), 315 (2.40), 206 (2.80) nm; IR (KBr) ν_{\max} 3398.5, 3107.2, 2924.6, 2852.4, 1690.8, 1635.7, 1615.3, 1356.2, 747.5 cm^{-1} ; HR-ESI-MS m/z 508.1867 ($[\text{M} + \text{H}]^+$, calcd for $\text{C}_{30}\text{H}_{25}\text{N}_3\text{O}_5$, 508.1869); ^1H and ^{13}C -NMR data assigned and listed in Table S3.

Single crystal X-ray diffraction

The structures were solved by direct methods (SHELXS-97) and refined using full-matrix least-squares difference Fourier techniques. Crystallographic data in CIF format have been deposited in the Cambridge Crystallographic Data Centre [available free of charge at <http://www.ccdc.cam.ac.uk/deposit> or from the CCDC, 12 Union Road, Cambridge CB21EZ, UK; fax: (+44) 1223-336-033; or e-mail: deposit@ccdc.cam.ac.uk].

Crystal data of chaetogline A (**1**): $\text{C}_{20}\text{H}_{18}\text{N}_2\text{O}_5$, Mr = 816.88, plate, space group $P2_1$, $a = 12.2455(2) \text{ \AA}$, $b = 13.1152(2) \text{ \AA}$, $c = 12.5043(2) \text{ \AA}$, $\alpha = \gamma = 90.00^\circ$, $\beta = 90.77^\circ$, $V = 208.04(6) \text{ \AA}^3$, $Z = 2$, $D_x = 1.351 \text{ g/cm}^3$, $\mu(\text{Cu K}\alpha) = 0.787 \text{ mm}^{-1}$, $F(000) = 864.0$. Crystal dimensions: $0.35 \times 0.20 \times 0.05 \text{ mm}^3$. Independent reflections: 8166 (Rint = 0.0363). The final R1 values were 0.0608, $wR^2 = 0.1682$ [$I > 2\sigma(I)$]. Flack parameter: 0.21(19). Supplementary publication no. CCDC 1018681.

Crystal data of chaetogline C (**3**): $\text{C}_{22}\text{H}_{22}\text{N}_2\text{O}_6$, Mr = 442.46, prism, space group $P2_12_12_1$, $a = 8.3110(2) \text{ \AA}$, $b = 15.6574(4) \text{ \AA}$, $c = 16.9836(5) \text{ \AA}$, $\alpha = \beta = \gamma = 90.00^\circ$, $V = 2210.05(10) \text{ \AA}^3$, $Z = 4$, $D_x = 1.330 \text{ g/cm}^3$, $\mu(\text{Cu K}\alpha) = 0.825 \text{ mm}^{-1}$, $F(000) = 936.0$. Crystal dimensions: $0.25 \times 0.23 \times 0.19 \text{ mm}^3$. Independent reflections: 3913 (Rint = 0.0304). The final R1 values were 0.0464, $wR^2 = 0.1361$ [$I > 2\sigma(I)$]. Flack parameter: 0.2(2). Supplementary publication no. CCDC 1018683.

Crystal data of chaetogline F (**6**): $\text{C}_{21}\text{H}_{18}\text{N}_2\text{O}_5$, Mr = 492.4, prism, space group $P2_1$, $a = 8.5420(1) \text{ \AA}$, $b = 11.9379(1) \text{ \AA}$, $c = 22.2441(2) \text{ \AA}$, $\alpha = \gamma = 90.00^\circ$, $\beta = 97.03^\circ$, $V = 2251.26(4) \text{ \AA}^3$, $Z = 4$, $D_x = 1.453 \text{ g/cm}^3$, $\mu(\text{Cu K}\alpha) = 1.075 \text{ mm}^{-1}$, $F(000) = 1016$. Crystal dimensions: $0.30 \times 0.15 \times 0.15 \text{ mm}^3$. Independent reflections: 4703 (Rint = 0.0630). The final R1 values were 0.0862, $wR^2 = 0.1200$ [$I > 2\sigma(I)$]. Supplementary

publication no. CCDC 1018682.

7. Antibacterial and AChE inhibitory assays

The in vitro antibacterial activity of **1–8** was determined against the bacteria listed in [Table S19](#) according to the protocol described ([3](#)). The minimum inhibitory concentrations (MICs) were determined after incubating the clinical anaerobic bacteria for 48 h at 35 °C in an atmosphere of 80% N₂, 10% CO₂ and 10% H₂. The microtiter plates were read visually and the minimum concentration of the sample, at which no turbidity was recorded. All assays were performed at Department of Clinical Laboratory of the First Affiliated Hospital of Nanjing Medical University (Nanjing, P. R. China), and repeated three times to maximize reliability and reproducibility. The acetylcholinesterase (AChE) inhibitory assay was performed as described ([4](#)).

8. Computational details

8.1 Electronic dichroism spectrum (ECD) calculation

The density functional theory (DFT) at B3LYP/6–31G(d,p) level was employed to optimize the geometries of the studied systems. The solvent effects on the electronic structures of the studied systems were evaluated by quantum chemistry method through the polarizable continuum model ([5](#), [6](#)) (PCM, dielectric constant $\epsilon = 32.63$ for CH₃OH). Then, the corresponding excited-state calculations were performed at the ground-state optimized geometries. Time-dependent DFT in combination with PCM model (TD-DFT/PCM) with the same basis set was carried out to calculate the spin-allowed excitation energy and rotatory strength of the lowest 100 excited states. The UV and ECD spectra were generated using the program SpecDis ([7](#)) by applying a Gaussian band shape with the width of 0.20 eV, from oscillator strengths and dipole-velocity rotational strengths, respectively.

8.2 Chemical reactivity prediction

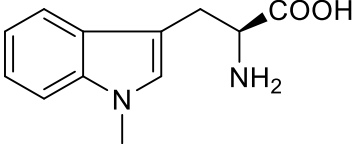
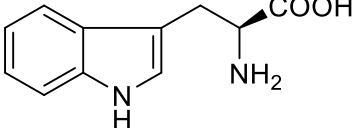
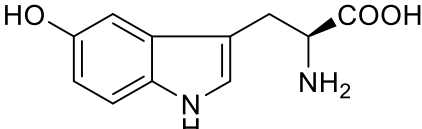
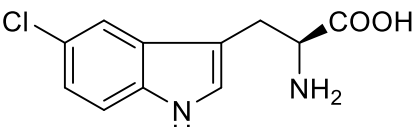
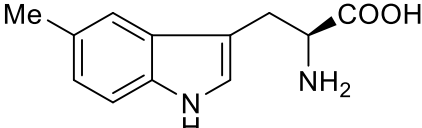
The geometries of the studied systems were optimized by B3LYP/6–31G(d,p) method. Then, the vibrational frequency calculation was performed to all stationary points to check whether the optimized geometry corresponds to a minimum or a transition state and to obtain Gibbs free energies at the temperature of 298.15 K. In order to consider the bulk solvent effects on the free energies of all species, we have employed the PCM ([5](#), [6](#)) method with water as the solvent to calculate the Gibbs free energy of solvation using gas-phase optimized geometries. All the calculations were performed with Gaussian 09 program ([8](#)).

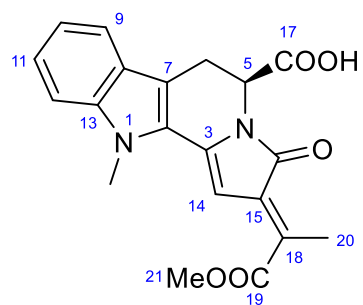
References

1. Miners JO, Birkett DJ (1998) Cytochrome P4502C9: an enzyme of major importance in human drug metabolism. *Br J Clin Pharmacol* 45: 525–538.
2. Lee JW, Shin KD, Lee M, Kim EJ., Han SS, Han MY, Ha H, Jeong TC, Koh WS (2003) Role of metabolism by flavin-containing monooxygenase in thioacetamide-induced immunosuppression. *Toxicol Lett* 136:163–172.

3. Wei W, Jiang N, Mei YN, Chu YL, Ge HM, Song YC, Ng SW, Tan RX (2014) An antibacterial metabolite from *Lasiodiplodia pseudotheobromae* F2. *Phytochemistry* 100:103–109.
4. Ge HM, Zhu CH, Shi DH, Zhang LD, Xie DQ, Yang J, Ng SW, Tan RX (2008) Hopeahainol A: an acetylcholinesterase inhibitor from *Hopea hainanensis*. *Chem Eur J* 14:376–381.
5. Barone V, Cossi M (1998) Quantum calculation of molecular energies and energy gradients in solution by a conductor solvent model. *J Phys Chem A* 102:1995–2001.
6. Cossi M, Rega N, Scalmani G, Barone V (2003) Energies, structures, and electronic properties of molecules in solution with the C-PCM solvation model. *J Comput Chem* 24:669–681.
7. Bruhn T, Hemberger Y, Schaumlöffe A, Bringmann G SpecDis version 1.50; University of Wuerzburg: Germany, 2010.
8. Frisch MJ, et al. Gaussian 09, Revision A.1, Gaussian, Inc., Wallingford CT, 2009.

Table S1. Tryptophan derivatives screened for the *FPS* gene up-regulator.

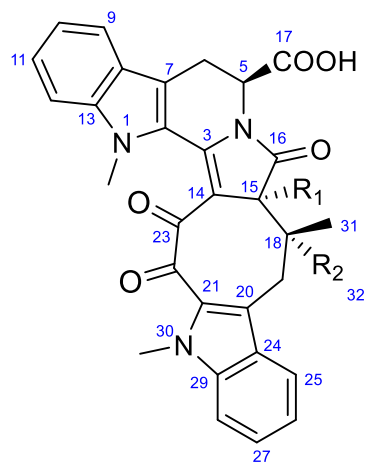
Shortened names	Structures
1-MT	
Trp	
L-5-HTP	
5-Cl-Trp	
5-MT	



chaetogline A (**1**)

Table S2. ^1H and ^{13}C -NMR data for **1** in acetone- d_6 .

position	δ_{C}	δ_{H} (mult. J in Hz)	position	δ_{C}	δ_{H} (mult. J in Hz)
2	126.8		13	141.2	
3	136.3		14	98.6	7.01 (s)
5	50.5	5.21 (d, 7.2)	15	137.1	
6	24.4	3.41 (dd, 7.2, 16.2)	16	169.3	
		3.78 (d, 16.2)			
7	114.0		17	171.8	
8	126.4		18	131.9	
9	120.6	7.67 (d, 7.5)	19	169.0	
10	125.6	7.33 (t, 7.5)	20	14.7	2.51 (s)
11	121.1	7.15 (t, 7.5)	21	52.5	3.87 (s)
12	110.8	7.50 (d, 7.5)	1-NMe	31.8	3.98 (s)



chaetogline B (**2**), R_1+R_2 =double bond

chaetogline G (**7**), R_1 =H, R_2 =COOH

chaetogline H (**8**), $R_1=R_2$ =H

Table S3. ^1H and ^{13}C -NMR data for **2**, **7** and **8** in acetone- d_6 .

position	chaetogline B (2)		chaetogline G (7)		chaetogline H (8)	
	δ_{C}	δ_{H} (mult. J in Hz)	δ_{C}	δ_{H} (mult. J in Hz)	δ_{C}	δ_{H} (mult. J in Hz)
2	127.1		127.0		127.3	
3	134.5		139.5		139.4	
5	50.1	5.20 (d, 7.2)	49.7	5.23 (d, 6.5)	49.5	5.17 (d, 7.2)
6	24.7	3.32 (dd, 7.2, 16.4)	24.0	3.33 (dd, 6.5, 16.3)	24.7	3.32 (dd, 7.2, 16.4)
		3.82 (d, 16.4)		3.88 (d, 16.3)		3.84 (d, 16.4)
7	118.5		116.9		116.4	

8	126.4		125.1		125.2	
9	126.1	7.70 (d, 7.5)	120.1	7.78 (d, 7.5)	120.8	7.76 (d, 7.5)
10	120.8	7.18 (t, 7.5)	120.8	7.24 (t, 7.5)	120.7	7.21 (t, 7.5)
11	126.4	7.39 (t, 7.5)	125.7	7.44 (t, 7.5)	125.5	7.41 (t, 7.5)
12	111.7	7.52 (d, 7.5)	110.8	7.60 (d, 7.5)	110.9	7.56 (d, 7.5)
13	142.6		141.6		141.5	
14	106.7		106.7		106.8	
15	126.8		51.3	4.54 (s)	50.8	3.84 (m)
16	165.7		174.2		175.6	
17	171.7		169.7		169.8	
18	154.2		49.7		35.8	2.59 (m)
19	33.6	4.04 (m) 4.08 (m)	34.1	3.10 (d, 15.8) 3.65 (d, 15.8)	34.1	2.74 (dd, 5.2, 16.1) 3.54 (dd, 12.5, 16.1)
20	125.8		124.0		120.0	
21	127.9		129.0		129.7	
22	187.0		186.6		186.6	
23	193.5		191.9		191.6	
24	126.2		127.0		125.9	
25	121.9	8.05 (d, 7.5)	121.4	7.73 (d, 7.5)	121.2	7.94 (d, 7.5)
26	122.2	7.30 (t, 7.5)	120.7	7.18 (t, 7.5)	120.7	7.23 (t, 7.5)
27	128.9	7.54 (t, 7.5)	127.7	7.50 (t, 7.5)	127.7	7.51 (t, 7.5)

28	111.9	7.62 (d, 7.5)	110.9	7.61 (d, 7.5)	110.8	7.62 (d, 7.5)
29	141.7		140.7		140.9	
31	20.7	2.64 (s)	18.2	1.31 (s)	14.6	1.01 (d, 6.5)
32			173.7			
N1-Me	35.9	3.85 (s)	34.9	3.77 (s)	34.2	3.72 (s)
N30-Me	32.6	4.13 (s)	31.9	4.22 (s)	31.8	4.18 (s)

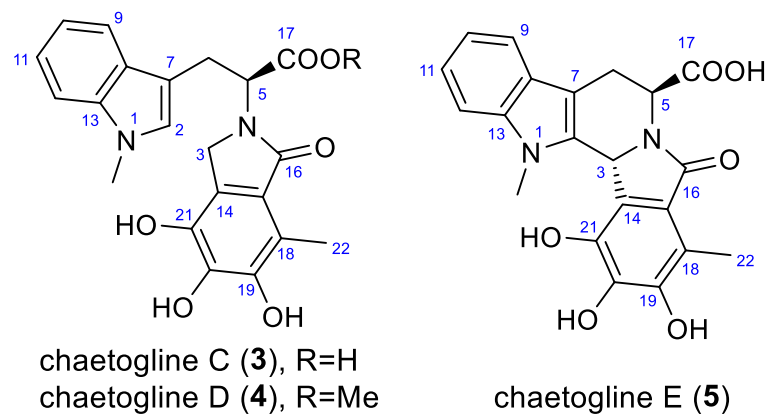
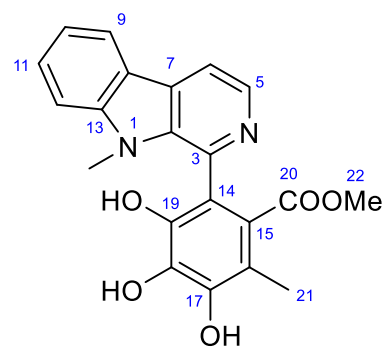


Table S4. ^1H and ^{13}C -NMR data for **3–5** in acetone- d_6 .

position	3		4		5	
	δ_{C}	δ_{H} (mult. J in Hz)	δ_{C}	δ_{H} (mult. J in Hz)	δ_{C}	δ_{H} (mult. J in Hz)
2	128.6	7.07 (s)	128.0	7.04 (s)	134.9	

3	44.5	4.34 (d, 16.1) 4.45 (d, 16.1)	44.5	4.33 (d, 16.1) 4.39 (d, 16.1)	55.1	6.22 (s)
5	54.8	5.39 (dd, 4.9, 10.9)	55.0	5.35 (dd, 5.3, 10.0)	52.9	5.55 (d, 5.6)
6	26.1	3.40 (dd, 10.9, 15.5) 3.57 (dd, 4.9, 15.5)	22.6	3.35 (dd, 10.0, 15.2) 3.52 (dd, 5.3, 15.2)	25.1	3.10 (dd, 5.6, 15.3) 3.40 (d, 15.3)
7	110.2		110.4		108.5	
8	127.9		128.7		127.8	
9	119.2	7.67 (d, 7.7)	119.2	7.64 (d, 7.8)	119.1	7.47 (d, 7.8)
10	119.5	7.04 (t, 7.7)	119.6	7.04 (t, 7.8)	120.1	7.03 (t, 7.8)
11	122.2	7.13 (t, 7.7)	122.3	7.14 (t, 7.8)	122.7	7.15 (t, 7.8)
12	110.5	7.26 (d, 7.7)	110.2	7.28 (d, 7.8)	110.7	7.33 (d, 7.8)
13	137.9		138.0		140.0	
14	122.1		122.2		125.0	
15	121.1		121.2		121.2	
16	171.1		170.7		172.1	
17	173.3		172.6		173.3	
18	116.2		116.3		117.3	
19	144.9		145.0		145.7	
20	137.5		137.6		138.5	
21	138.4		138.5		140.3	

22	9.6	2.47 (s)	9.6	2.47 (s)	10.0	2.55 (s)
N1-Me	32.6	3.63 (s)	32.7	3.67 (s)	32.8	4.01 (s)
C17-OMe			52.4	3.68 (s)		



chaetogline F (**6**)

Table S5. ^1H and ^{13}C -NMR data for **6** in acetone- d_6 .

position	δ_{C}	δ_{H} (mult. J in Hz)	position	δ_{C}	δ_{H} (mult. J in Hz)
2	135.9		14	109.9	
3	137.7		15	125.6	
5	129.8	8.72 (br s)	16	118.5	
6	116.9	8.63 (br s)	17	149.1	
7	134.6		18	136.6	
8	120.3		19	144.9	

9	122.7	8.48 (d, 7.5)	20	168.4	
10	122.7	7.46 (t, 7.5)	21	13.2	2.33 (s)
11	132.8	7.82 (t, 7.5)	1-NMe	31.3	3.71 (s)
12	111.8	7.77 (d, 7.5)	C22	52.1	3.31 (s)
13	146.0				

Table S6. Monooxygenase genes of *Chaetomium globosum* CBS 148.51.

		Genome locus							
	CHGG_00014	CHGG_01243	CHGG_02305	CHGG_04104	CHGG_05281	CHGG_07681	CHGG_08936	CHGG_09395	CHGG_10078
	CHGG_00033	CHGG_01306	CHGG_02308	CHGG_04362	CHGG_05285	CHGG_07836	CHGG_09072	CHGG_09397	CHGG_10133
	CHGG_00044	CHGG_01325	CHGG_02312	CHGG_04428	CHGG_05293	CHGG_08027	CHGG_09080	CHGG_09440	CHGG_10649
	CHGG_00208	CHGG_01339	CHGG_02341	CHGG_04572	CHGG_05325	CHGG_08218	CHGG_09255	CHGG_09459	CHGG_10717
CYP450	CHGG_00240	CHGG_01465	CHGG_02966	CHGG_04654	CHGG_06520	CHGG_08337	CHGG_09276	CHGG_09528	CHGG_10746
	CHGG_00261	CHGG_01610	CHGG_03082	CHGG_04825	CHGG_06764	CHGG_08360	CHGG_09310	CHGG_09832	CHGG_10810
	CHGG_00353	CHGG_01652	CHGG_03508	CHGG_05142	CHGG_07101	CHGG_08480	CHGG_09318	CHGG_09834	CHGG_10816
	CHGG_00771	CHGG_02003	CHGG_03590	CHGG_05242	CHGG_07393	CHGG_08596	CHGG_09344	CHGG_09876	CHGG_10894
	CHGG_00898	CHGG_02069	CHGG_03669	CHGG_05254	CHGG_07425	CHGG_08794	CHGG_09366	CHGG_09957	CHGG_11051
	CHGG_01242	CHGG_02147	CHGG_04063	CHGG_05266	CHGG_07508	CHGG_08890	CHGG_09392	CHGG_09989	CHGG_11059
FMO	CHGG_05522	CHGG_07152							

Table S7. Incorporation of ^{13}C -labeled acetate and methionine into chaetogline A (**1**).

position	δ_{C}	Relative enhancement ^a by $[1-^{13}\text{C}]$ -acetate	Relative enhancement ^a by $[2-^{13}\text{C}]$ -acetate	$J_{\text{C-C}}/\text{Hz}$ observed with $[1,2-^{13}\text{C}_2]$ -acetate	Relative enhancement ^a by $[\text{methyl-}^{13}\text{C}]$ -L-methionine	Absolute enhancement ^b by $[\text{methyl-}^{13}\text{C}]$ -L-methionine(%)
C-3	136.3	2.2	0.7	70.4	1.4	ND ^b
C-14	98.6	0.7	4.8	70.4	1.4	ND ^b
C-15	137.1	2.0	0.6	60.5	1.2	ND ^b
C-16	169.3	1.1	4.0	60.5	1.4	ND ^b
C-18	131.9	1.0	4.9	71.6	1.2	ND ^b
C-19	169.0	2.2	0.7	71.6	1.1	ND ^b
C-20	14.7	0.7	1.3		9.5	7.2
C-21	52.5	0.9	0.8		0.8	ND ^b

^aRelative enhancements were determined by calculating the carbon signal intensity ratios of **1** (labeled to unlabeled). ^bThe absolute abundance of the protonated ^{13}C was measured by the satellites of ^1H signal in its $^1\text{H-NMR}$, but that of quaternary carbon was unable to be measured. Enhancements resulting likely from specific incorporation are highlighted in bold.

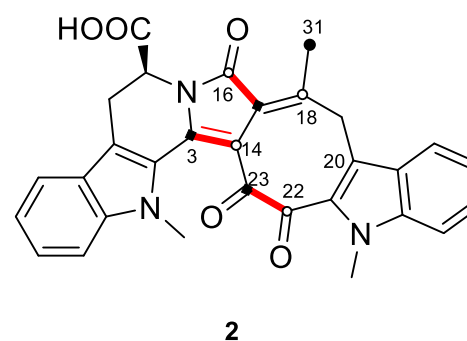
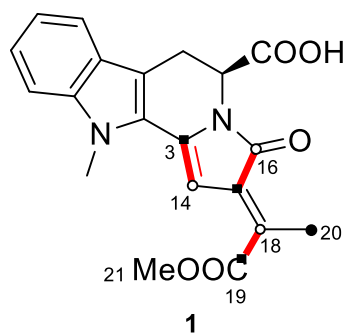


Table S8. Incorporation of ^{13}C -labeled acetate and methionine into chaetogline B (**2**).

position	δ_{C}		Relative enhancement ^a	Relative enhancement ^a	$J_{\text{C-C}}/\text{Hz}$	Relative enhancement ^a	Absolute enhancement ^b by
	acetone- d_6	CDCl_3	by $[1-^{13}\text{C}]$ -acetate	by $[2-^{13}\text{C}]$ -acetate	$[1,2-^{13}\text{C}_2]$ -acetate	by $[\text{methyl-}^{13}\text{C}]$ -L-methionine	$[\text{methyl-}^{13}\text{C}]$ -L-methionine(%)
C-3	134.5	133.9	11.2	2.0	72.7	1.0	ND ^b
C-14	106.7	106.4	0.6	8.2	72.7	ND ^d	ND ^b
C-23	ND ^c	193.7	10.4	1.6	52.7	ND ^d	ND ^b
C-22	187.0	185.7	0.9	12.8	52.7	ND ^d	ND ^b
C-18	154.2	153.9	1.3	13.5	75.2	1.3	ND ^b
C-15	126.8	125.9	3.9	1.1	64.8	1.5	ND ^b
C-16	165.7	165.3	1.0	9.8	64.8	0.6	ND ^b
C-31	20.7	21.1	1.2	1.9		7.9	12.7
C-19	33.6	33.5	0.9	0.8		1.3	ND ^b

^aRelative enhancements were determined by calculating the carbon signal intensity ratios of **2** (labeled to unlabeled). ^bThe absolute abundance of the protonated ^{13}C was measured by the satellites of ^1H signal in its ^1H -NMR, but that of quaternary carbon was unable to be determined. Enhancements resulting likely from specific incorporation are highlighted in bold. ^cLow abundance measured in acetone- d_6 . ^dSignal intensities were too low to be measured due to sample scarcity.

Table S9. Incorporation of ^{13}C -labeled acetate and methionine into chaetogline E (**5**).

position	δ_{C}	Relative enhancement ^a by $[1-^{13}\text{C}]$ -acetate	Relative enhancement ^a by $[2-^{13}\text{C}]$ -acetate	$J_{\text{C-C}}/\text{Hz}$ observed with $[1,2-^{13}\text{C}_2]$ -acetate	Relative enhancement ^a by $[\text{methyl-}^{13}\text{C}]$ -L-methionine	Absolute enhancement ^b by $[\text{methyl-}^{13}\text{C}]$ -L-methionine(%)
C-3	55	3.3	1.4	44.6	1.0	ND ^b
C-14	124.9	1.2	3.5	44.6	0.6	ND ^b
C-15	121.1	2.8	0.6	66.4	0.5	ND ^b
C-16	172.1	0.8	2.8	66.4	0.5	ND ^b
C-18	117.2	0.6	3.3	69.7	0.5	ND ^b
C-19	145.5	3.4	0.8	69.7	0.7	ND ^b
C-20	138.4	0.9	2.8	75.2	0.9	ND ^b
C-21	140.2	2.9	0.4	75.2	0.6	ND ^b
C-22	9.9	1.2	1.3		21.5	36.0

^aRelative enhancements were determined by calculating the carbon signal intensity ratios of **5** (labeled to unlabeled). ^bThe absolute abundance of the protonated ^{13}C was measured by the satellites of ^1H signal in its $^1\text{H-NMR}$, but that of quaternary carbon was unable to be measured. Enhancements resulting likely from specific incorporation are highlighted in bold.

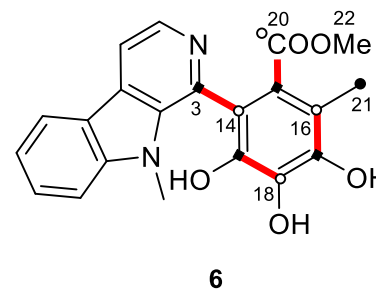
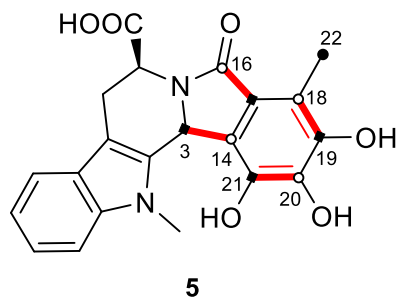


Table S10. Incorporation of ^{13}C -labeled acetate and methionine into chaetogline F (**6**).

position	δ_{C}	Relative enhancement ^a by [1- ^{13}C]-acetate	Relative enhancement ^a by [2- ^{13}C]-acetate	$J_{\text{C-C}}/\text{Hz}$ observed with [1,2- $^{13}\text{C}_2$]-acetate	Relative enhancement ^a by [methyl- ^{13}C]-L-methionine	Absolute enhancement ^b by [methyl- ^{13}C]-L-methionine(%)
C-3	137.7	9.5	2.5	62.5	1.5	ND ^b
C-14	109.9	1.3	11.6	62.5	1.4	ND ^b
C-15	125.6	8.4	2.3	75.9	1.3	ND ^b
C-16	118.5	1.8	10.8	69.5	1.3	ND ^b
C-17	149.1	8.4	2.4	69.5	1.5	ND ^b
C-18	136.6	1.3	10.6	73.2	1.3	ND ^b
C-19	144.9	8.4	2.3	73.2	1.4	ND ^b
C-20	168.4	1.1	10.5	75.9	1.2	ND ^b
C-21	13.2	1.0	1.6		7.0	7.2
C-22	52.1	0.9	1.1		0.9	ND ^b

^aRelative enhancements were determined by calculating the carbon signal intensity ratios of **6** (labeled to unlabeled). ^bThe absolute abundance of the protonated ^{13}C was measured by the satellites of ^1H signal in its ^1H -NMR, but that of quaternary carbon was unable to be determined. Enhancements resulting likely from specific incorporation are highlighted in bold.

Table S11. Primers used in the work.

Primers for qPCR	5'-3'
18sRNA-RT-F	CGTGACCTACTTCCTCCTCCC
18sRNA-RT-R	CGCACCTGGCTCGCAA
actinRT-F	ATGGTATTATGATCGGTATGGG
actinRT-R	GATGGGAGCCTCGGTTAG
06703RT-F	CAGCAGCACTGGAGGATT
06703RT-R	CTCGATACACCGTAAACCC

Table S12. The Mulliken partial charges on carbon atoms of flavipin.

Carbon atom	Mulliken partial charges
1	-0.024
2	-0.031
3	0.048
4	0.283
5	0.302
6	0.280
7	0.270
8	0.253

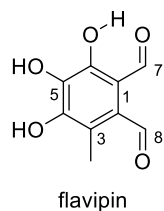
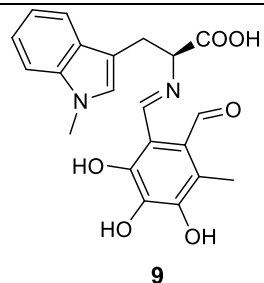


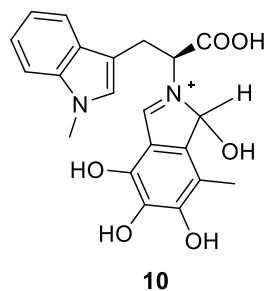
Table S13. The optimized XYZ coordinates of **9** at B3LYP/6-31G(d,p) level.



Atom	X	Y	Z	Atom	X	Y	Z
C	-3.200	-0.405	-0.698	O	2.405	2.609	0.868
C	-4.197	-1.346	-0.622	O	5.004	3.085	0.333
C	1.215	0.133	0.548	O	6.643	1.139	-0.530
N	0.521	-0.791	0.002	C	5.844	-1.594	-0.874
C	-0.902	-0.841	0.317	H	-4.125	-2.419	-0.727
C	-1.742	-0.648	-0.964	H	0.758	0.890	1.198
C	-1.170	-2.211	0.950	H	-1.183	-0.079	1.063
O	-1.815	-3.114	0.468	H	-1.599	-1.526	-1.599
O	-0.560	-2.316	2.155	H	-1.316	0.206	-1.501
C	-3.832	0.867	-0.455	H	-0.747	-3.215	2.475
C	-5.217	0.614	-0.243	H	-2.322	2.422	-0.562
N	-5.415	-0.748	-0.351	H	-3.933	4.244	-0.100
C	-3.373	2.195	-0.402	H	-6.331	3.759	0.264
C	-4.280	3.216	-0.143	H	-7.187	1.430	0.174
C	-5.646	2.940	0.064	H	-6.531	-2.500	-0.347
C	-6.134	1.639	0.016	H	-7.107	-1.268	0.792

C	-6.684	-1.429	-0.205	H	-7.408	-1.079	-0.950
C	2.657	0.286	0.318	H	2.959	3.404	0.905
C	3.504	-0.777	-0.110	H	5.933	3.100	0.057
C	2.965	-2.170	-0.075	H	5.425	-2.593	-0.797
O	3.358	-3.094	-0.767	H	6.113	-1.453	-1.930
C	3.195	1.573	0.473	H	6.769	-1.556	-0.282
C	4.539	1.808	0.183	H	2.188	-2.337	0.687
C	5.347	0.769	-0.268	H	7.123	0.396	-0.918
C	4.860	-0.538	-0.419				

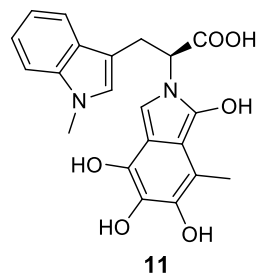
Table S14. The optimized XYZ coordinates of **10** at B3LYP/6-31G(d,p) level.



Atom	X	Y	Z	Atom	X	Y	Z
C	-2.833	-0.241	-0.735	O	3.641	3.089	0.122
C	-3.622	-1.335	-1.016	O	6.127	2.135	-0.439
C	1.436	1.072	0.466	O	6.580	-0.502	-0.650
N	0.767	-0.056	0.570	C	4.538	-2.564	-0.297
C	-0.699	-0.145	0.650	H	-3.330	-2.325	-1.340
C	-1.341	-0.191	-0.777	H	-1.053	0.742	1.176

C	-1.125	-1.376	1.451	H	-0.929	-1.052	-1.308
O	-0.741	-2.511	1.226	H	-0.988	0.707	-1.299
O	-1.997	-1.066	2.404	H	-2.292	-1.890	2.833
C	-3.731	0.825	-0.372	H	-2.558	2.605	0.056
C	-5.050	0.299	-0.458	H	-4.544	3.985	0.567
N	-4.952	-1.026	-0.856	H	-6.821	3.033	0.422
C	-3.553	2.169	0.000	H	-7.182	0.681	-0.240
C	-4.668	2.945	0.282	H	-6.002	-2.808	-0.439
C	-5.966	2.403	0.197	H	-6.997	-1.432	-0.940
C	-6.176	1.081	-0.174	H	-6.032	-2.295	-2.146
C	-6.051	-1.944	-1.109	H	4.478	3.558	-0.038
C	2.808	0.852	0.206	H	6.951	1.665	-0.640
C	3.020	-0.547	0.110	H	6.679	-1.462	-0.706
C	1.712	-1.245	0.413	H	3.616	-3.142	-0.240
O	1.311	-2.135	-0.561	H	4.995	-2.804	-1.266
C	3.857	1.768	0.024	H	5.213	-2.917	0.492
C	5.120	1.241	-0.260	H	0.593	-2.665	-0.161
C	5.307	-0.145	-0.358	H	0.944	2.033	0.576
C	4.257	-1.087	-0.172	H	1.740	-1.712	1.408

Table S15. The optimized XYZ coordinates of **11** at B3LYP/6-31G(d,p) level.



Atom	X	Y	Z	Atom	X	Y	Z
C	-2.884	-0.407	-0.651	O	3.965	2.991	0.636
C	-3.680	-1.521	-0.543	O	6.364	1.845	-0.072
C	1.533	1.190	0.555	O	6.552	-0.707	-0.791
N	0.793	0.034	0.357	C	4.286	-2.564	-0.921
C	-0.653	-0.027	0.524	H	-3.401	-2.566	-0.564
C	-1.391	-0.390	-0.794	H	-0.974	0.961	0.853
C	-1.023	-1.017	1.631	H	-1.023	-1.360	-1.137
O	-0.708	-2.196	1.654	H	-1.075	0.350	-1.537
O	-1.758	-0.455	2.598	H	-1.964	-1.154	3.244
C	-3.769	0.727	-0.572	H	-2.589	2.540	-0.755
C	-5.088	0.217	-0.418	H	-4.556	4.030	-0.570
N	-5.008	-1.162	-0.401	H	-6.832	3.103	-0.296
C	-3.583	2.119	-0.628	H	-7.207	0.651	-0.201
C	-4.689	2.953	-0.527	H	-5.762	-3.096	-0.296
C	-5.987	2.425	-0.372	H	-6.682	-1.902	0.640
C	-6.205	1.053	-0.317	H	-6.823	-1.945	-1.132

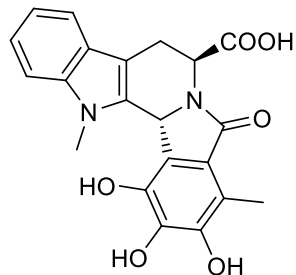
C	-6.131	-2.069	-0.291	H	4.865	3.346	0.583
C	2.849	0.891	0.247	H	7.092	1.273	-0.356
C	2.922	-0.504	-0.144	H	6.530	-1.631	-1.069
C	1.622	-0.994	-0.054	H	3.318	-3.061	-0.858
O	1.141	-2.230	-0.369	H	4.639	-2.675	-1.956
C	4.034	1.676	0.267	H	4.981	-3.119	-0.274
C	5.216	1.081	-0.089	H	0.550	-2.518	0.356
C	5.271	-0.295	-0.472	H	1.072	2.097	0.910
C	4.167	-1.114	-0.512				

Table S16. The optimized XYZ coordinates of chaetogline C (**3**) at B3LYP/6-31G(d,p) level.

<p style="text-align: center;">3</p>							
Atom	X	Y	Z	Atom	X	Y	Z
C	-3.040	-0.527	-0.564	O	3.763	2.816	1.164
C	-4.028	-1.464	-0.399	O	6.190	1.955	0.251
C	1.333	1.023	0.771	O	6.487	-0.406	-0.983
N	0.659	-0.141	0.202	C	4.251	-2.265	-1.461
C	-0.717	-0.492	0.512	H	-3.944	-2.541	-0.360
C	-1.570	-0.771	-0.754	H	1.221	1.042	1.863

C	-0.705	-1.610	1.570	H	-1.149	0.375	1.023
O	0.067	-1.633	2.502	H	-1.375	-1.788	-1.096
O	-1.662	-2.546	1.396	H	-1.188	-0.100	-1.532
C	-3.698	0.755	-0.520	H	-1.546	-3.176	2.128
C	-5.086	0.509	-0.322	H	-2.207	2.307	-0.801
N	-5.263	-0.858	-0.253	H	-3.855	4.147	-0.637
C	-3.258	2.085	-0.637	H	-6.256	3.674	-0.282
C	-4.186	3.116	-0.548	H	-7.080	1.341	-0.083
C	-5.555	2.848	-0.347	H	-6.358	-2.612	-0.052
C	-6.024	1.544	-0.234	H	-6.990	-1.248	0.890
C	-6.529	-1.535	-0.061	H	-7.229	-1.301	-0.871
C	2.760	0.793	0.357	H	4.648	3.211	1.190
C	2.883	-0.441	-0.285	H	6.963	1.499	-0.112
C	1.536	-1.070	-0.321	H	6.492	-1.282	-1.388
O	1.205	-2.187	-0.715	H	3.287	-2.772	-1.504
C	3.869	1.609	0.540	H	4.621	-2.149	-2.489
C	5.101	1.146	0.064	H	4.951	-2.923	-0.927
C	5.209	-0.096	-0.573	H	0.924	1.961	0.372
C	4.103	-0.932	-0.769				

Table S17. The optimized XYZ coordinates of chaetogline E (**5**) at B3LYP/6-31G(d,p) level.



chaetogline E (**5**)

Atom	X	Y	Z	Atom	X	Y	Z
C	-1.884	0.418	-0.672	C	3.619	0.509	-0.680
C	-1.099	-0.229	0.257	O	1.404	-2.513	1.266
C	0.181	0.341	0.826	O	3.878	-3.020	0.386
N	0.322	1.731	0.345	O	5.388	-1.177	-0.851
C	-0.827	2.541	-0.016	C	4.460	1.565	-1.357
C	-1.632	1.827	-1.124	H	0.124	0.350	1.926
C	-1.725	2.914	1.158	H	-0.411	3.480	-0.397
O	-2.818	3.418	1.030	H	-1.058	1.883	-2.057
O	-1.172	2.665	2.368	H	-2.576	2.356	-1.285
C	-3.010	-0.429	-0.939	H	-1.825	2.974	3.020
C	-2.863	-1.571	-0.108	H	-4.268	0.534	-2.420
N	-1.696	-1.435	0.625	H	-5.950	-1.285	-2.401
C	-4.135	-0.329	-1.774	H	-5.671	-3.254	-0.930
C	-5.077	-1.350	-1.759	H	-3.698	-3.464	0.558

C	-4.918	-2.472	-0.922	H	-2.318	-2.203	2.474
C	-3.814	-2.597	-0.084	H	-0.579	-1.845	2.349
C	-1.442	-2.230	1.815	H	-1.226	-3.270	1.553
C	1.528	-0.255	0.404	H	1.986	-3.289	1.282
C	2.313	0.725	-0.219	H	5.842	-0.447	-1.292
C	1.516	1.969	-0.315	H	3.893	2.489	-1.460
O	1.794	3.022	-0.881	H	4.770	1.247	-2.362
C	2.077	-1.515	0.625	H	5.369	1.785	-0.781
C	3.377	-1.764	0.167	H	4.774	-3.052	0.019
C	4.130	-0.774	-0.469				

Table S18. Up- and down-stream genes of *FPS* CHGG_06703 in *C. globosum* CBS148.51.

gene	Length (aa)	Identity/ similarity (%)	protein homolog	predicted function
CHGG_06693	206	73/75	XP_003666373.1	hypothetical protein
CHGG_06694	207	81/88	EPE06955.1	protein sorting and transport
CHGG_06695	1286	85/91	XP_006691628.1	RNA helicase
CHGG_06696	175	65/78	GAA88272.1	dUTPase
CHGG_06697	285	88/95	CCE34298.1	alcohol dehydrogenase
CHGG_06698	567	82/90	XP_965075.1	mitochondrial 2-methylisocitrate lyase
CHGG_06699	431	52/60	EGZ78081.1	chromosome segregation
CHGG_06700	317	62/72	XP_007811025.1	3-hydroxybutyryl-CoA dehydratase
CHGG_06701	255	84/92	XP_006691630.1	NADH-ubiquinone oxidoreductase
CHGG_06702	310	73/80	XP_003653731.1	glycoside hydrolase
CHGG_06703	446	64/69	XP_003651251.1	strictosidine synthase

CHGG_06704	415	51/65	XP_003007719.1	unknown
CHGG_06705	84	36/47	WP_006063371.1	oxidoreductase
CHGG_06706	332	80/88	XP_003666384.1	histone acetyltransferase
CHGG_06707	298	72/83	CAE81960.1	oxidoreductase
CHGG_06708	245	56/61	XP_003349077.1	unknown
CHGG_06709	192	70/77	XP_003651242.1	unknown
CHGG_06710	173	59/65	EFX04837.1	U1-like zinc finger
CHGG_06711	720	47/60	ESA43884.1	transcription factor
CHGG_06712	705	68/78	XP_009219360.1	copper amine oxidase
CHGG_06713	352	44/62	CCT69936.1	dihydroflavonol 4-reductase

Table S19. Antibacterial activity of **1–8** (MICs in μM).

	<i>Veillonella parvula</i>	<i>Actinomyces israelii</i>	<i>Streptococcus</i> sp.	<i>Bacteroides vulgatus</i>	<i>Peptostreptococcus</i> sp.
1	5.46	>10	>10	>10	>10
2	0.24	>10	>10	0.24	0.24
3	2.44	>10	>10	4.88	4.88
4	>10	>10	>10	>10	>10
5	5.08	>10	>10	>10	>10
6	0.32	>10	0.66	>10	0.32
7	3.94	>10	>10	>10	>10
8	3.77	>10	>10	>10	>10
tinidazole	0.49	32.4	1.01	2.02	2.02

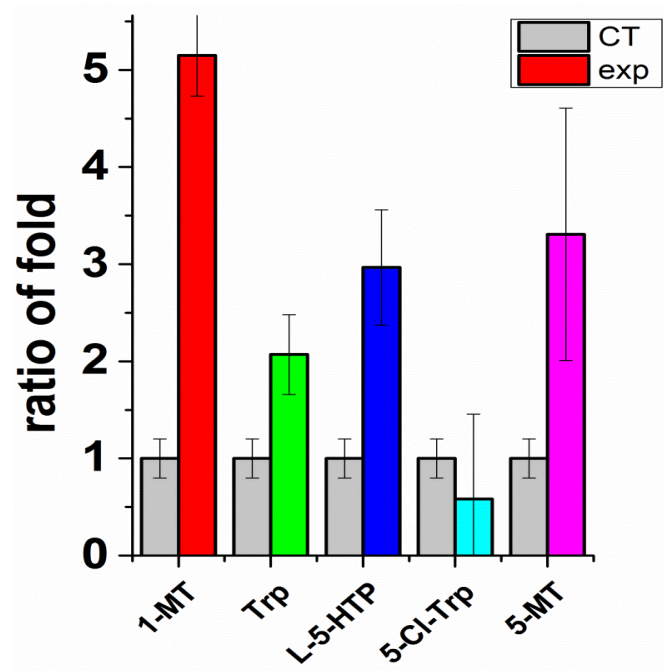
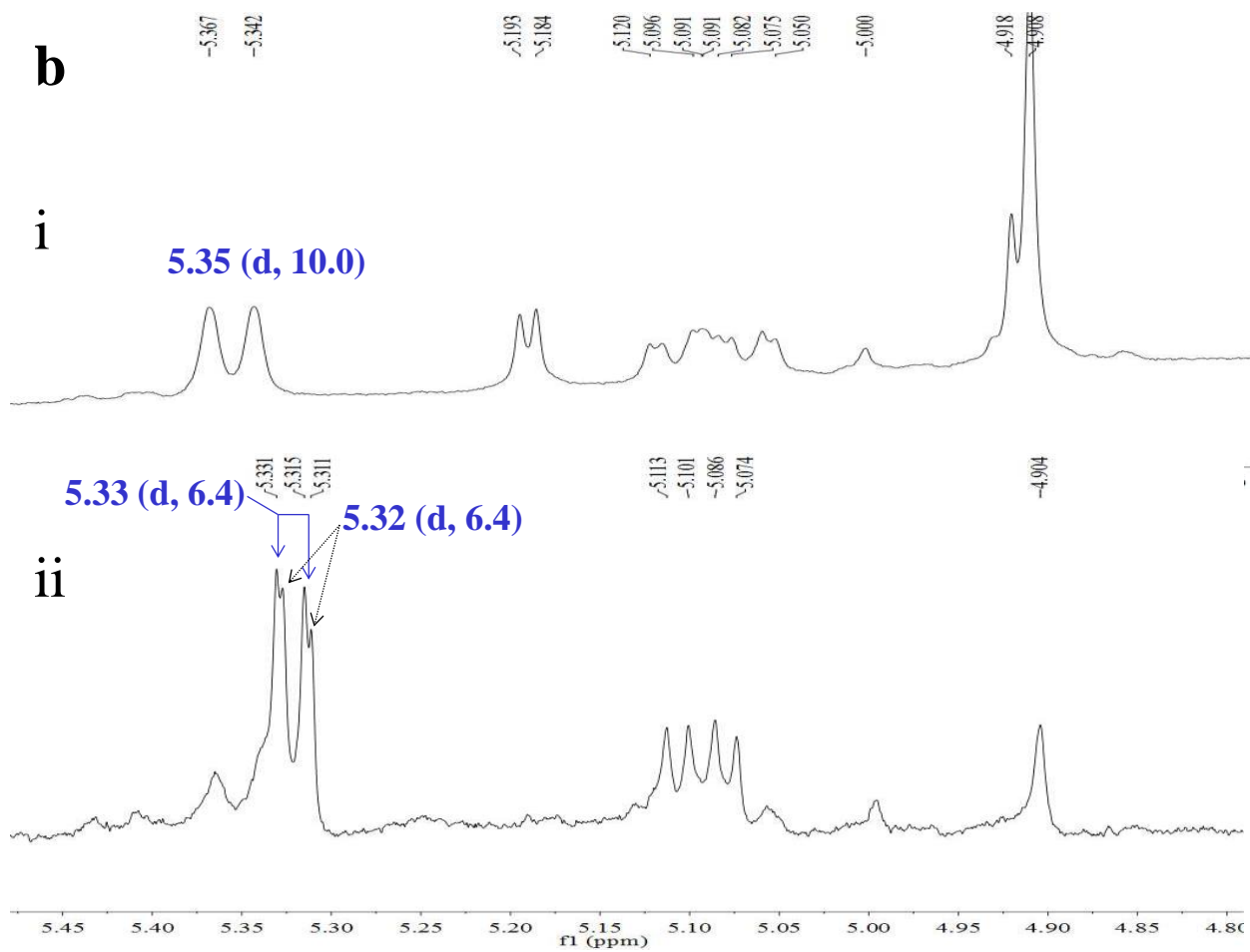


Figure S1. qPCR screening of tryptophan derivatives for *FPS* gene up-regulators.



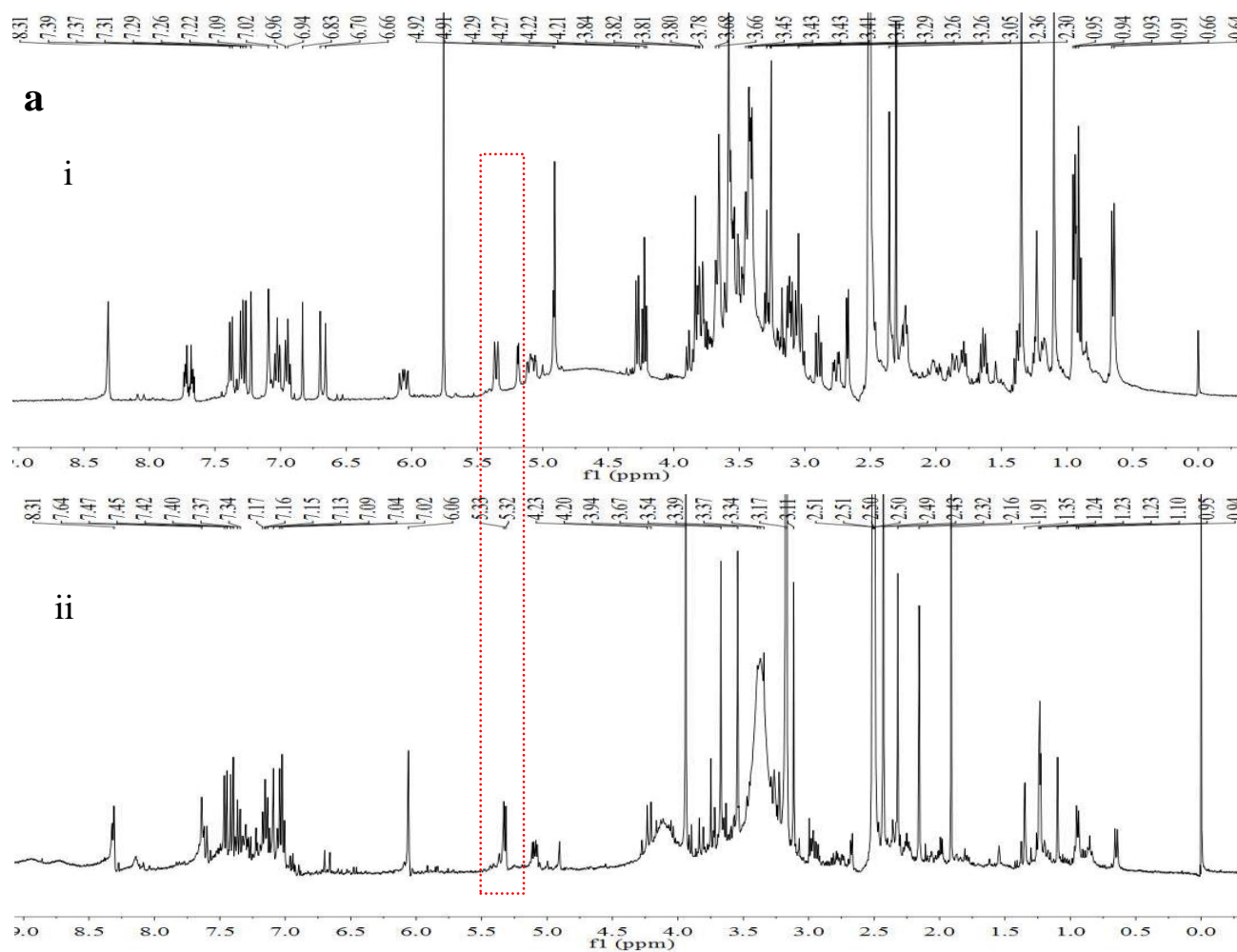


Figure S2. $^1\text{H-NMR}$ spectral comparison of crude extracts from cultures of *C. globosum* 1C51 without (i) and with (ii) exposure to 1-MT (a). Doublets around δ_{H} 5.3 ($J = 6.4$ Hz) in the enlarged window (b, up) were likely due to the aminomethine proton of 1-MT derived structures.

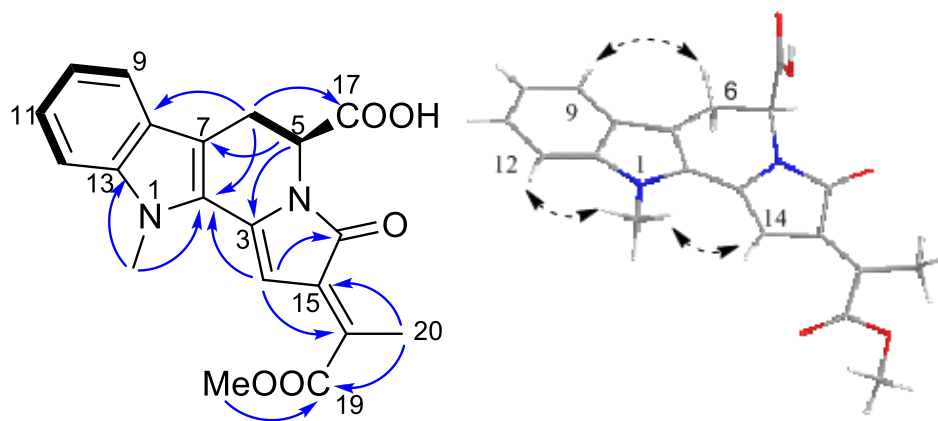


Figure S3. Key ^1H - ^1H COSY (bold lines), HMBC (solid arrows) and ROESY (dashed arrows) correlations of chaetogline A (**1**).

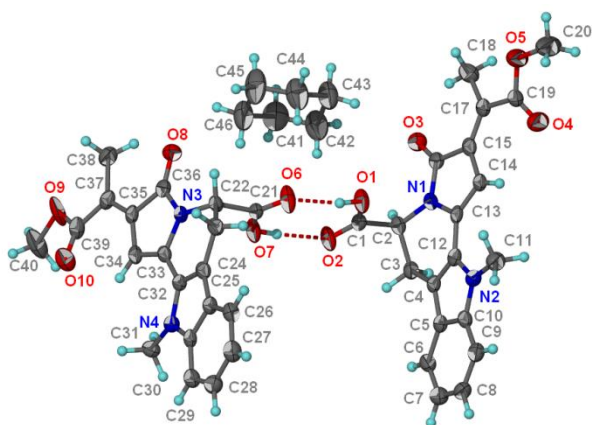


Figure S4. Single-crystal X-ray structure of chaetogline A (**1**).

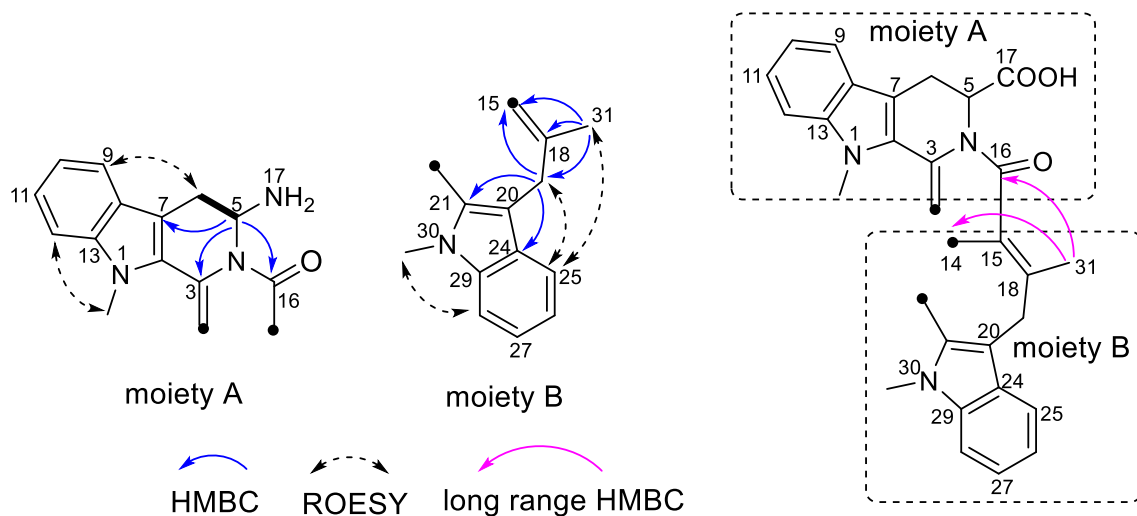


Figure S5. Key HMBC and ROESY correlations for chaetogline B (**2**) as represented by moieties A and B.

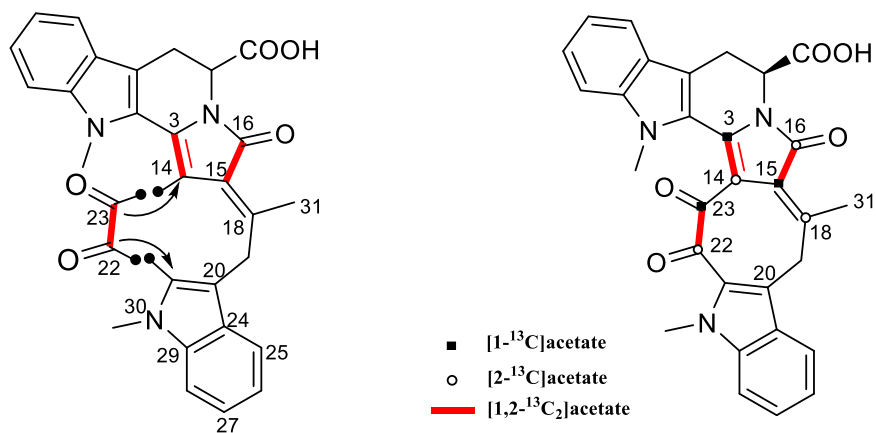


Figure S6. ¹³C-labeling pattern for **2** ascertained by feeding sodium [1-¹³C]-, [2-¹³C]-, and [1,2-¹³C₂]-acetates feeding experiments.

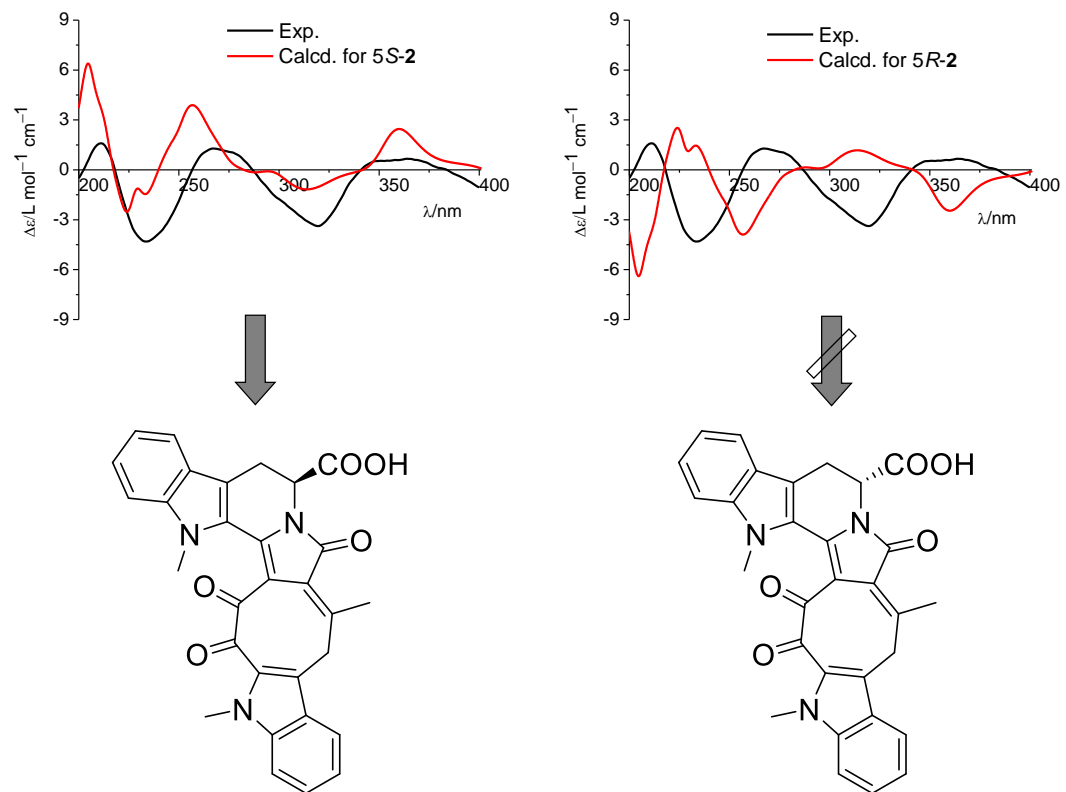


Figure S7. Comparison of experimental CD spectrum of **2** with calculated ECD curves for 5S- (left) and 5R-2 (right).

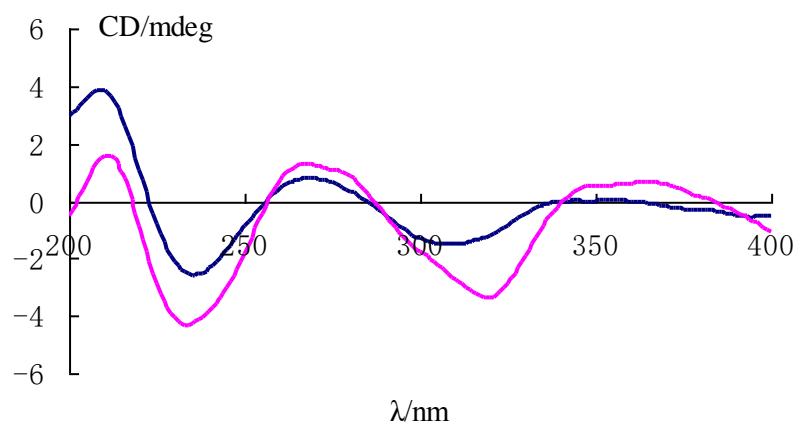


Figure S8. CD spectra of chaetoglines A (**1**, blue) and B (**2**, pink).

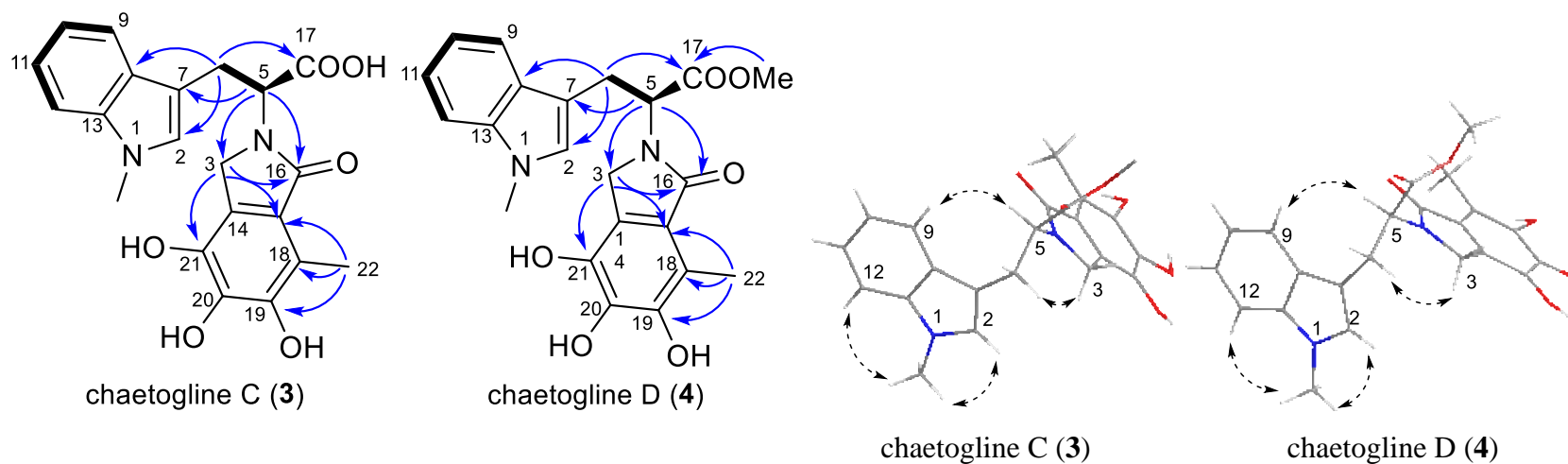


Figure S9. Key ^1H - ^1H COSY (bold), HMBC (solid arrows) and ROESY (dashed arrows) correlations of chaetoglines C (**3**) and D (**4**).

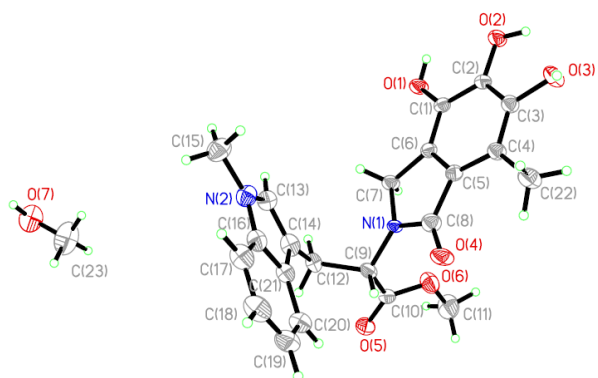


Figure S10. Single-crystal X-ray structure of chaetogline D (**4**)

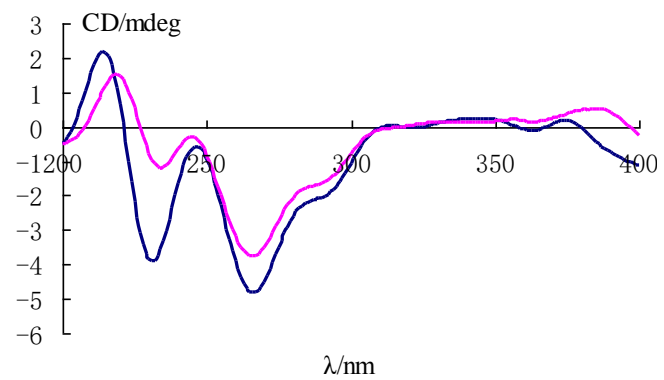


Figure S11. CD spectra of chaetoglines C (**3**, blue) and D (**4**, pink).

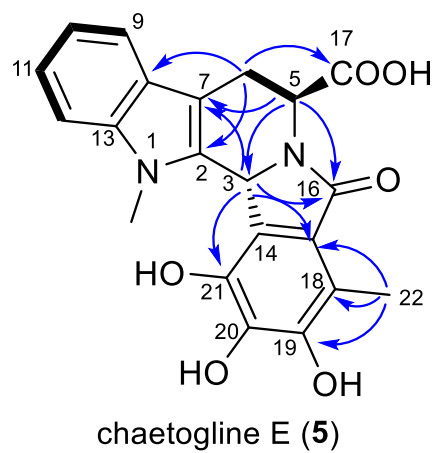


Figure S12. Key ^1H - ^1H COSY (bold) and HMBC (solid arrows) correlations of chaetogline E (5).

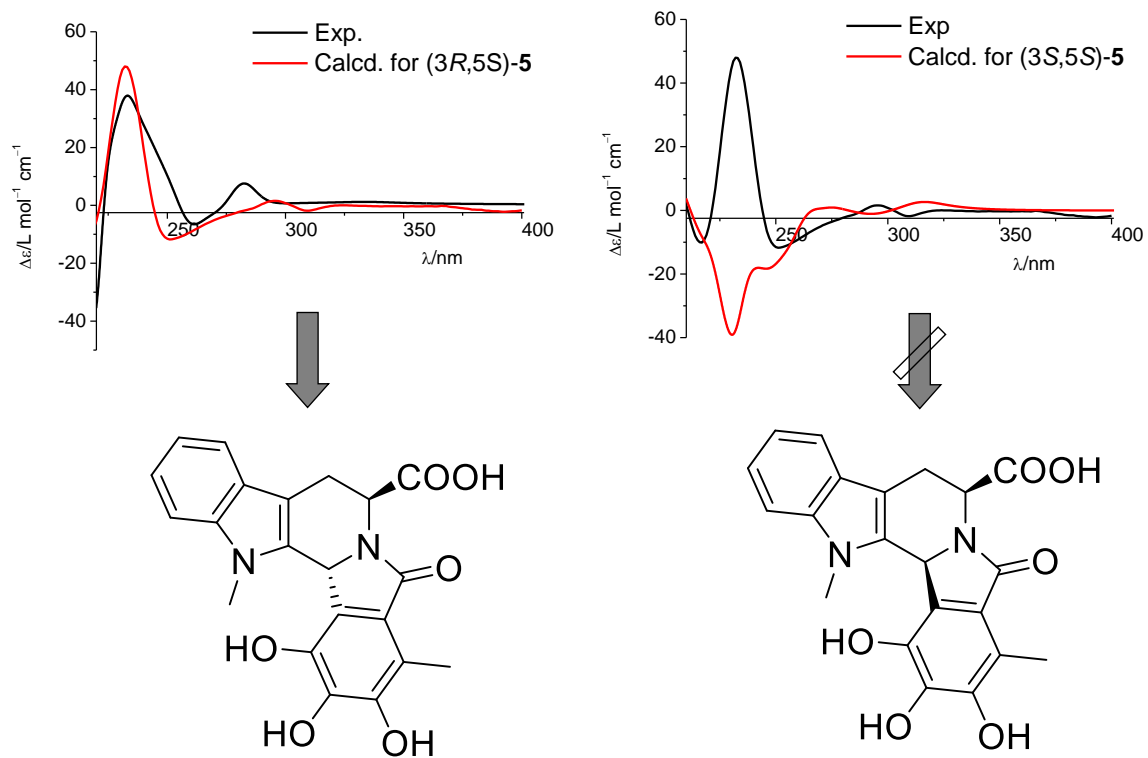


Figure S13. Comparison of experimental CD spectrum with calculated ECD curves for (3*R*,5*S*)- (left) and (3*S*,5*S*)-**5** (right).

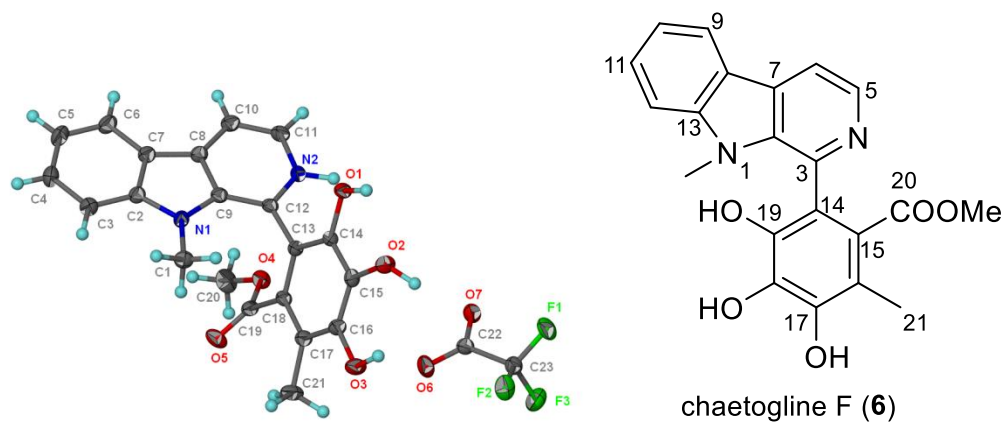


Figure S14. Single-crystal X-ray structure of chaetogline F (6).

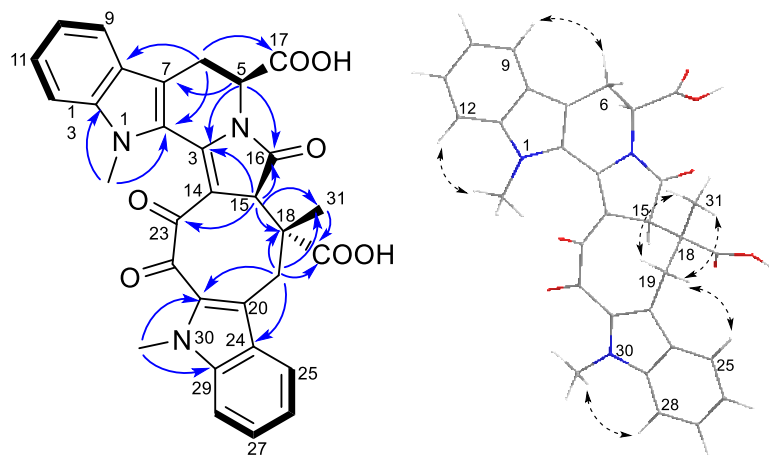


Figure S15. Key ^1H - ^1H COSY (bold), HMBC (solid arrows) and ROESY (dashed arrows) correlations of chaetogline G (7).

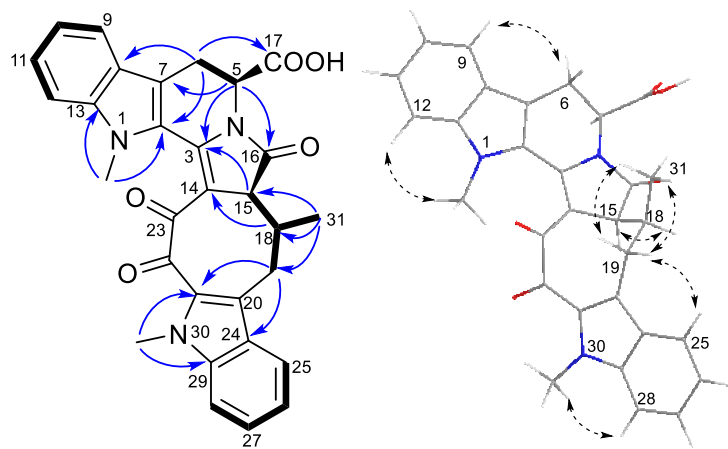


Figure S16. Key ^1H - ^1H COSY (bold), HMBC (solid arrows) and ROESY (dashed arrows) correlations of chaetogline H (**8**).

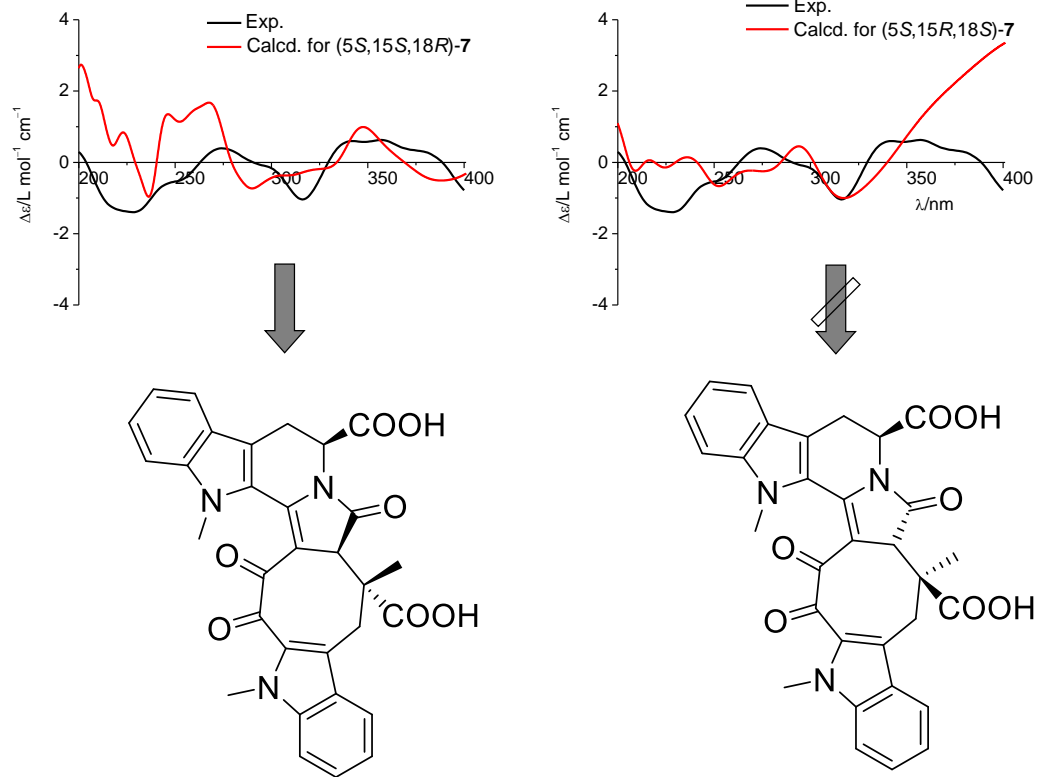


Figure S17. Comparison of experimental CD spectrum with calculated ECD curves for (5S,15R,18R)- (left) and (5S,15S,18S)-7 (right).

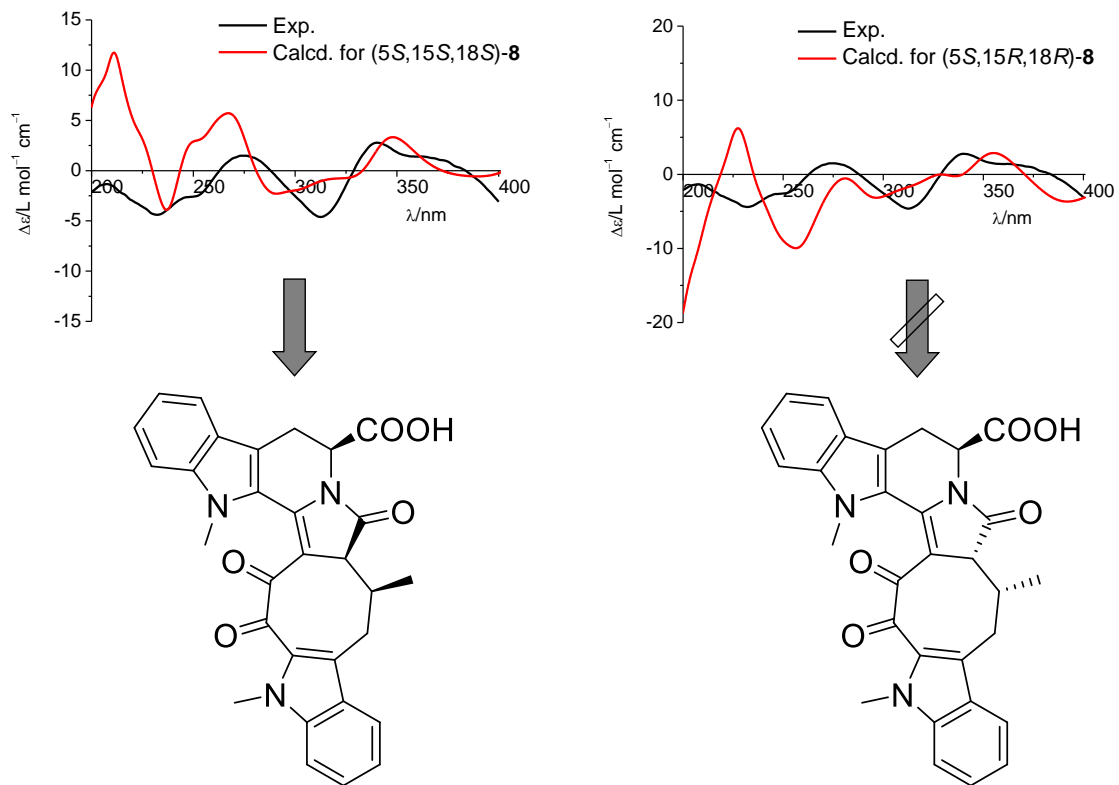


Figure S18. Comparison of experimental CD spectrum with calculated ECD curves for (5*S*,15*S*,18*S*)- (left) and (5*S*,15*R*,18*R*)-**8** (right).

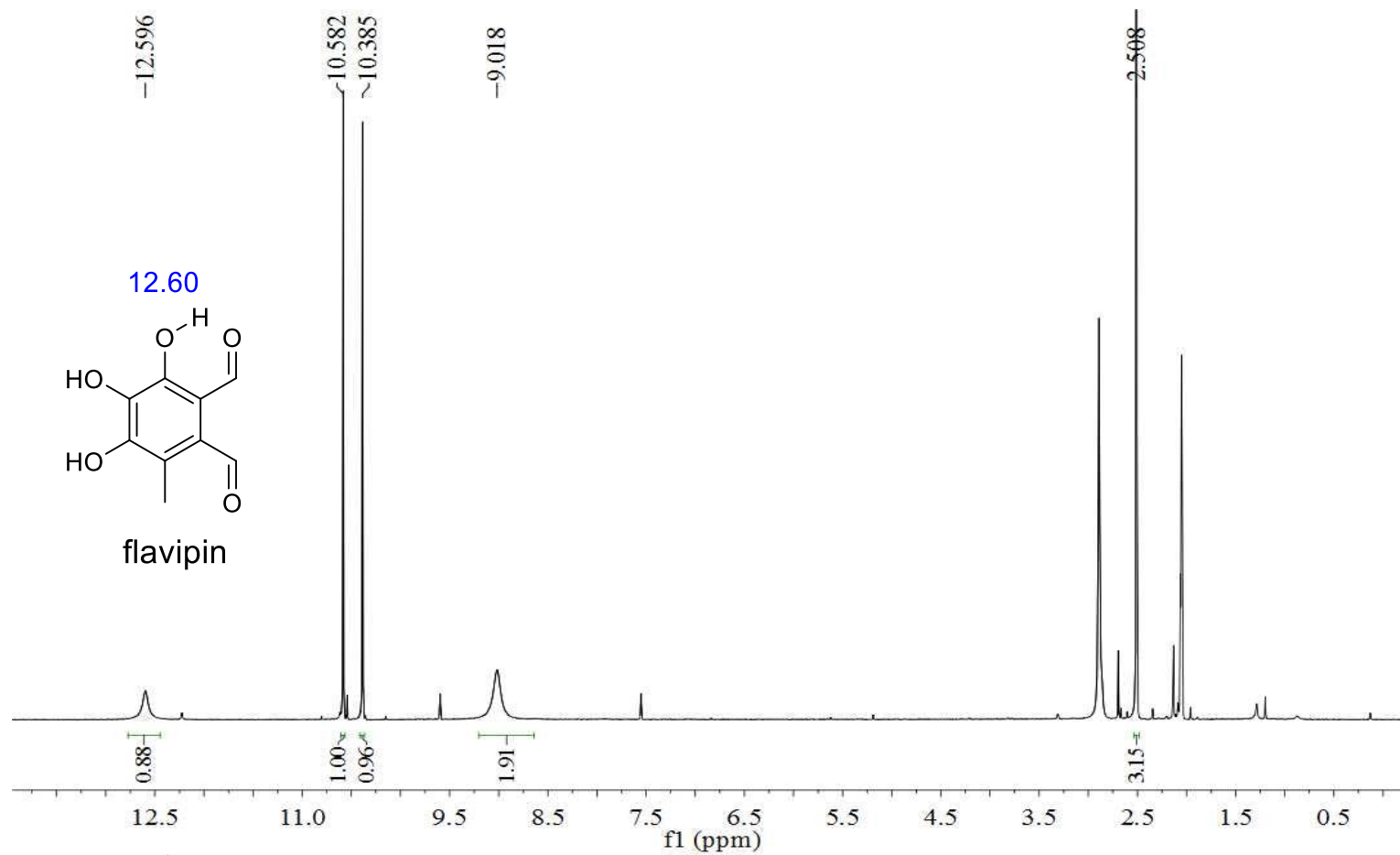


Figure S19. ¹H-NMR spectrum of flavipin.

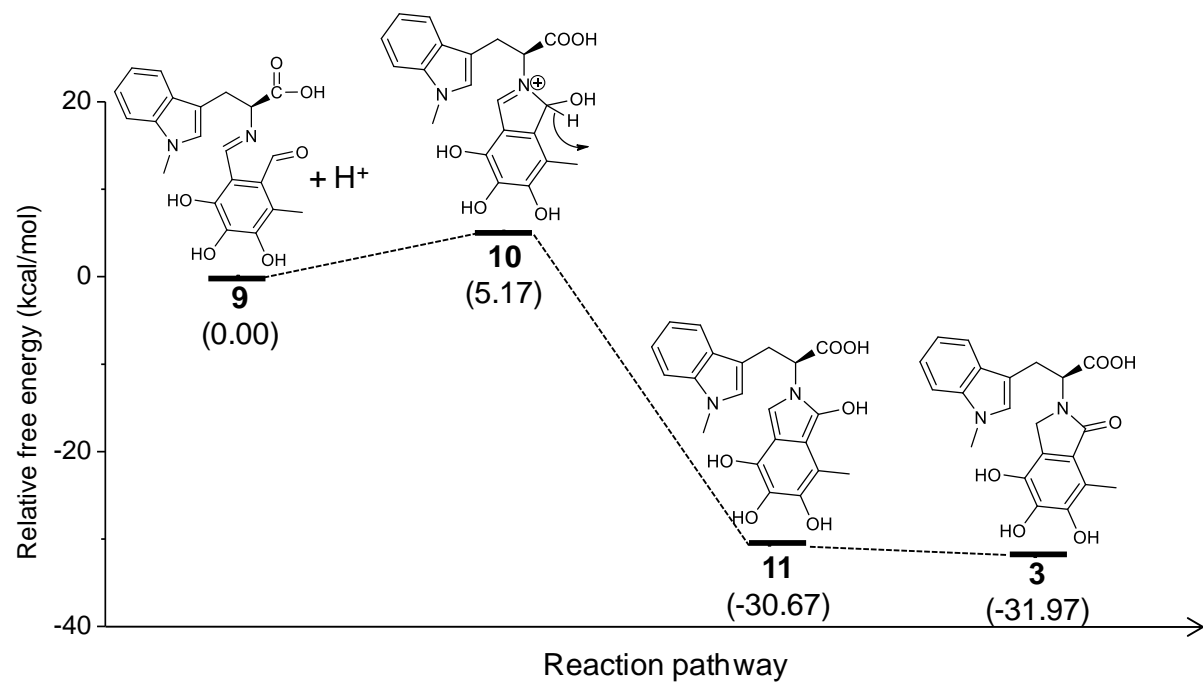


Figure S20. The free energy profile of the reaction pathway from **9** to **3**. Free energies in the solvent are given in parentheses.

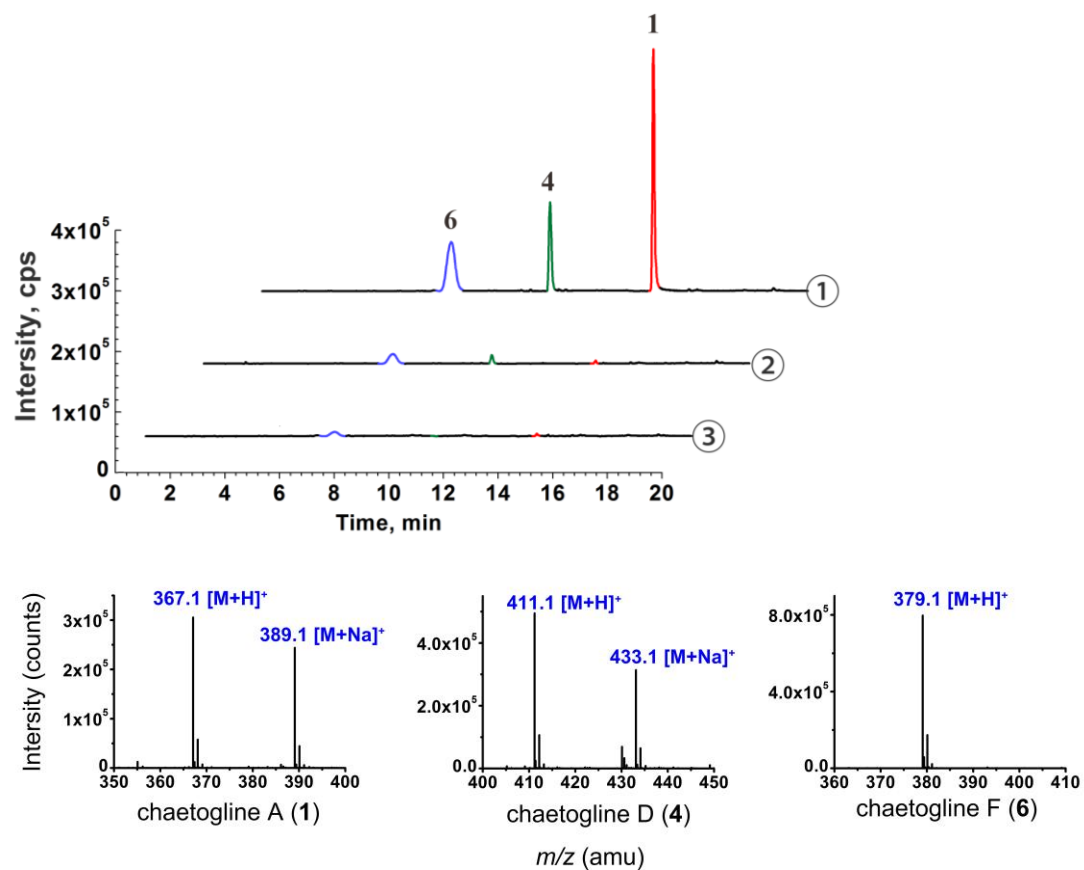


Figure S21. LC-MS profile of chaetoglines A (1), D (4) and F (6) from cultures without (①) and with exposures to 3-(trifluoromethyl)-phenylacetone at 0.5 (②) and 1.0 (③) mM, respectively.

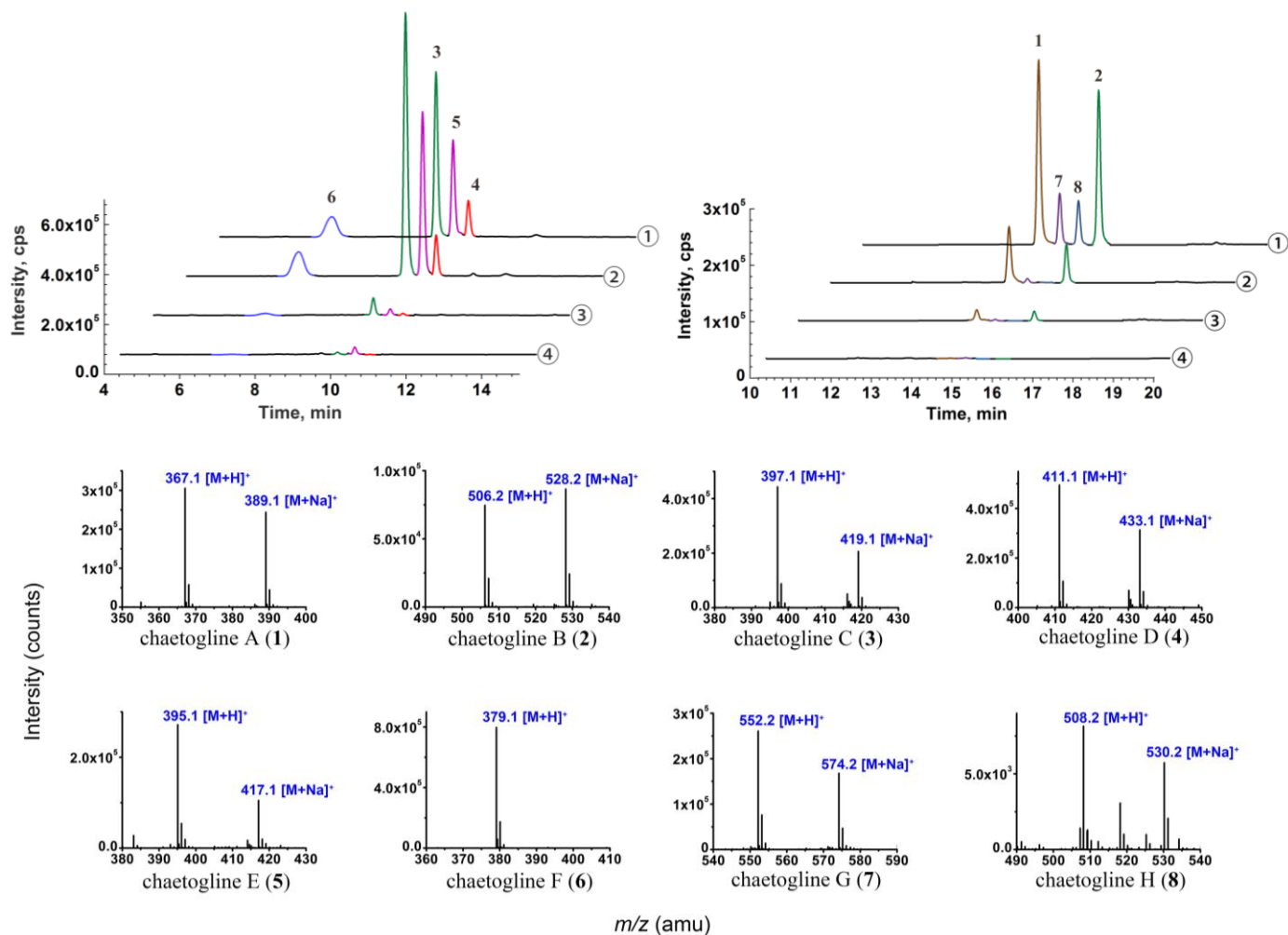


Figure S22. LC-MS profile of chaetoglines A–H (1–8) from cultures without (①) and with exposures to NaN_3 at 0.1 (①), 0.5 (②) and 1.0 (③) mM, respectively.

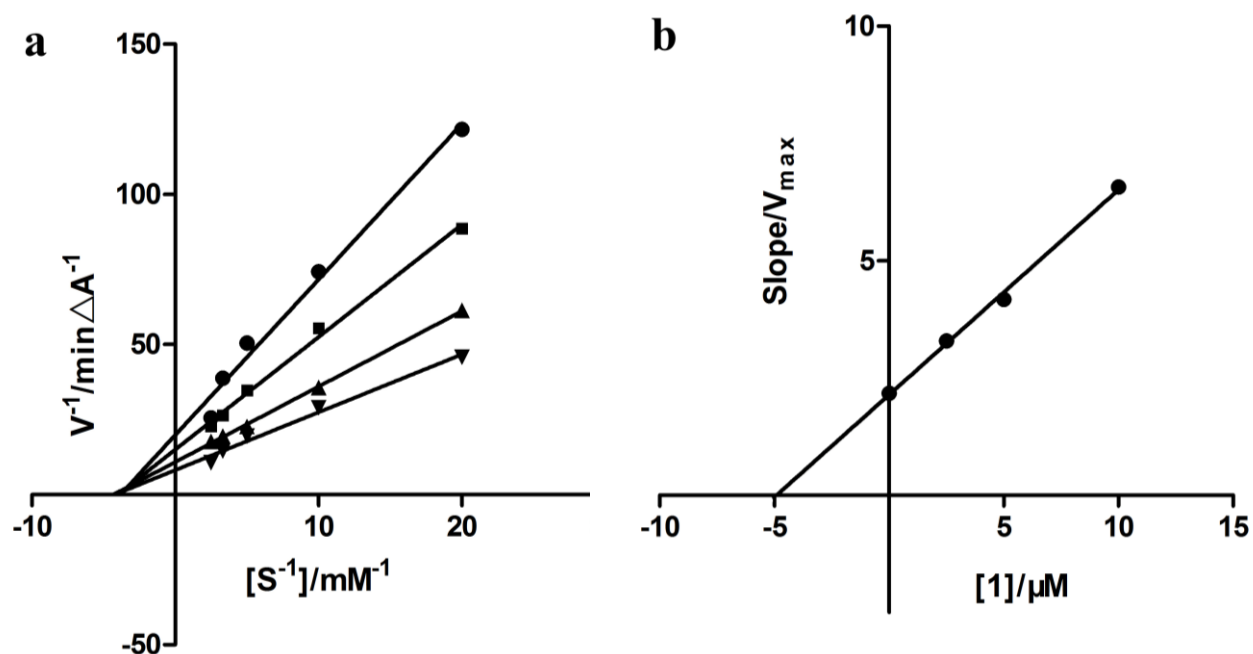


Figure S23. Steady-state inhibition of AChE by chaetogline F (**6**). a) Lineweaver-Burk plot of reciprocal of initial velocities versus reciprocal of five fixed acetylthiocholine iodide (ATCh) concentrations in the absence (\blacktriangledown) and presence of 10 μM (\blacktriangle), 20 μM (\blacksquare) and 40 μM (\bullet) of **6**. b) Secondary plots of the Lineweaver-Burk plot, slope versus various concentrations of **6**. x axis intercept represents the K_i (4.87 μM) of **6**.

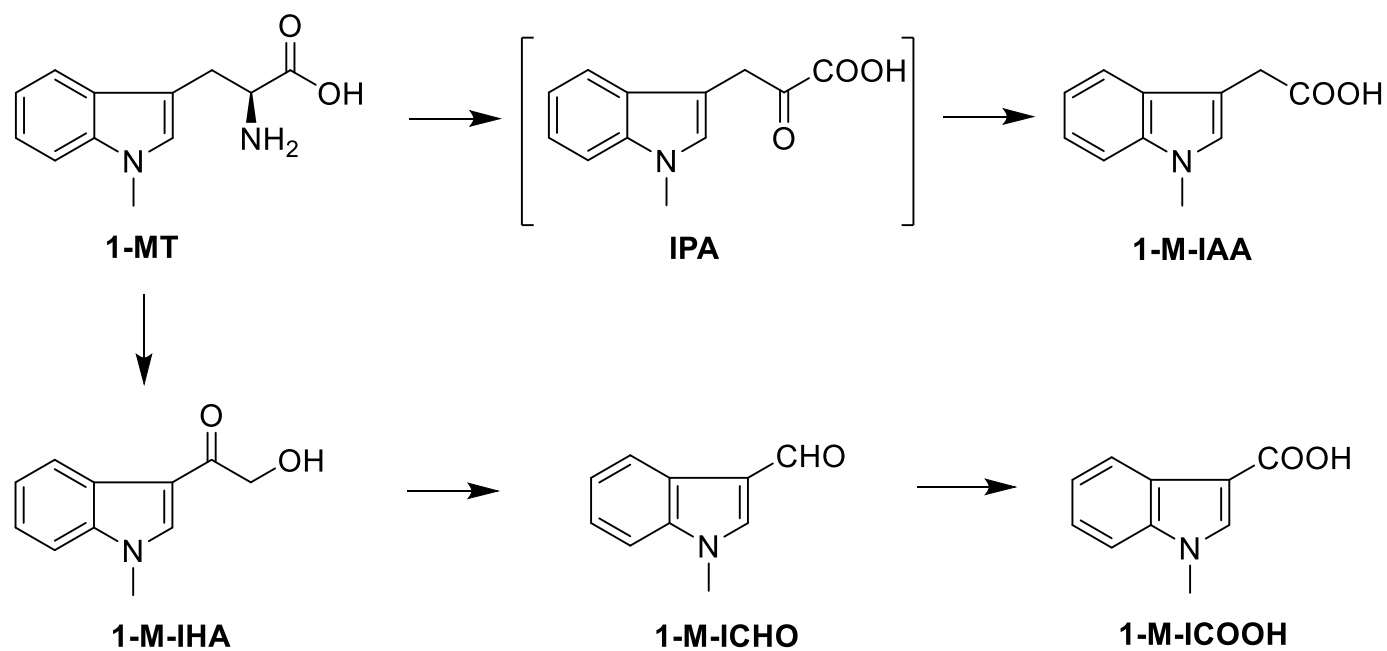


Figure S24. Isolated indole metabolites derived from 1-MT by *C. globosum* 1C51. 1-Methylindole-3-carboxylic acid (1-M-IAA), 1-methyl-3-hydroxyacetylindole (1-M-IHA), 1-methylindole-3-carboxaldehyde (1-M-ICHO) and 1-methylindole-3-carboxylic acid (1-M-ICOOH) were not detected in the 1-MT free culture by LC-MS.

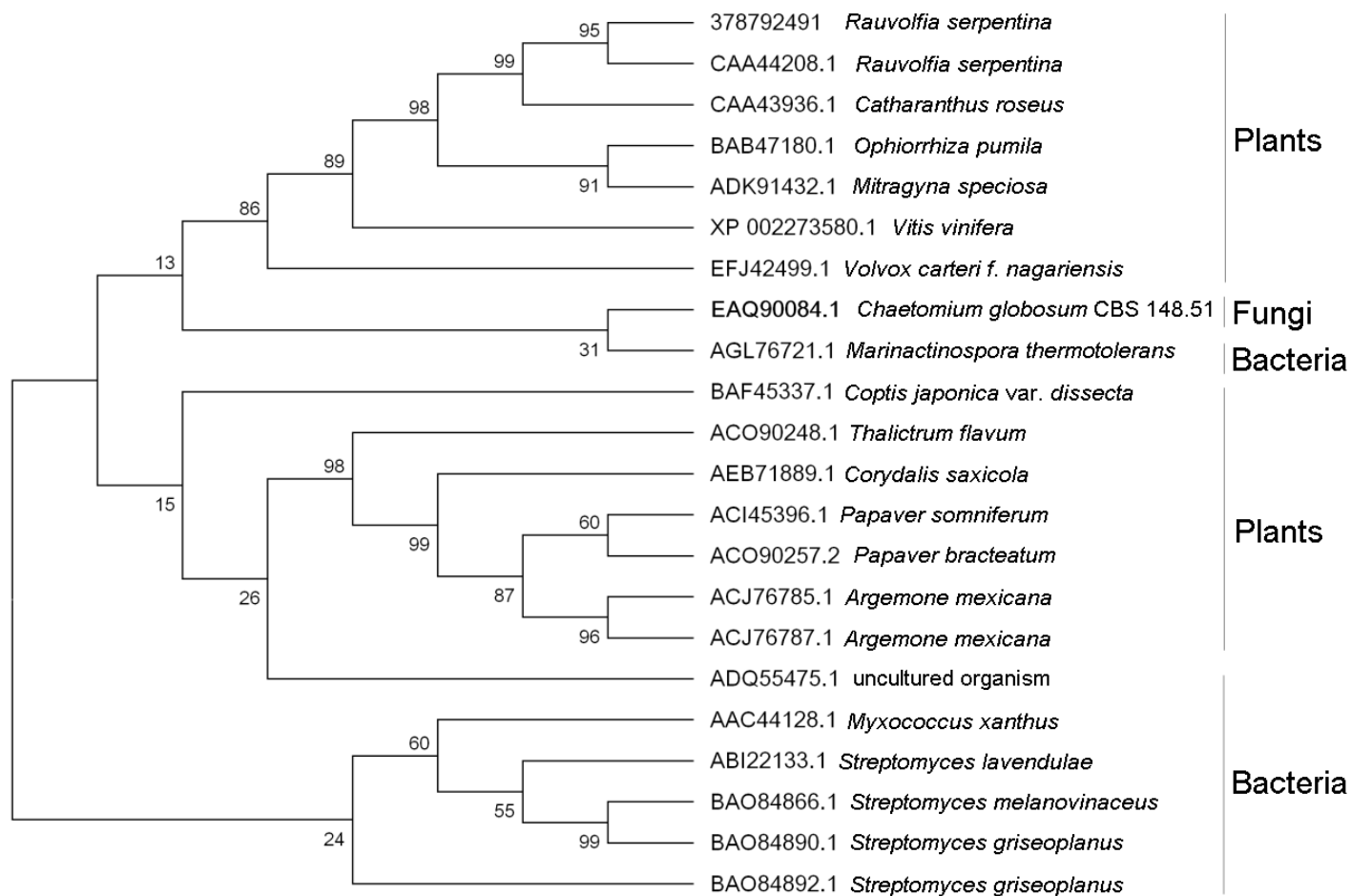


Figure S25. Phylogenetic analysis of 22 characterized Pictet–Spengler reaction enzymes, constructed using MEGA v5.0 with 1000 bootstrap replicates.

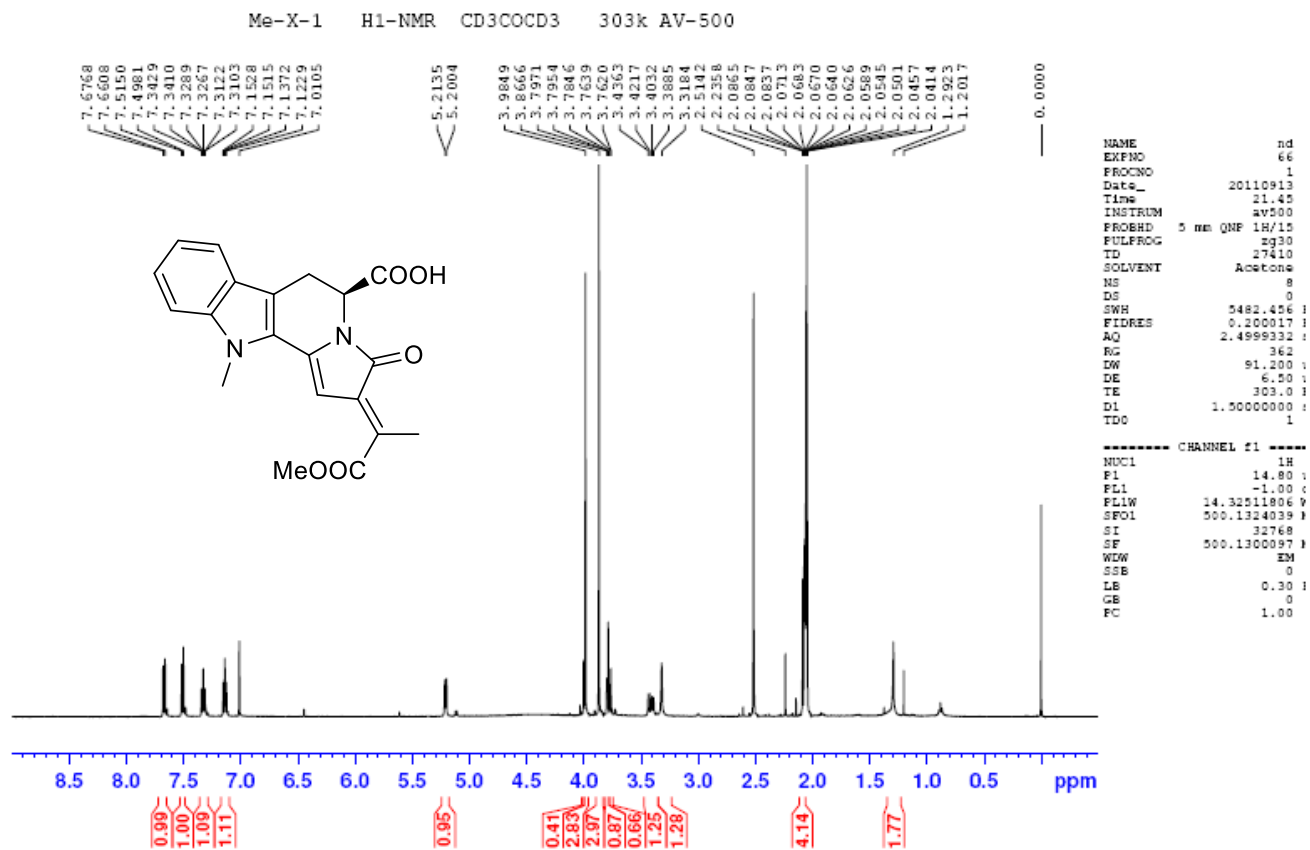


Figure S26. ¹H-NMR spectrum of chaetogline A (1) (acetone-*d*₆, 500 MHz).

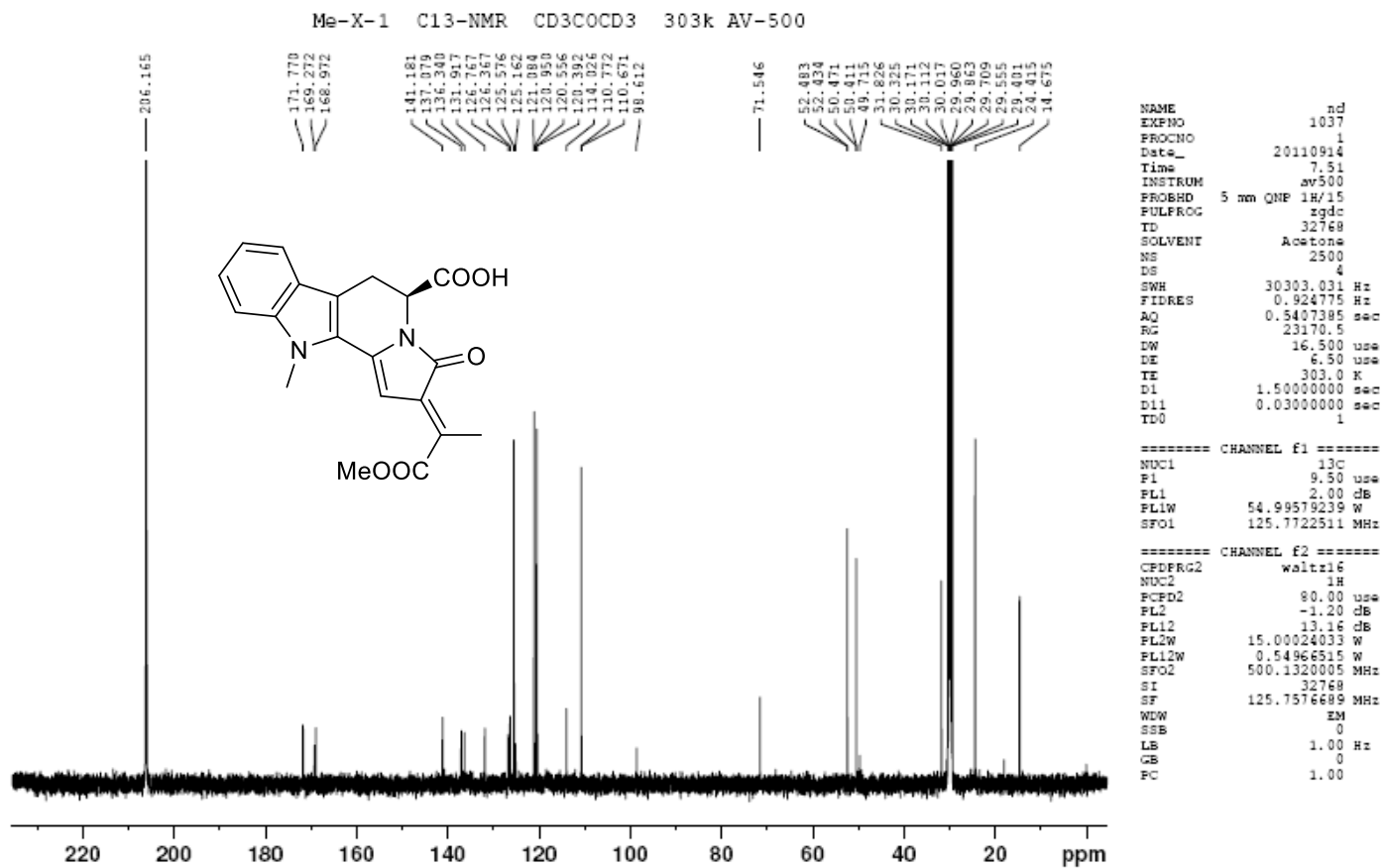


Figure S27. ^{13}C -NMR spectrum of chaetogline A (1) (acetone- d_6 , 500 MHz).

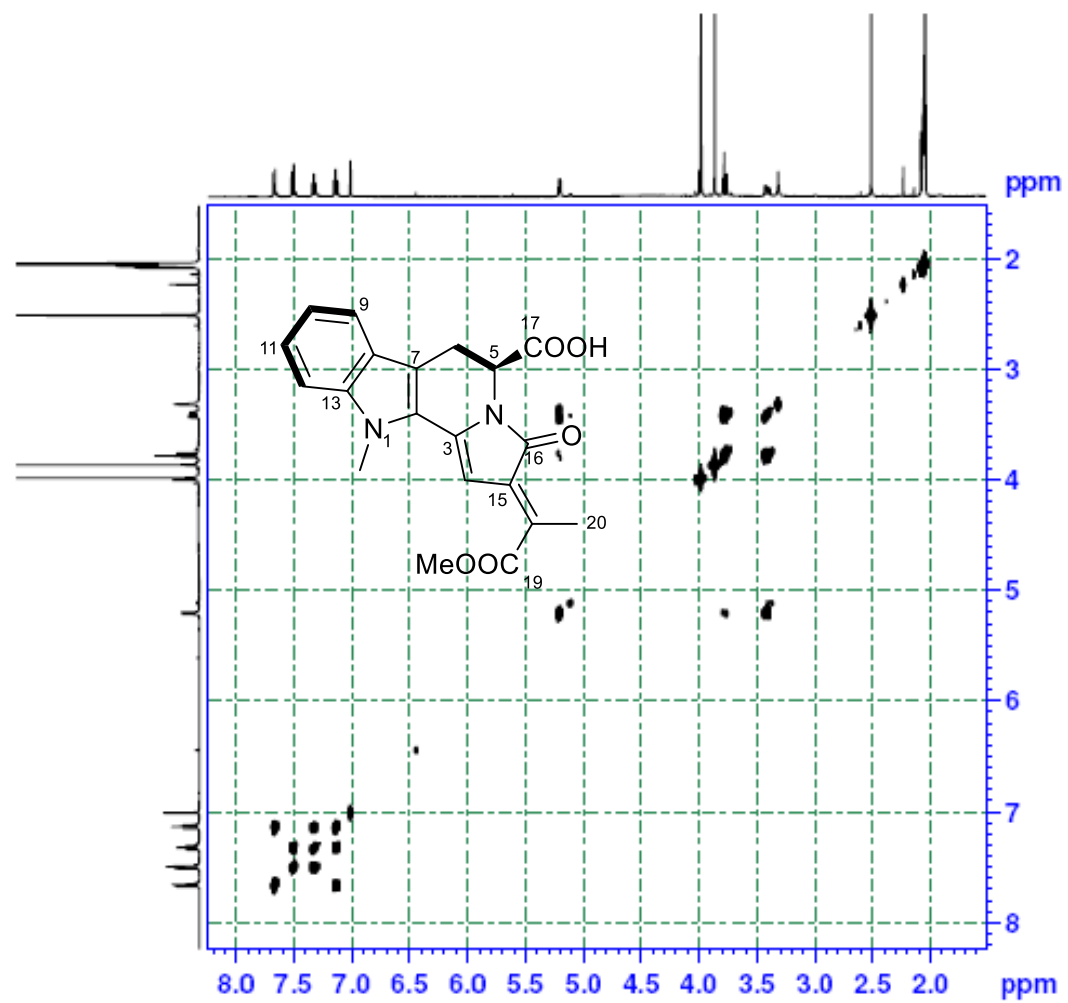


Figure S28. ^1H - ^1H COSY spectrum of chaetogline A (**1**) (acetone- d_6 , 500 MHz).

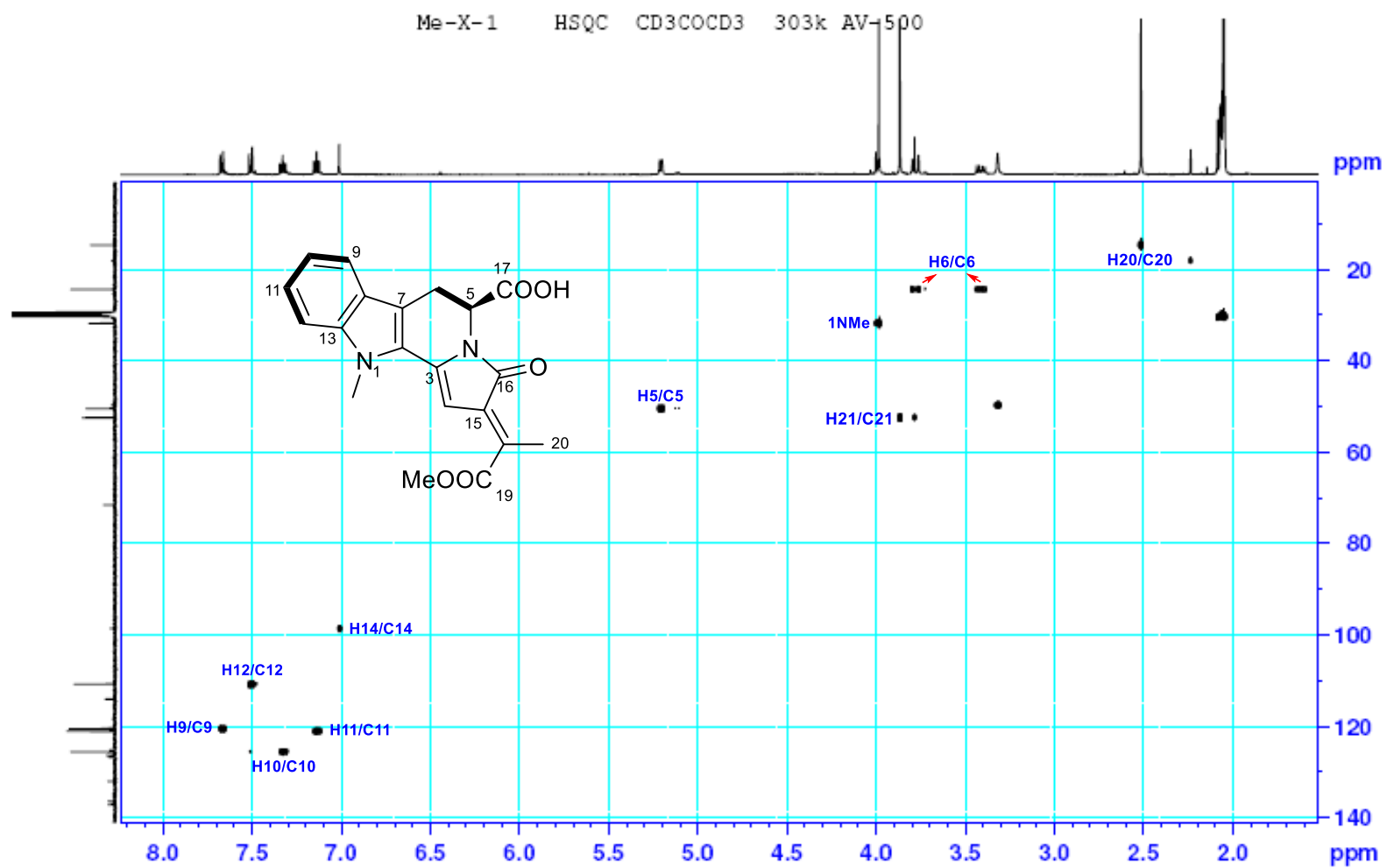


Figure S29. HSQC spectrum of chaetogline A (**1**) (acetone- d_6 , 500 MHz).

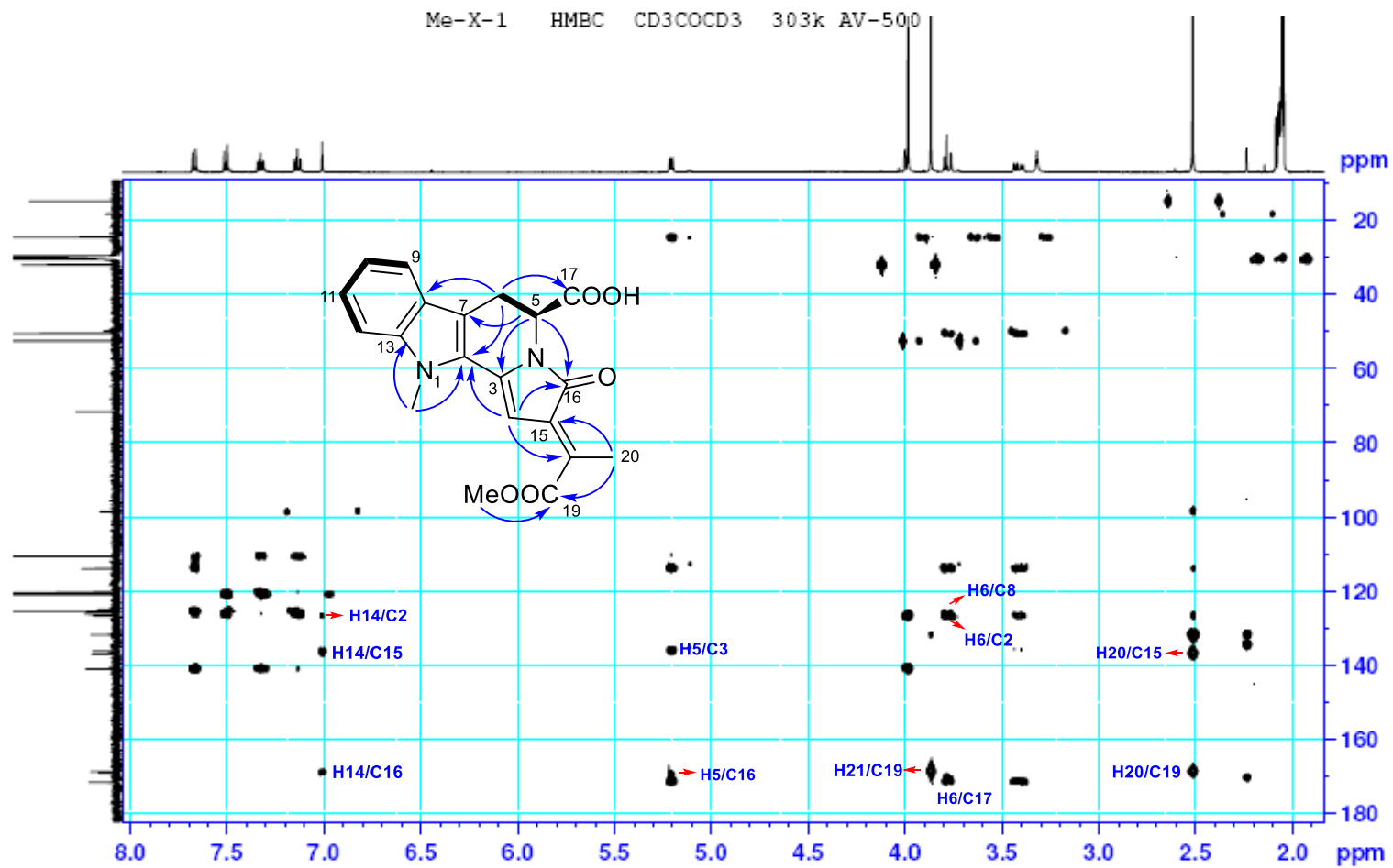


Figure S30. HMBC spectrum of chaetogline A (**1**) (acetone- d_6 , 500 MHz).

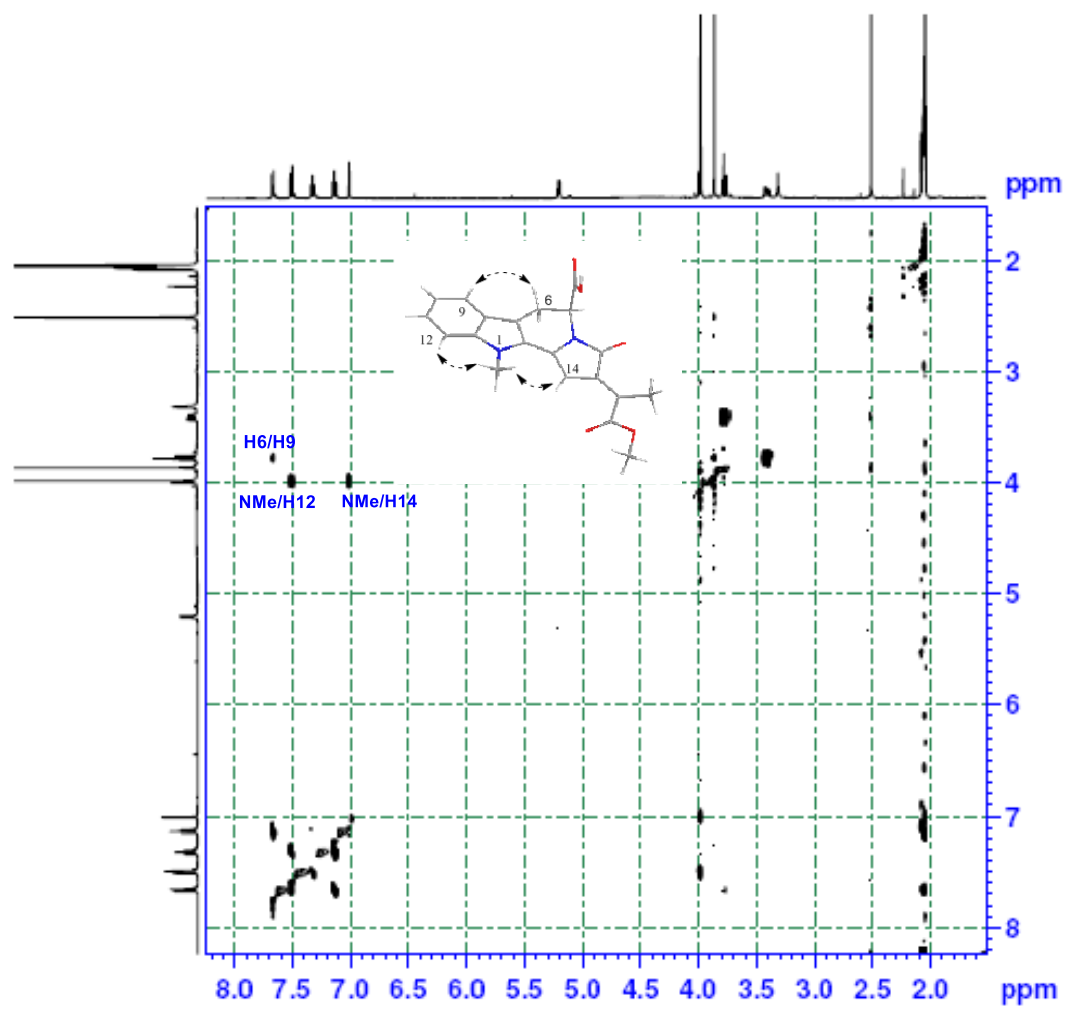


Figure S31. ROESY spectrum of chaetogline A (**1**) (acetone-*d*₆, 500 MHz).

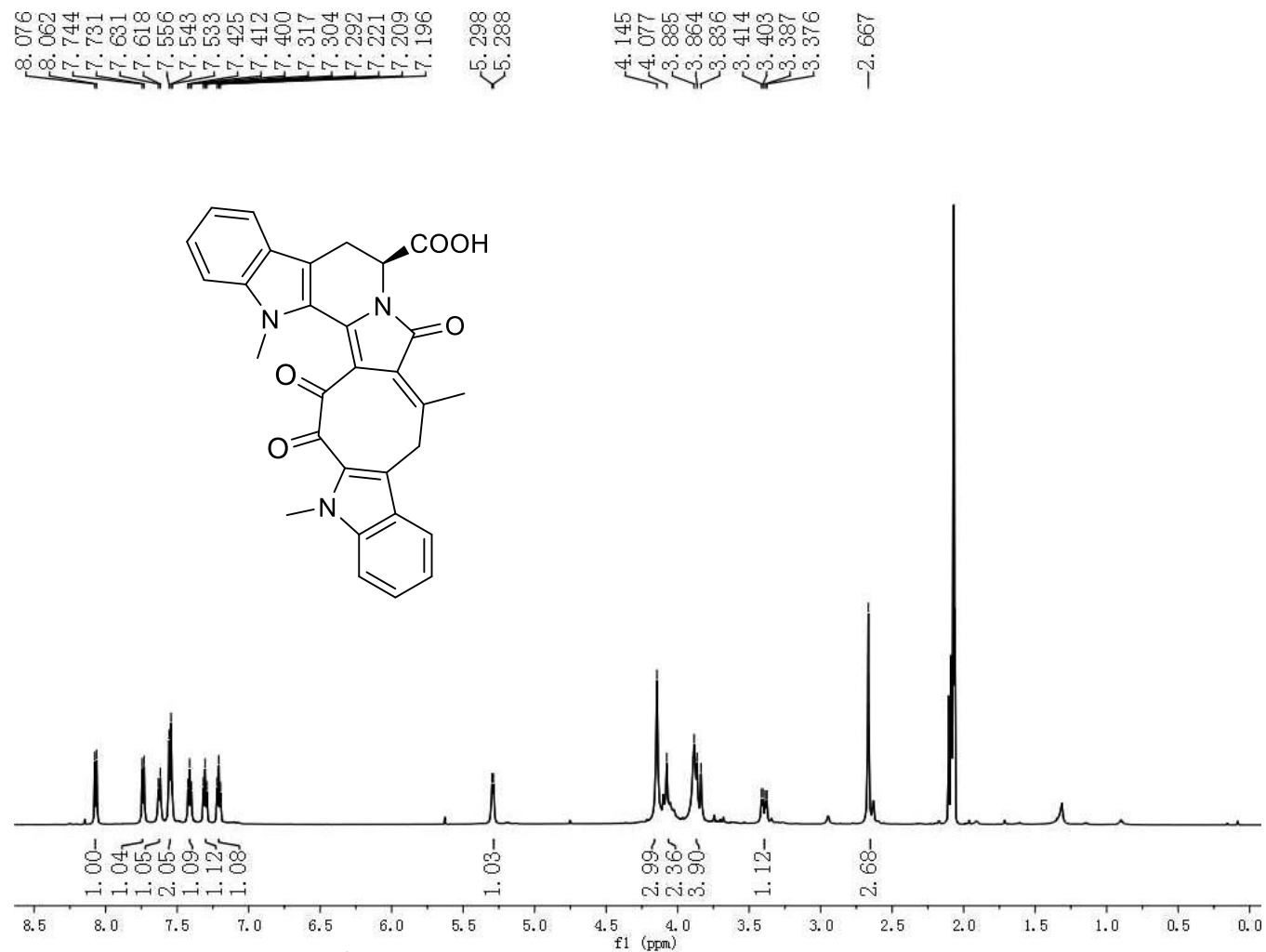


Figure S32. ¹H-NMR spectrum of chaetogline B (2) (acetone-*d*₆, 600 MHz).

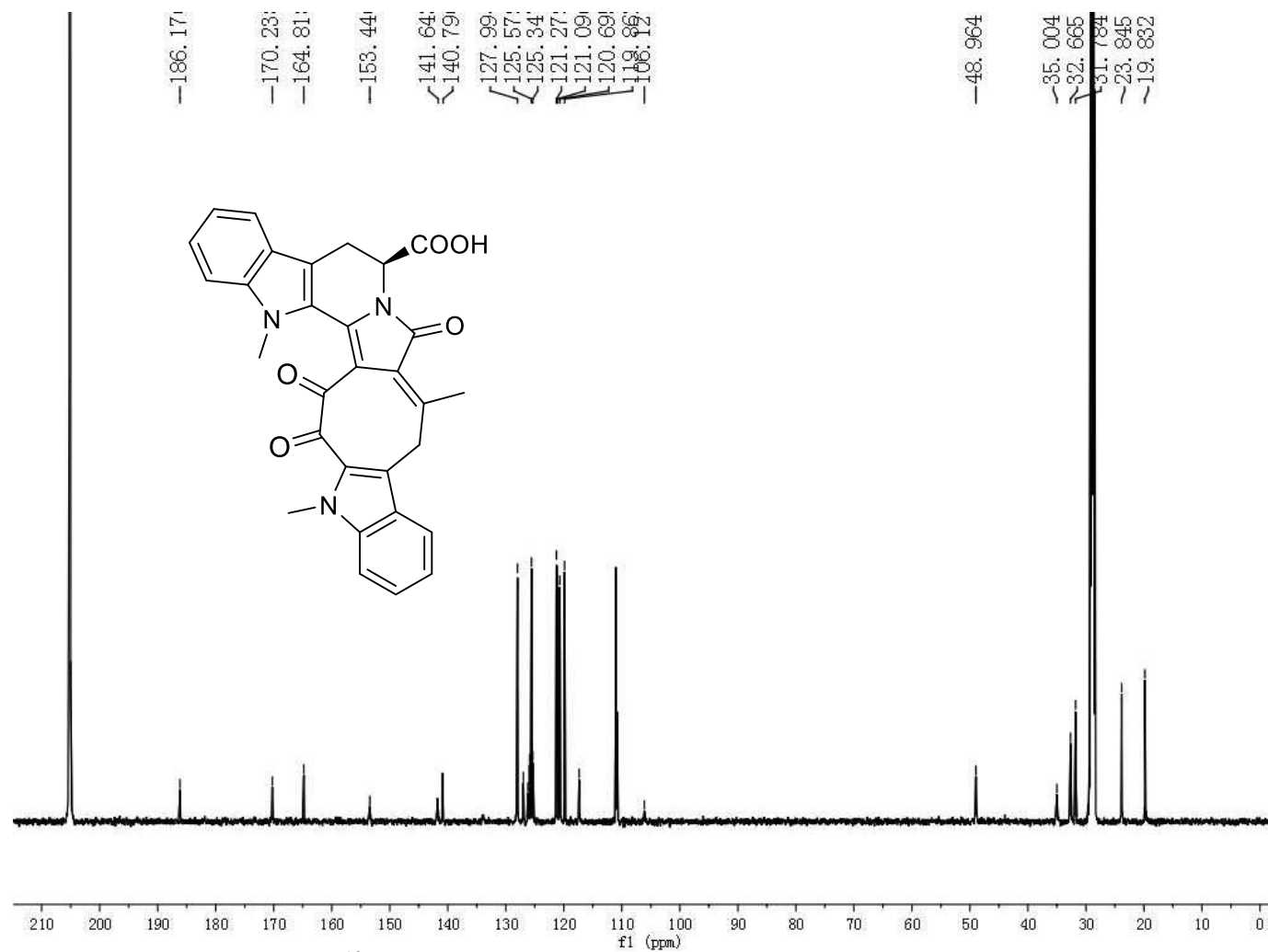


Figure S33. ¹³C-NMR spectrum of chaetogline B (**2**) (acetone-*d*₆, 600 MHz).

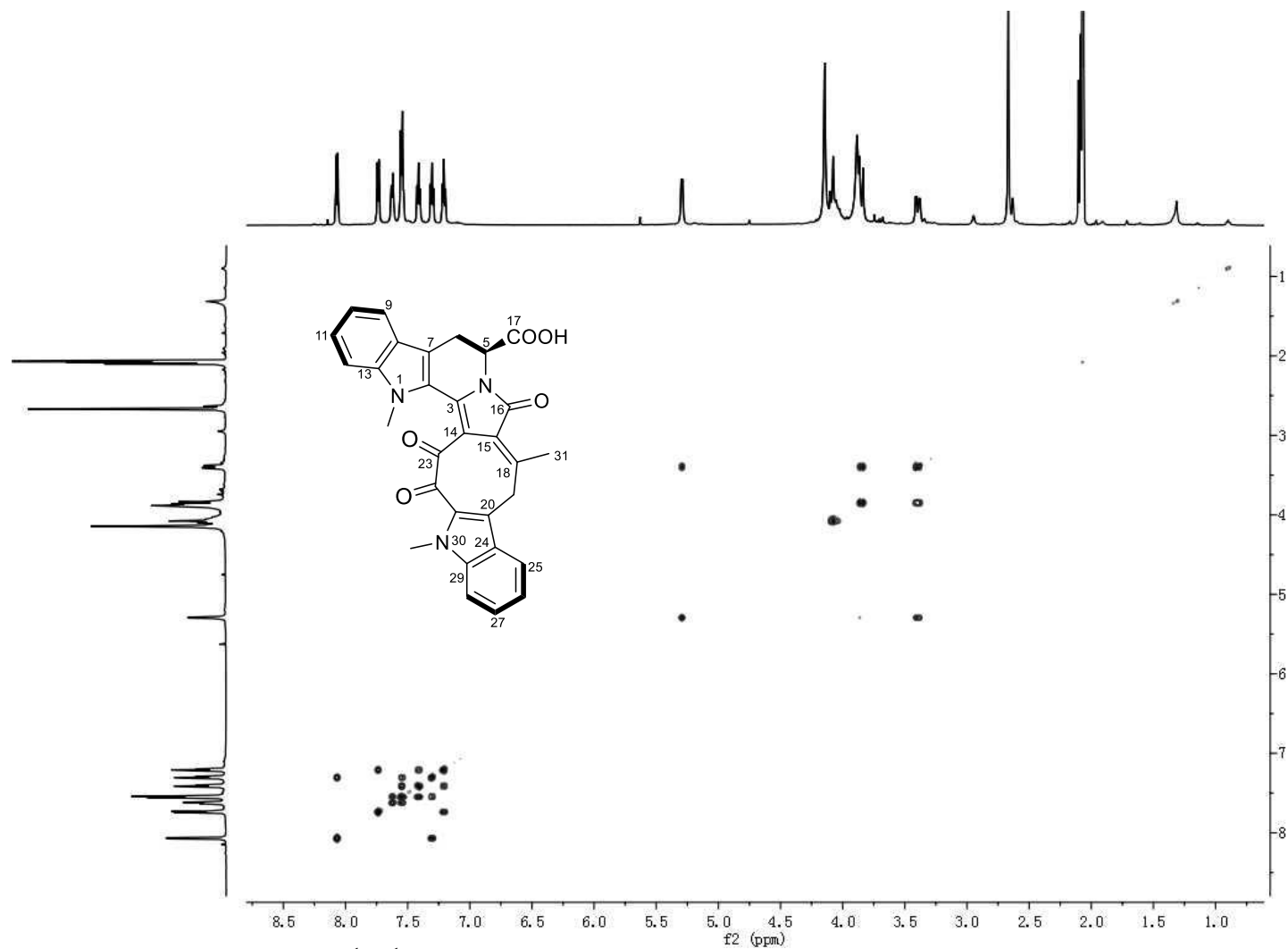


Figure S34. ^1H - ^1H COSY spectrum of chaetogline B (**2**) (acetone- d_6 , 600 MHz).

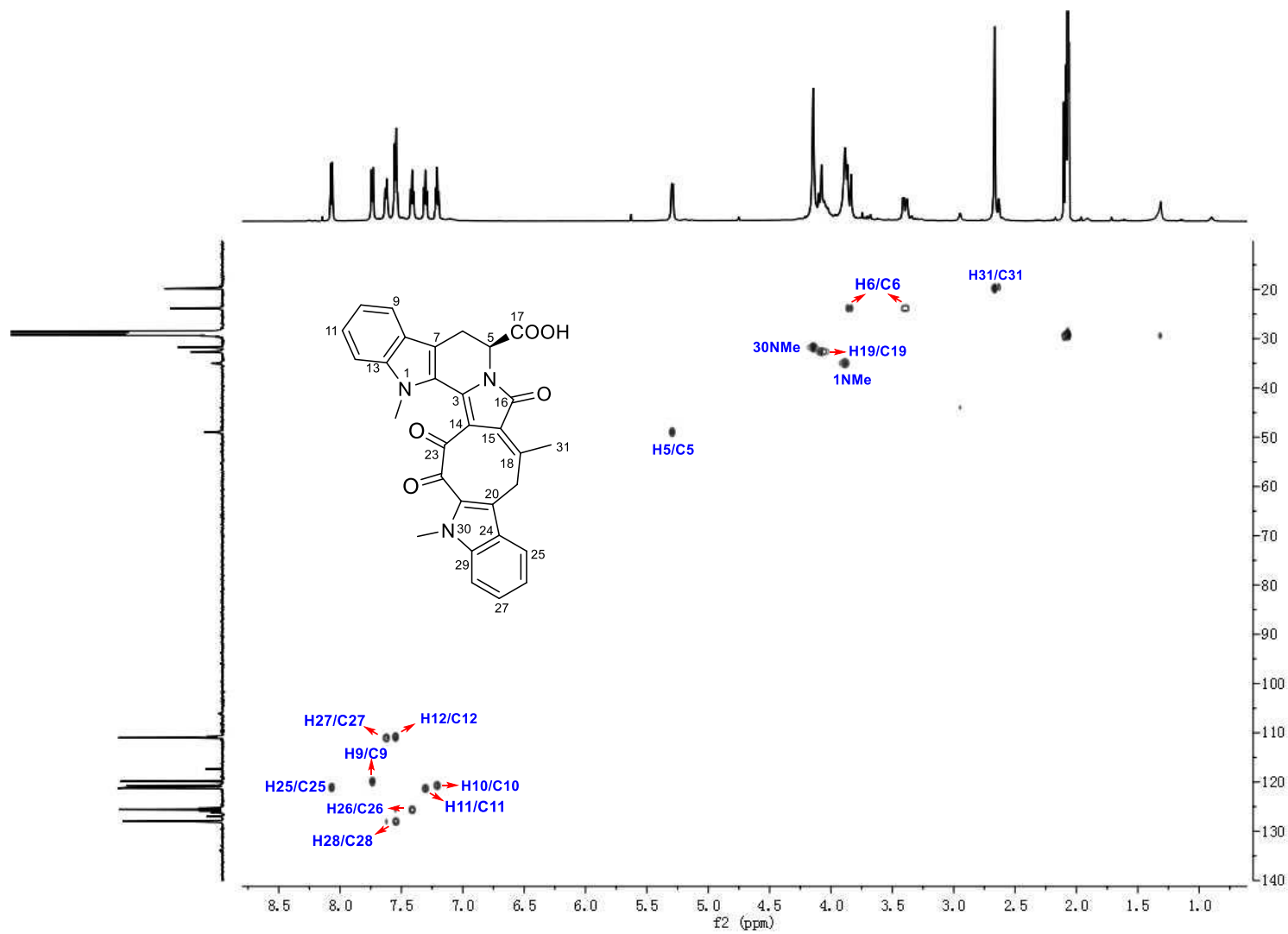


Figure S35. HSQC spectrum of chaetogline B (**2**) (acetone- d_6 , 600 MHz).

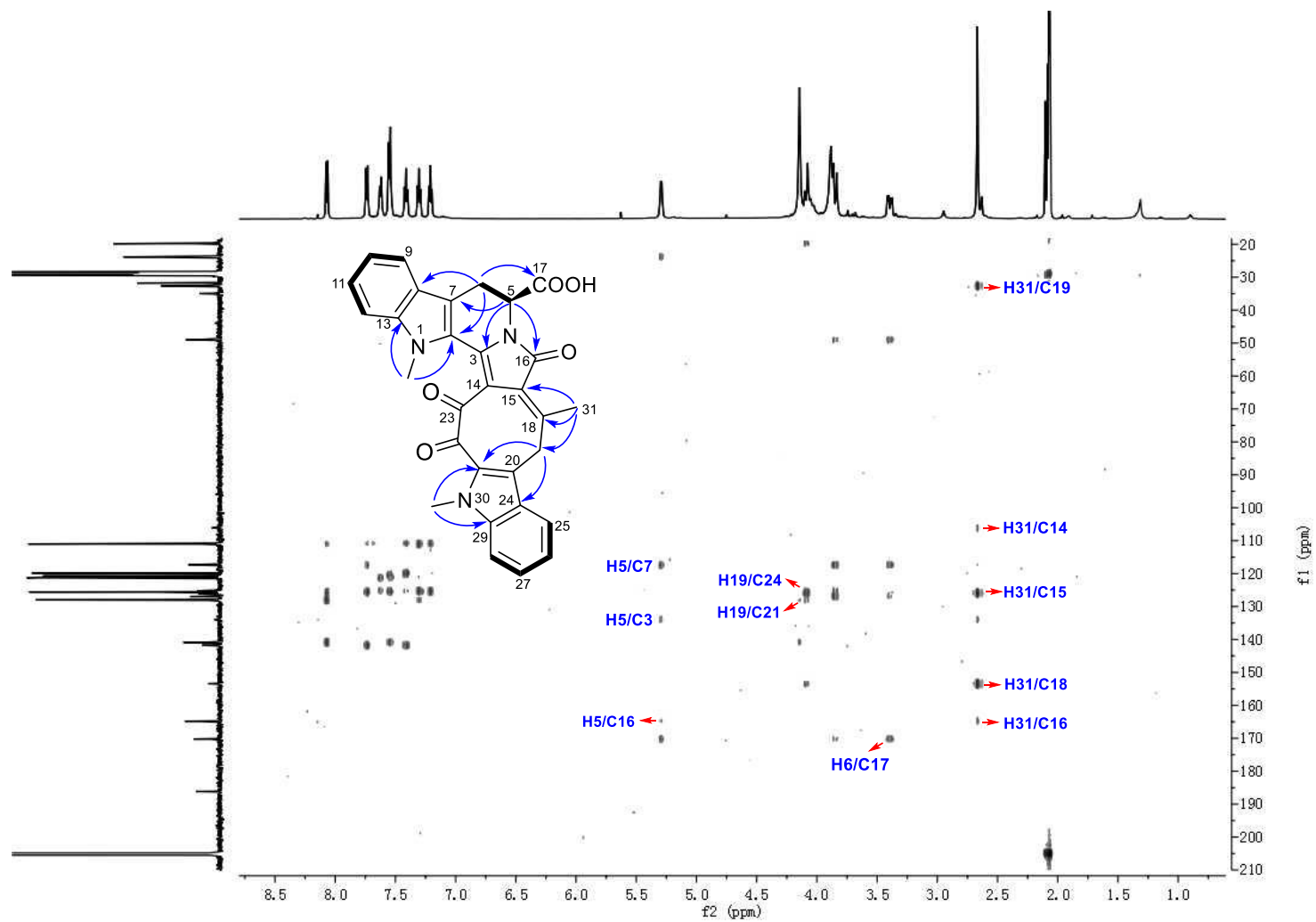


Figure S36. HMBC spectrum of chaetogline B (2) (acetone- d_6 , 600 MHz).

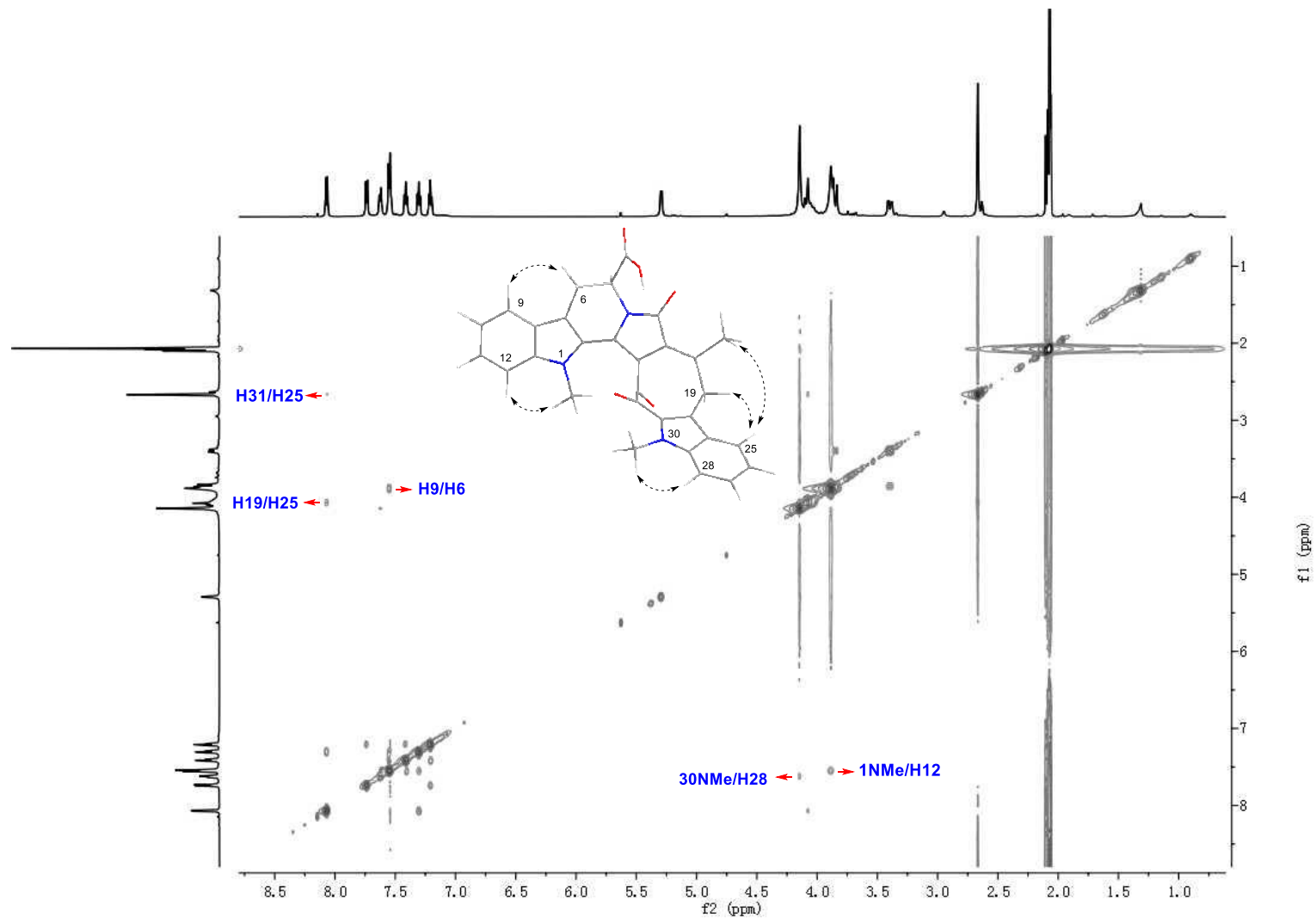


Figure S37. ROESY spectrum of chaetogline B (**2**) (acetone- d_6 , 600 MHz).

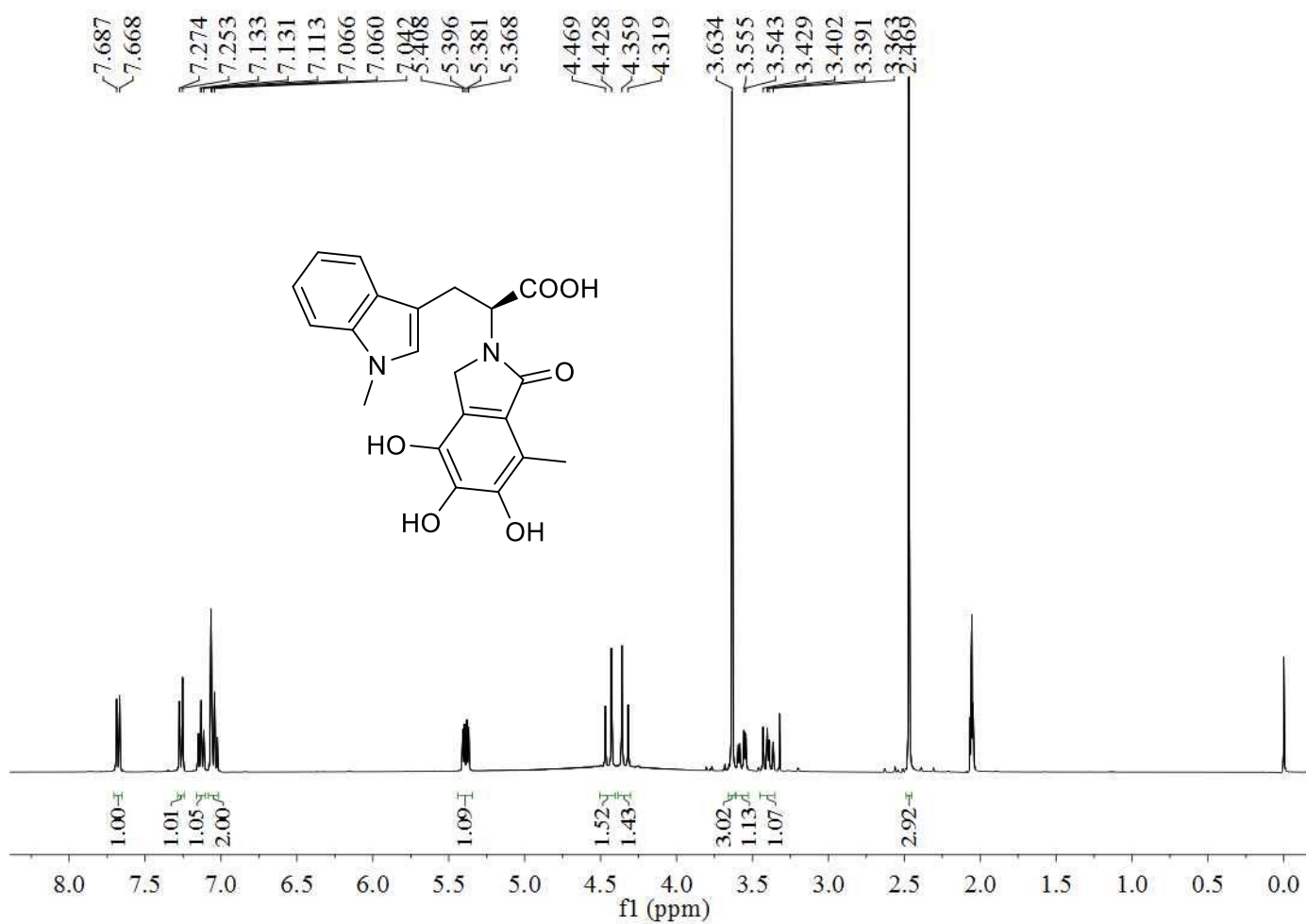


Figure S38. ¹H-NMR spectrum of chaetogline C (**3**) (acetone-*d*₆, 400 MHz).

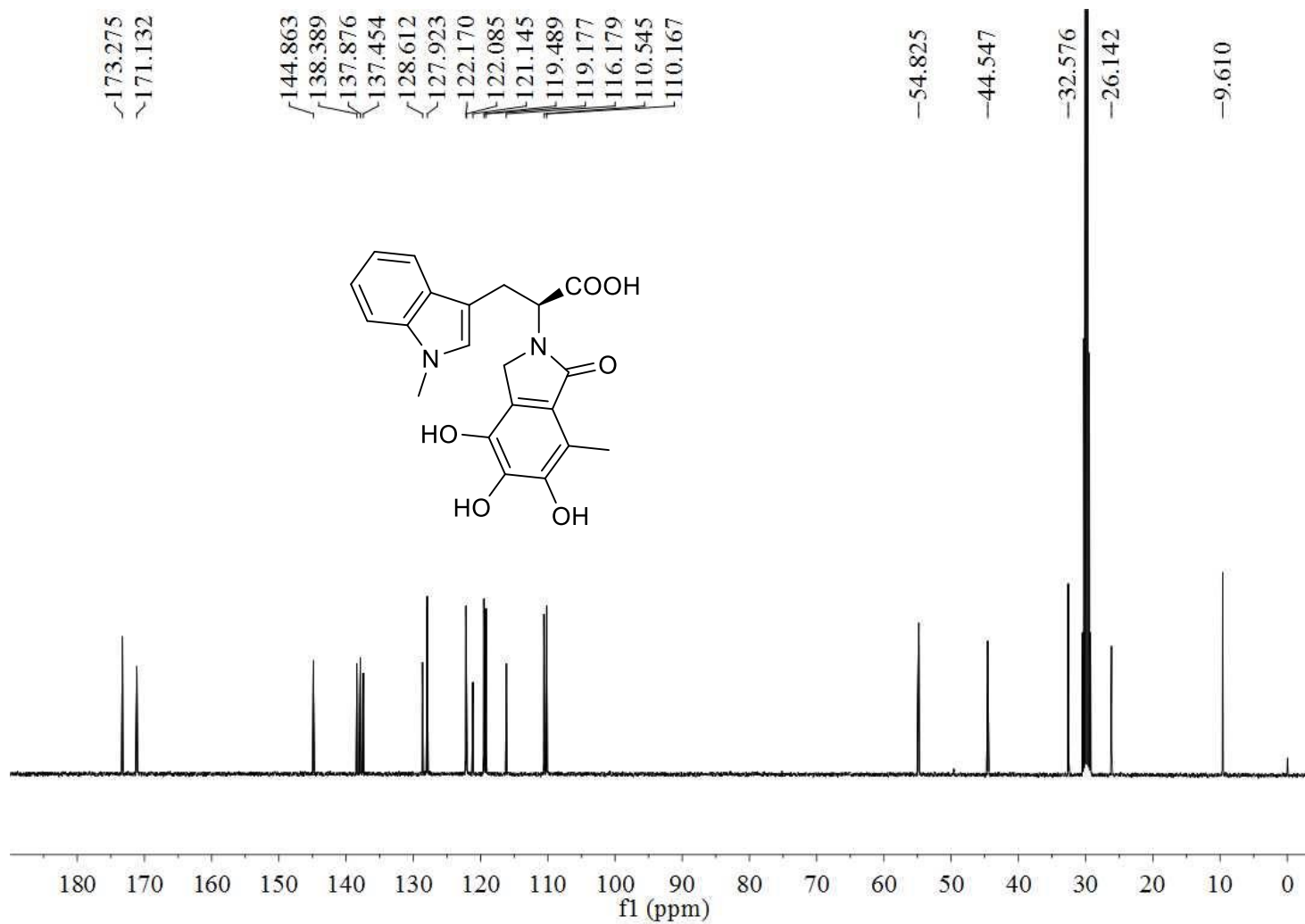


Figure S39. ^{13}C -NMR spectrum of chaetogline C (**3**) (acetone- d_6 , 400 MHz).

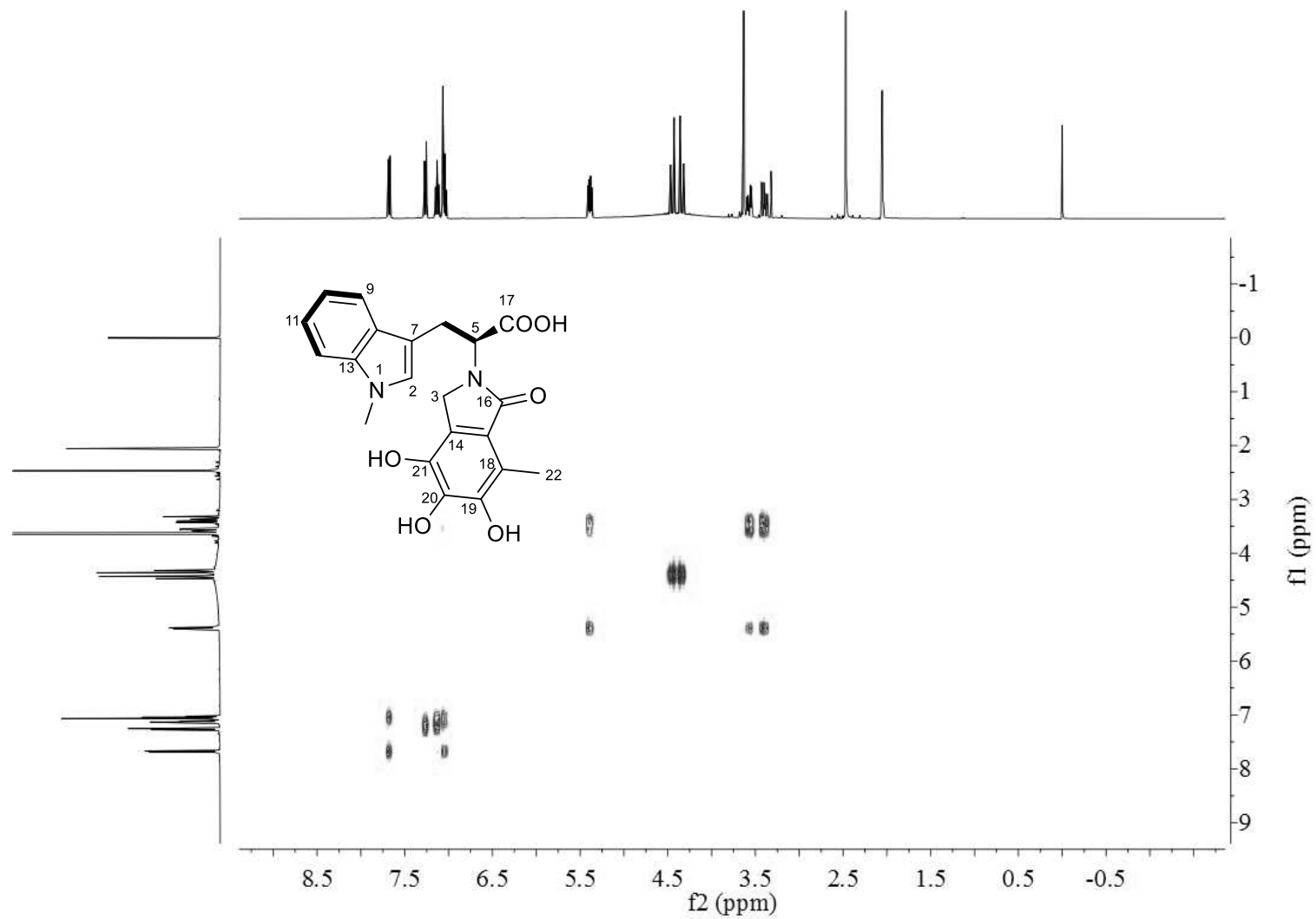


Figure S40. ^1H - ^1H COSY spectrum of chaetogline C (**3**) (acetone- d_6 , 400 MHz).

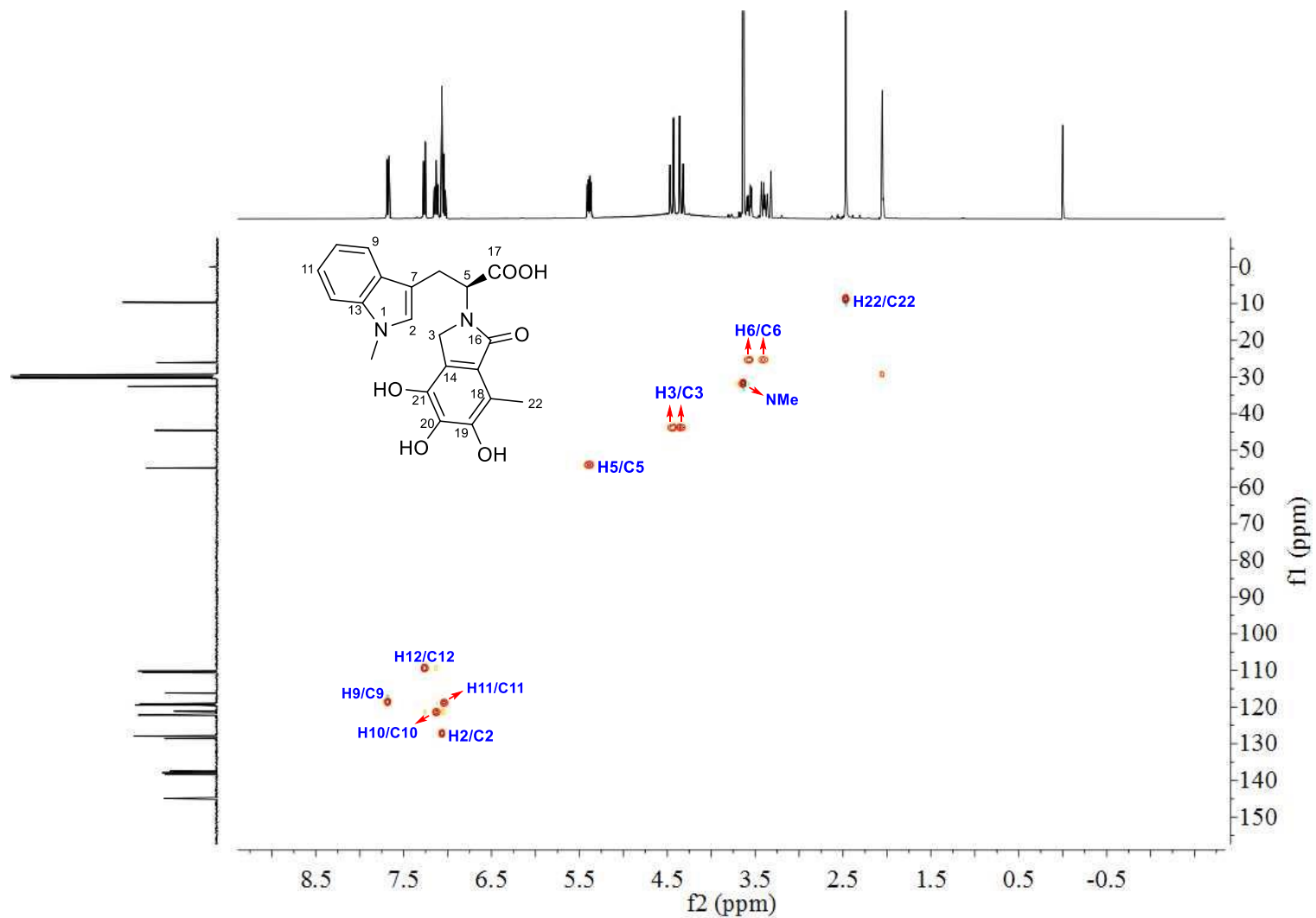


Figure S41. HSQC spectrum of chaetogline C (**3**) (acetone- d_6 , 400 MHz).

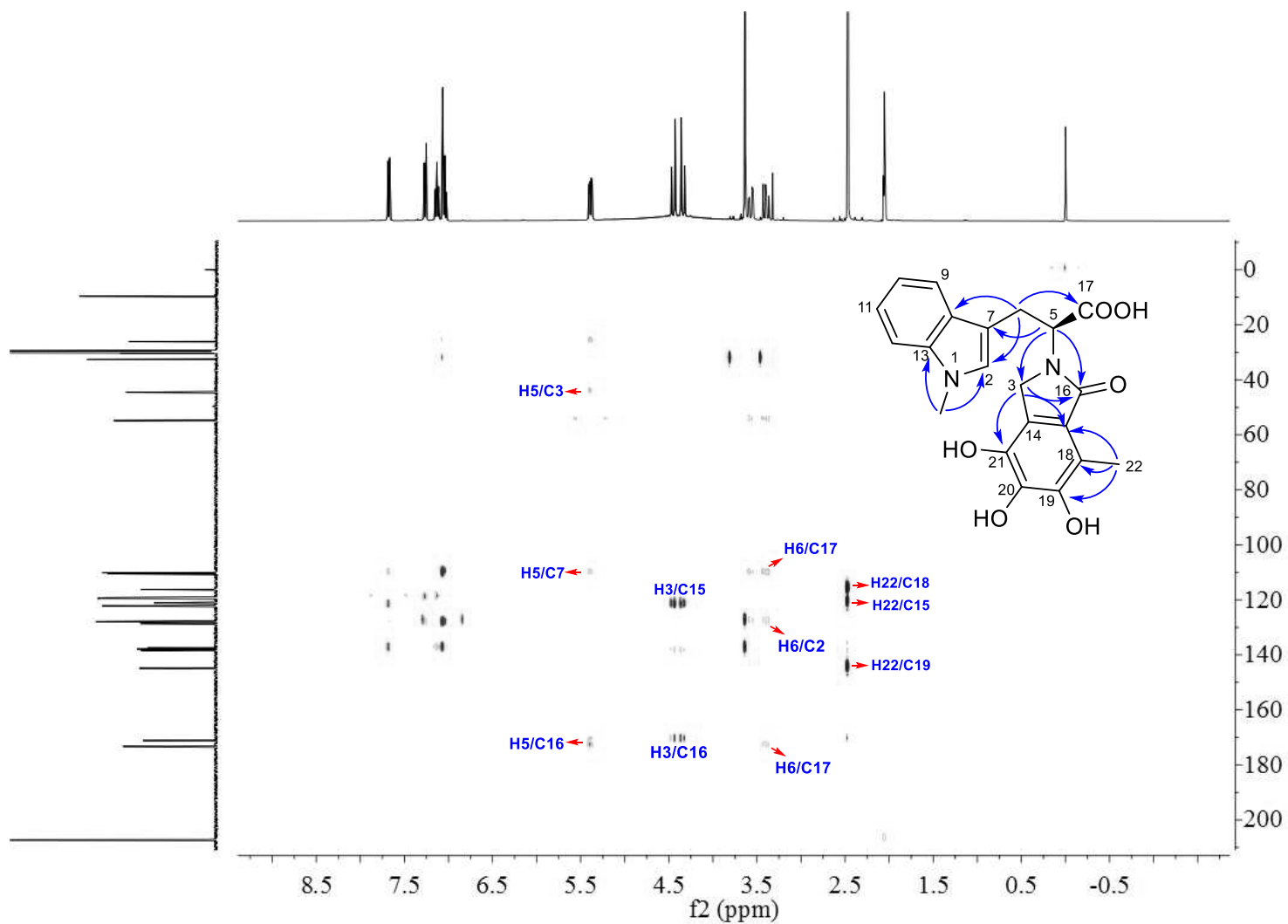


Figure S42. HMBC spectrum of chaetogline C (**3**) (acetone-*d*₆, 400 MHz).

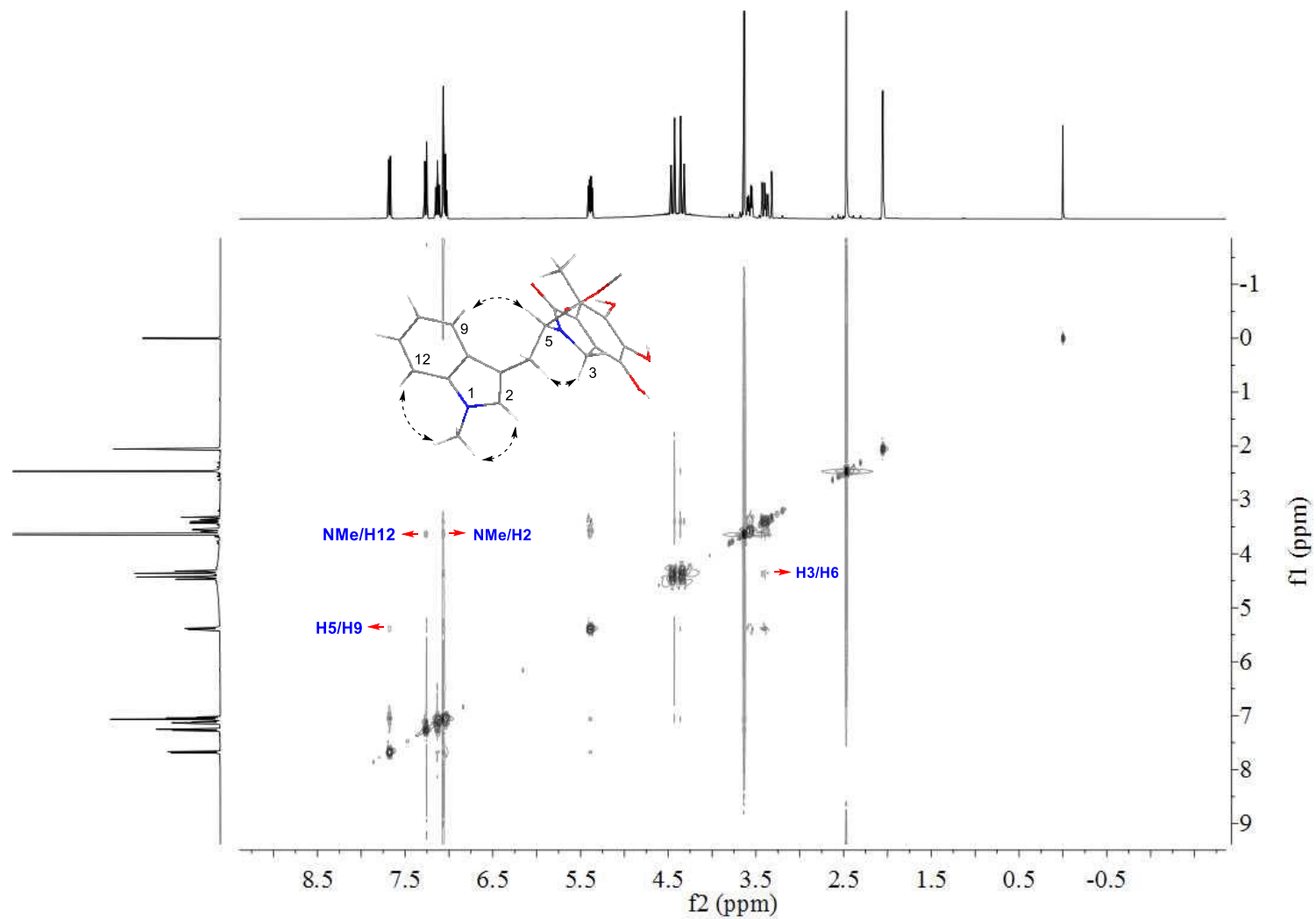


Figure S43. ROESY spectrum of chaetogline C (**3**) (acetone- d_6 , 400 MHz).

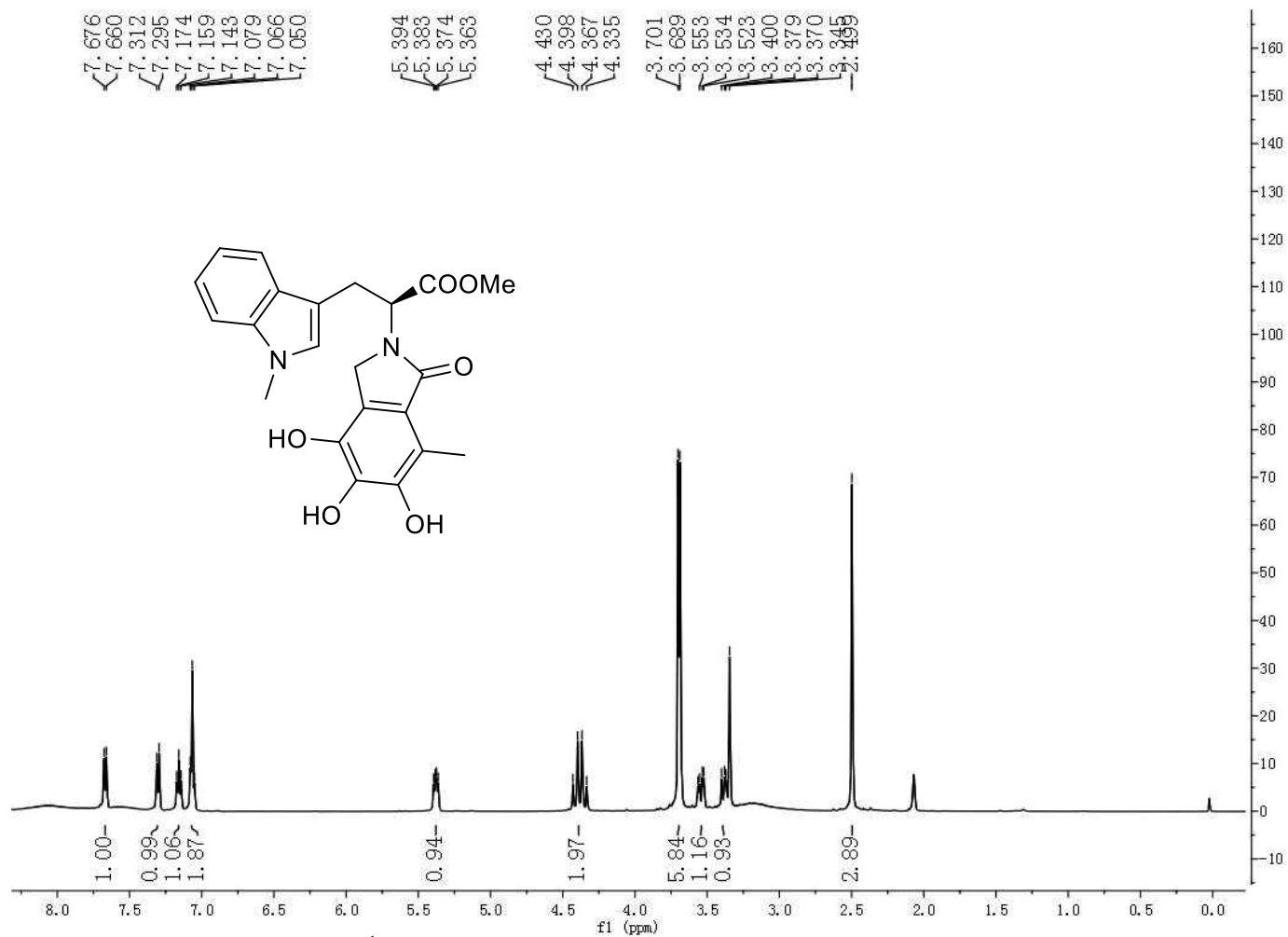


Figure S44. ¹H-NMR spectrum of chaetogline D (**4**) (acetone-*d*₆, 400 MHz).

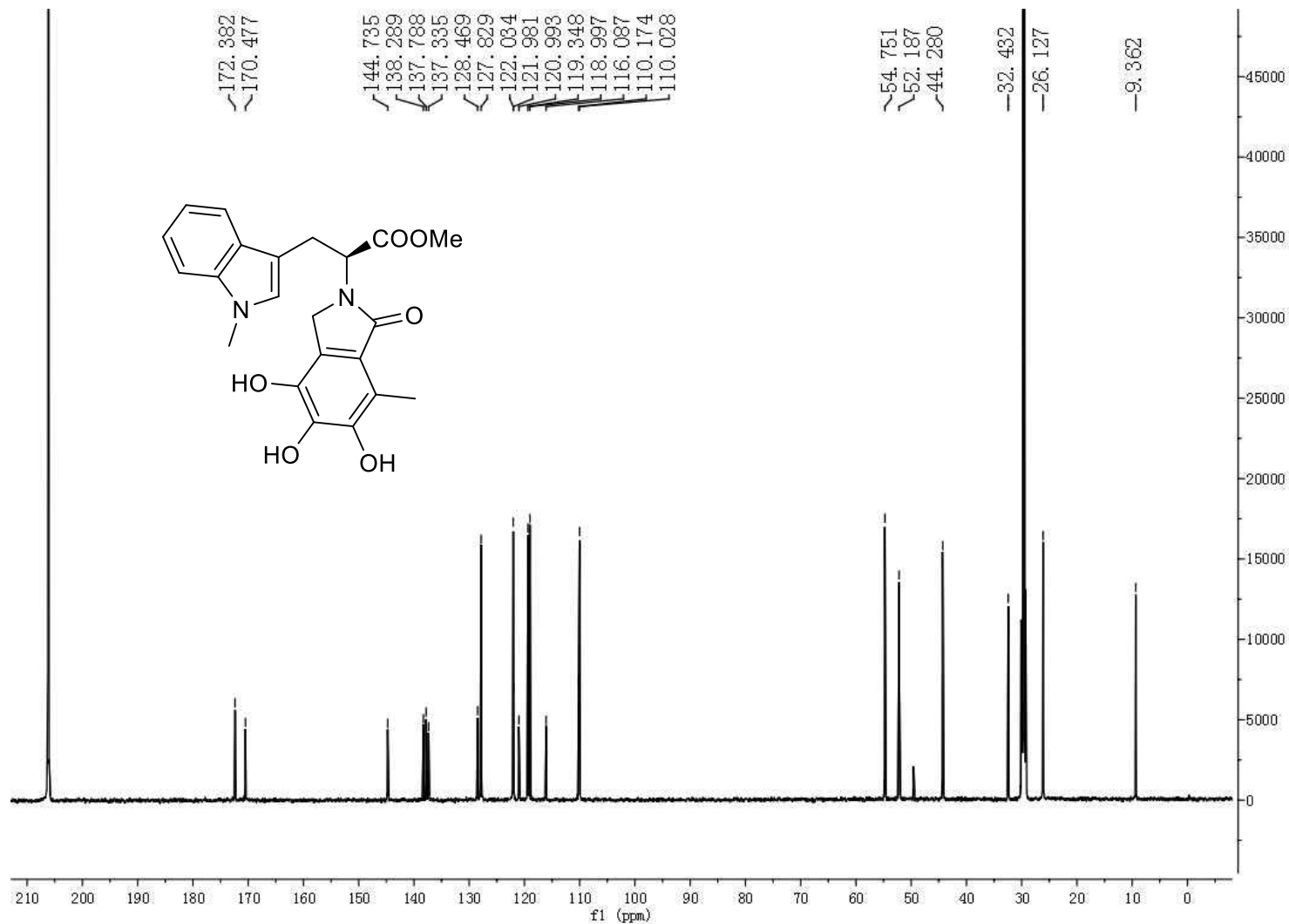


Figure S45. $^{13}\text{C-NMR}$ spectrum of chaetogline D (**4**) (acetone- d_6 , 400 MHz).

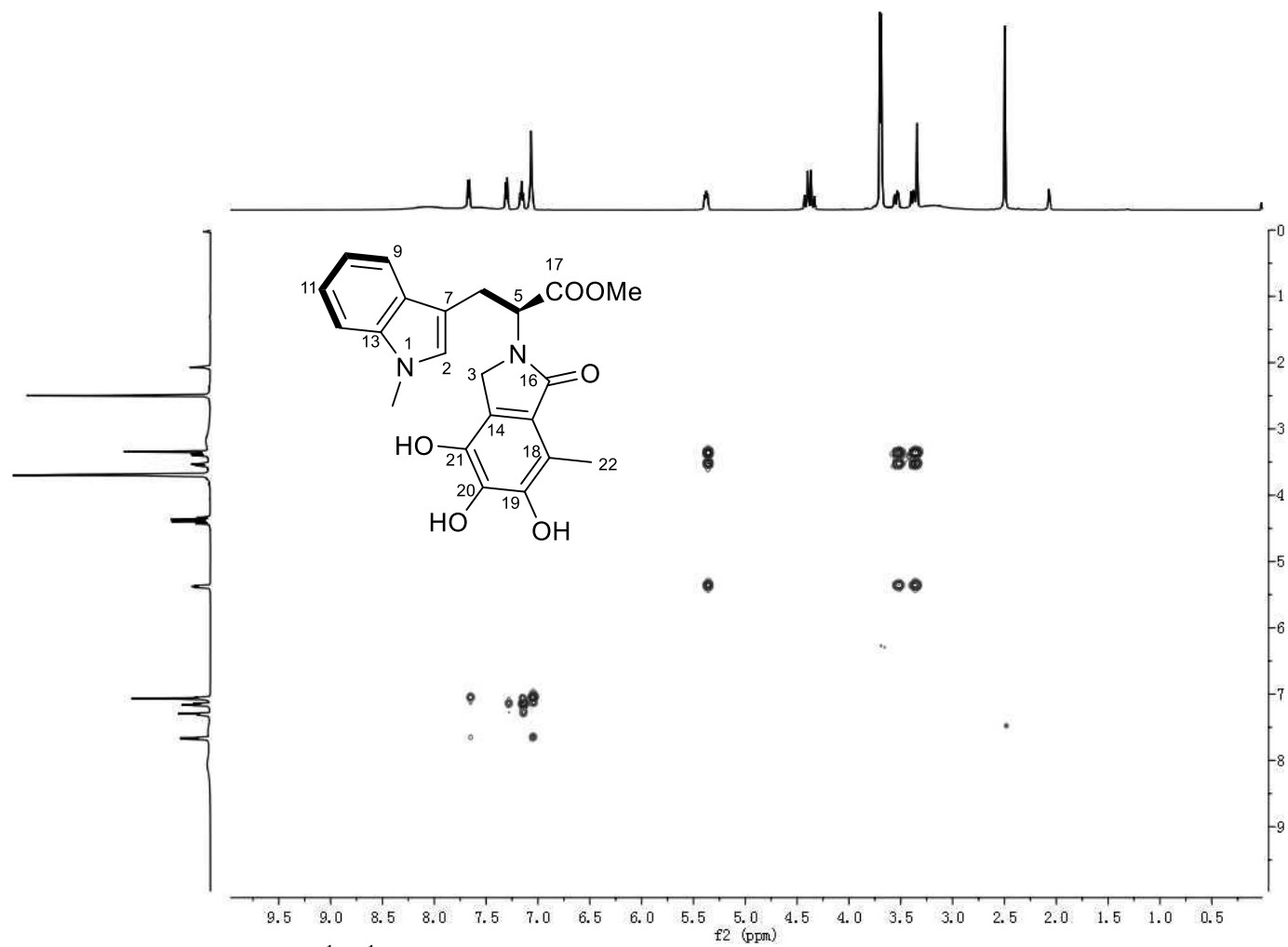


Figure S46. ^1H - ^1H COSY spectrum of chaetogline D (**4**) (acetone- d_6 , 400 MHz).

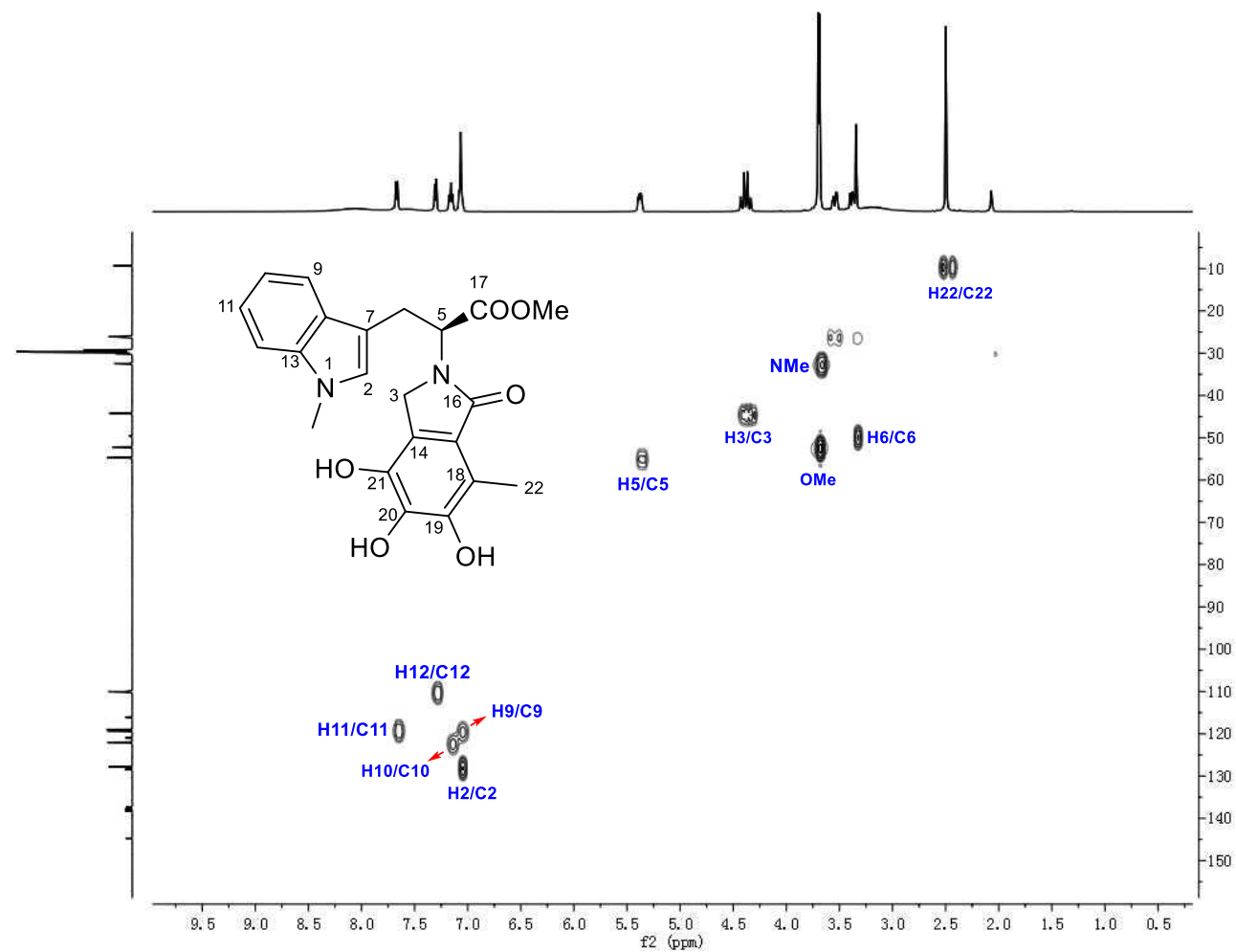
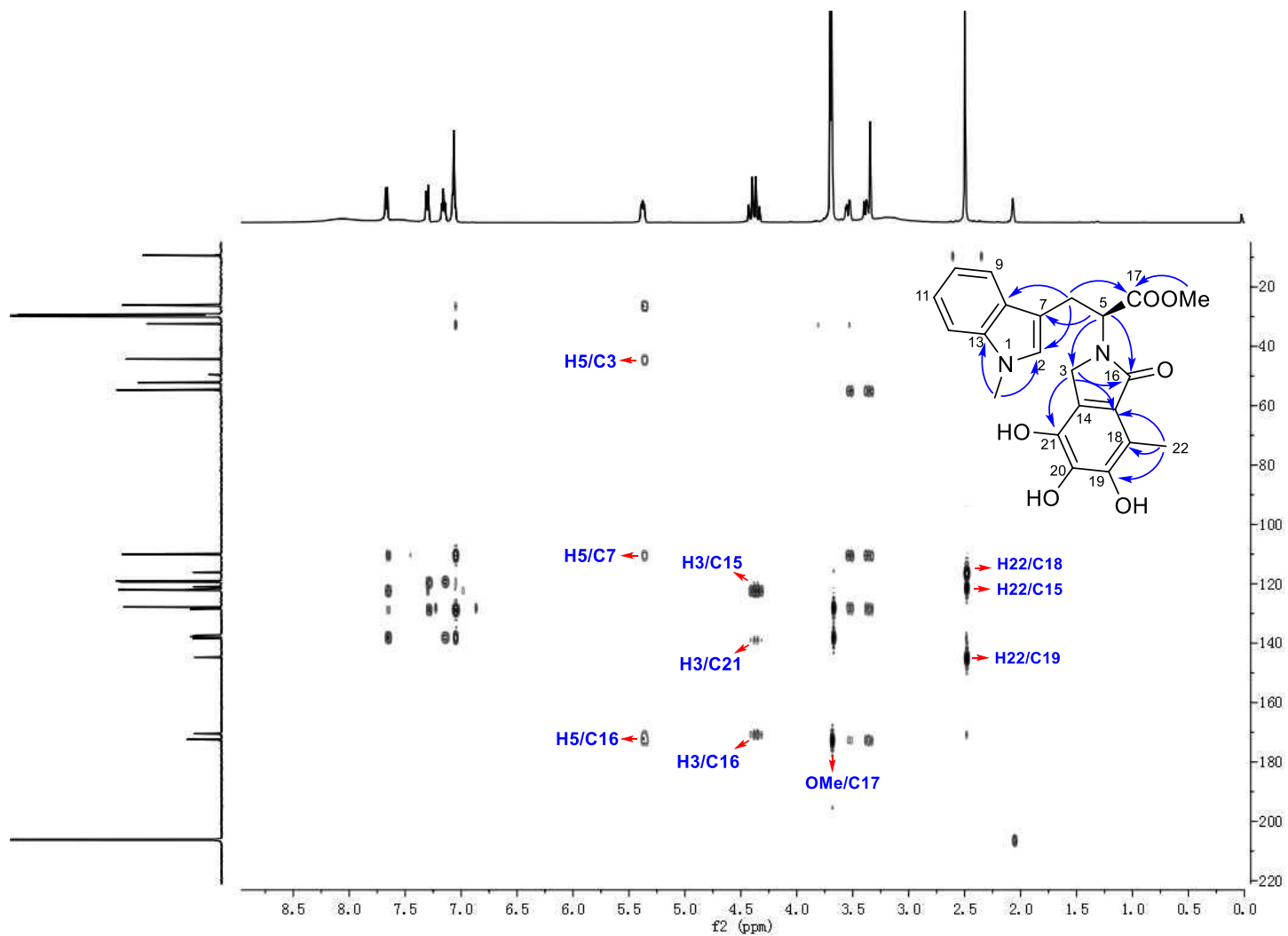


Figure S47. HSQC spectrum of chaetogline D (4) (acetone- d_6 , 400 MHz).



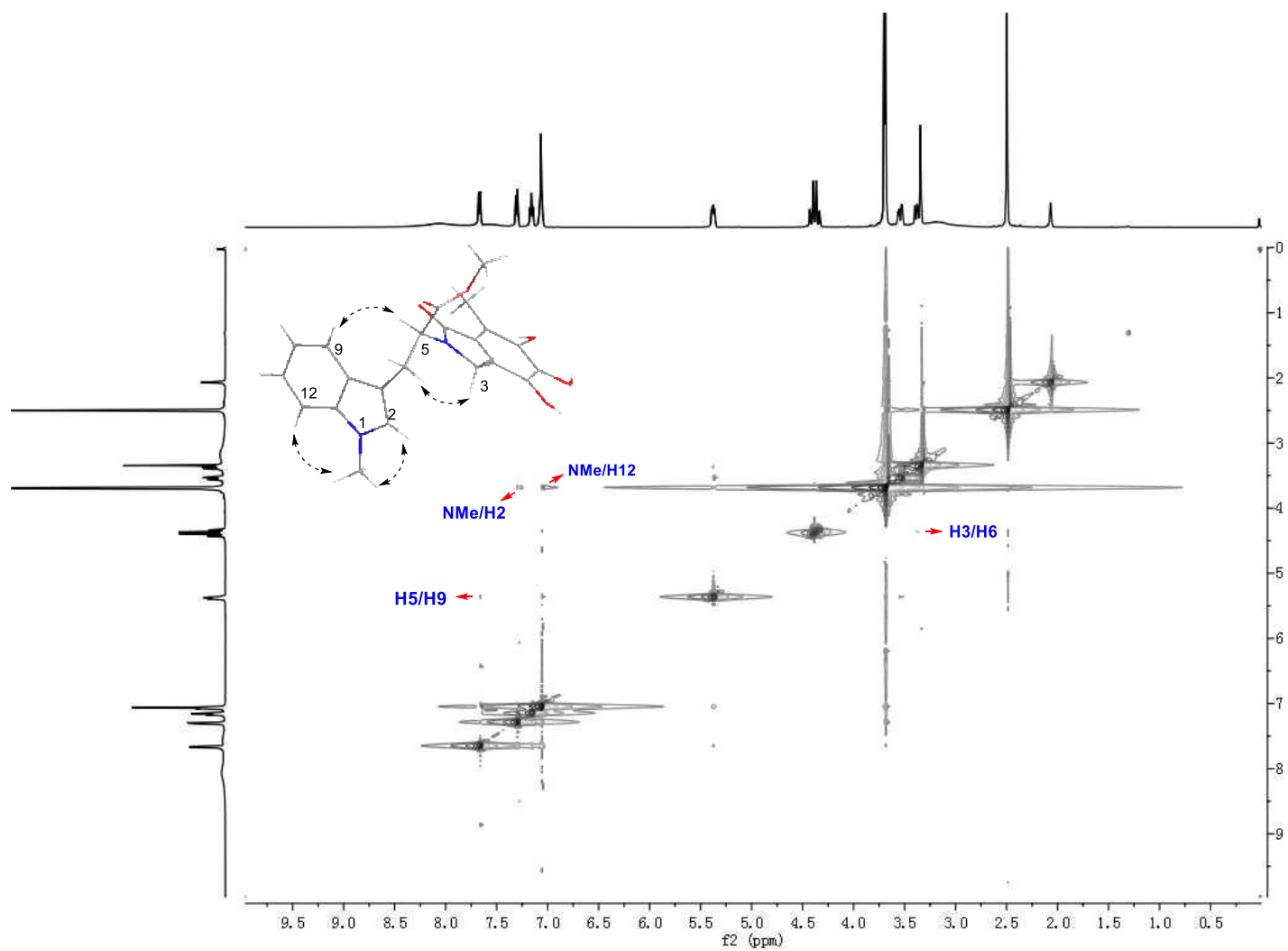


Figure S49. ROESY spectrum of chaetogline D (**4**) (acetone-*d*₆, 400 MHz).

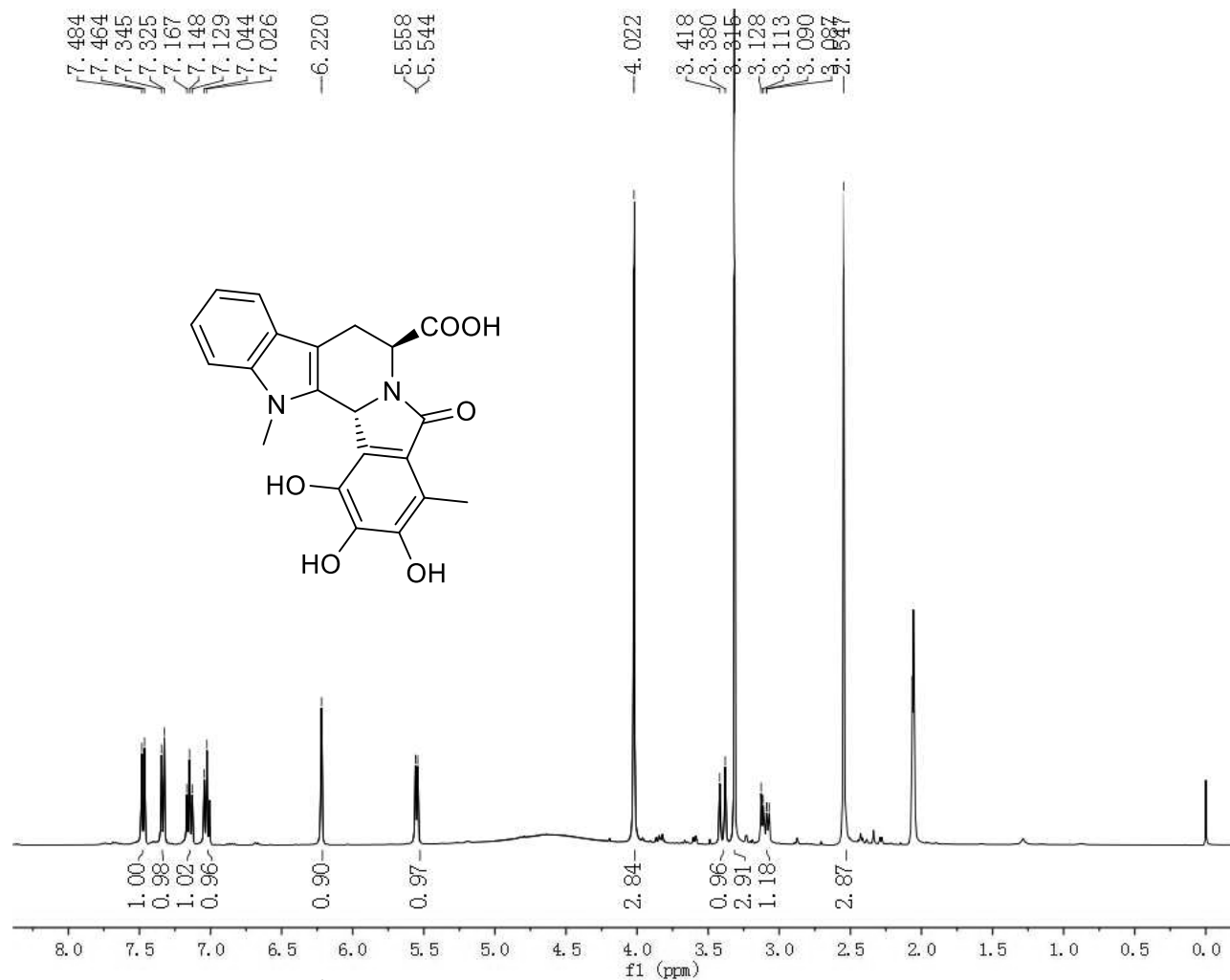


Figure S50. ¹H-NMR spectrum of chaetogline E (**5**) (acetone-*d*₆, 400 MHz).

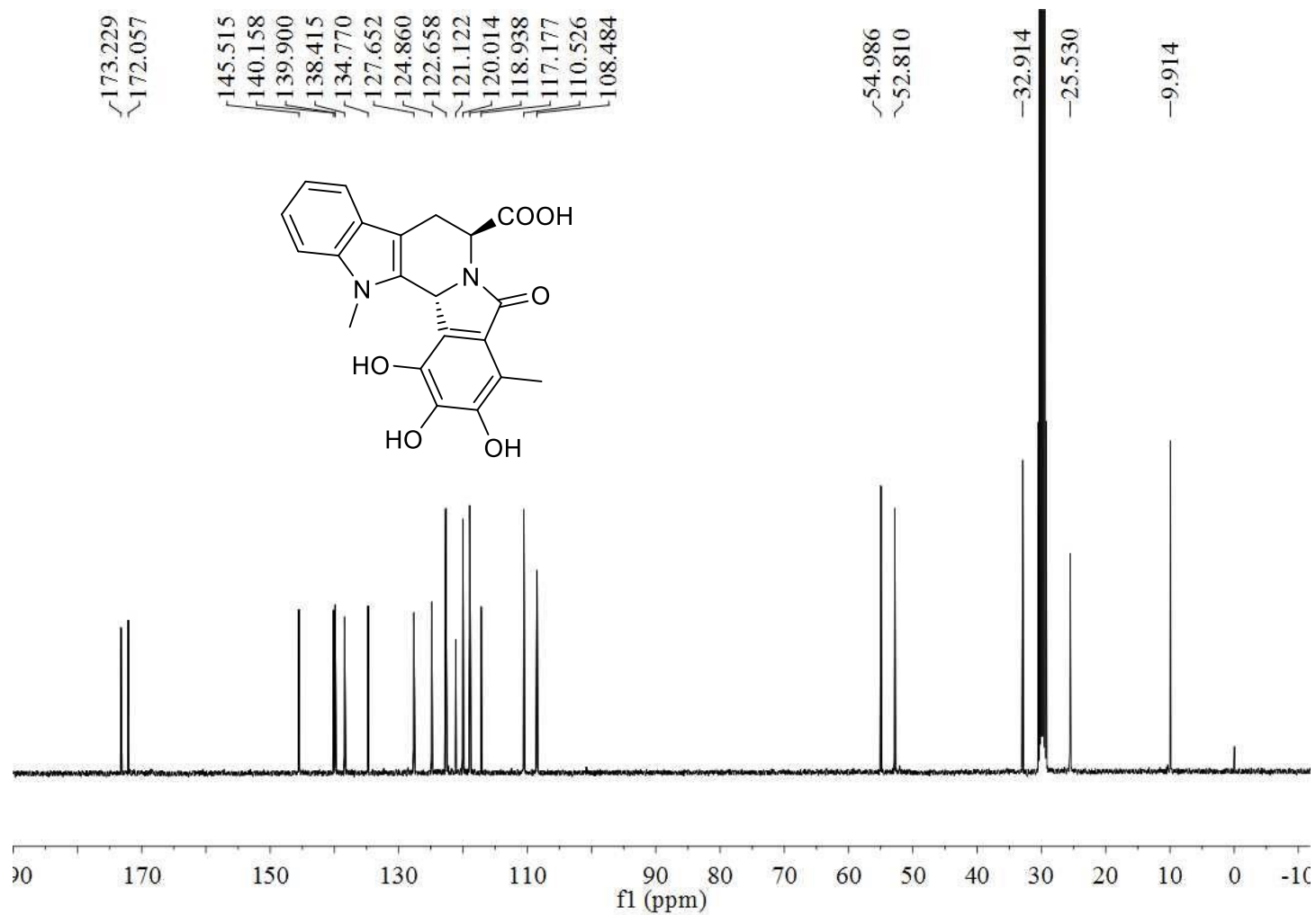


Figure S51. ¹³C-NMR spectrum of chaetogline E (**5**) (acetone-*d*₆, 400 MHz).

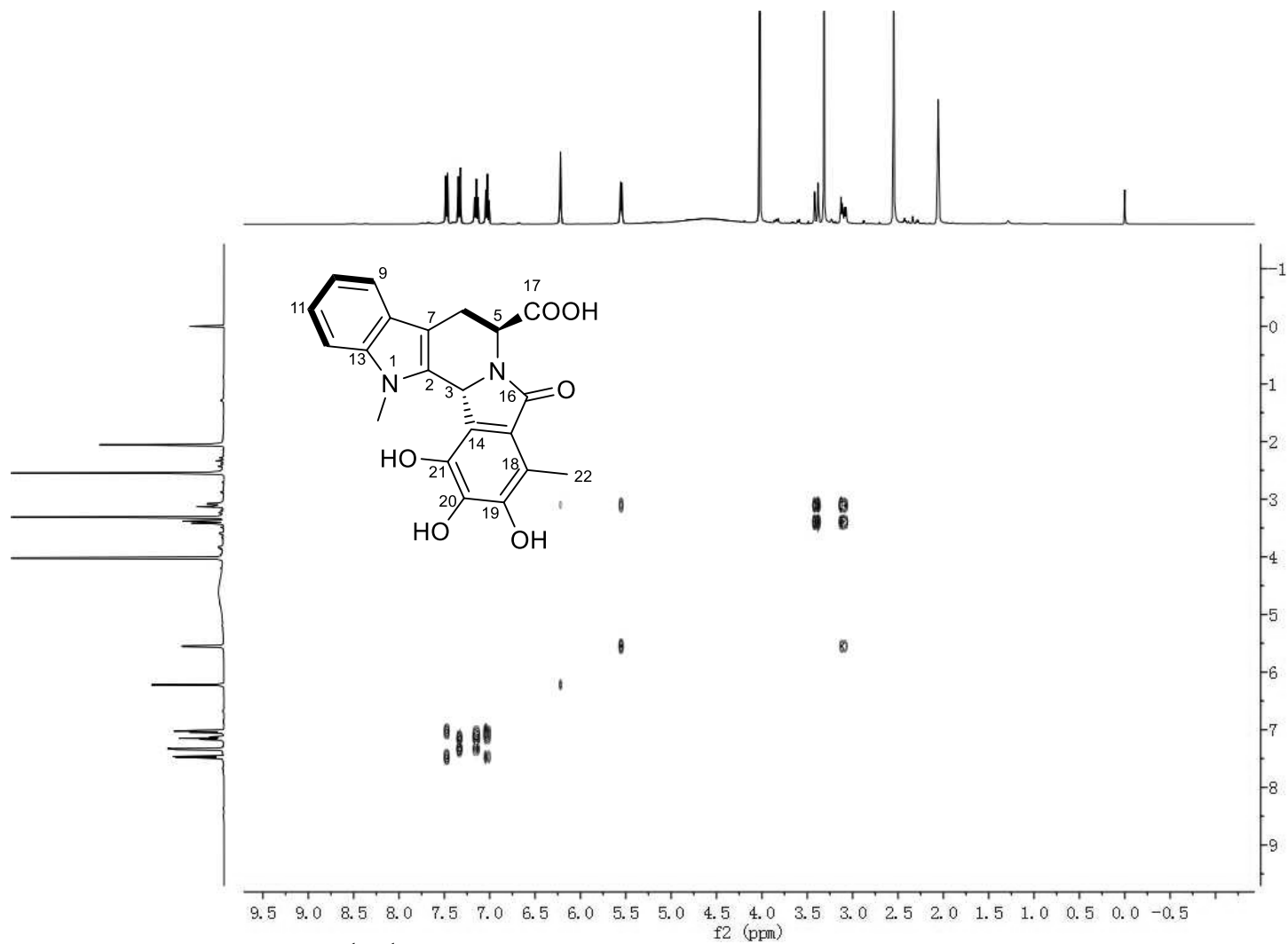


Figure S52. ^1H - ^1H COSY spectrum of chaetogline E (**5**) (acetone- d_6 , 400 MHz).

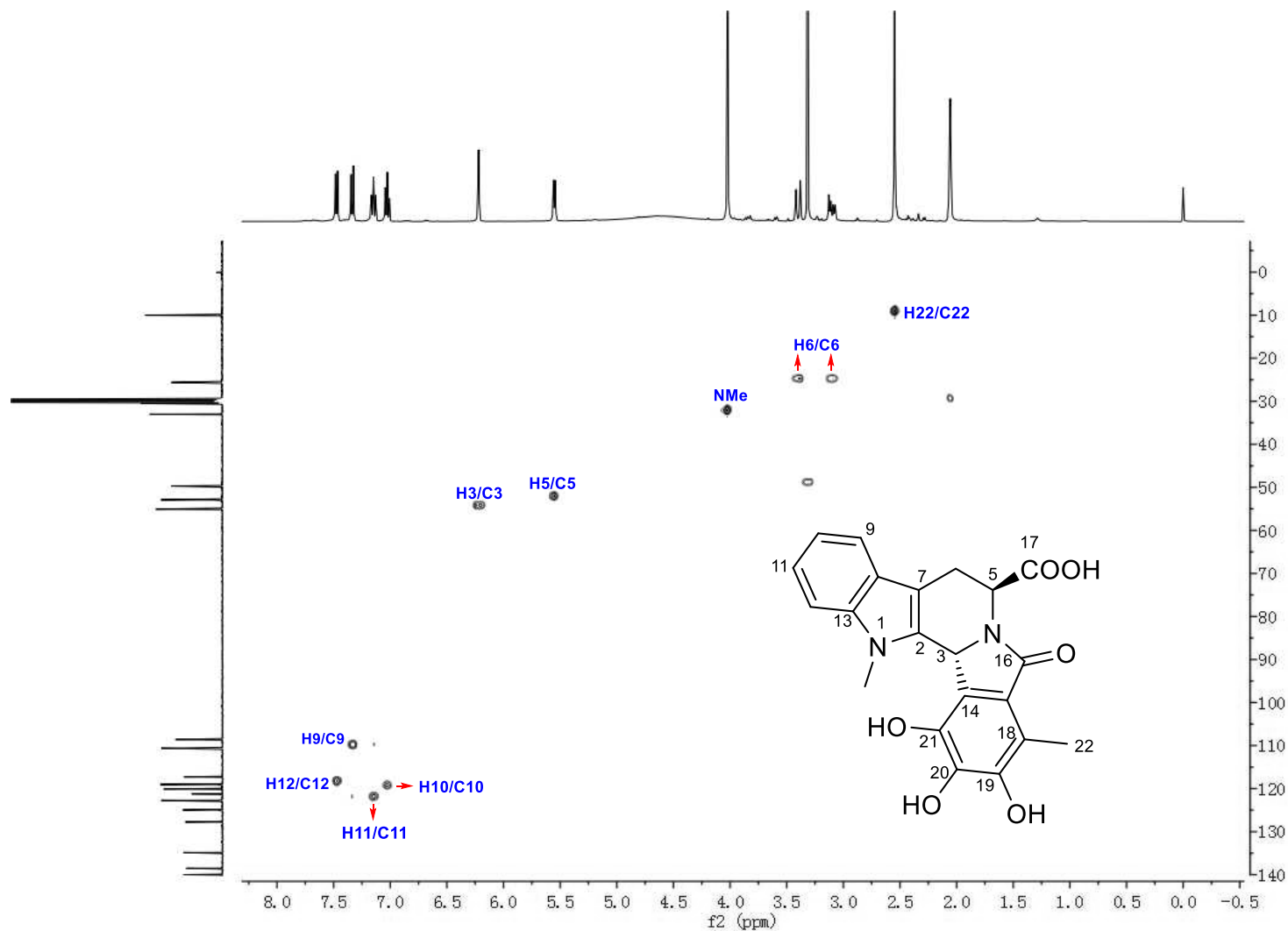


Figure S53. HSQC spectrum of chaetogline E (**5**) (acetone-*d*₆, 400 MHz).

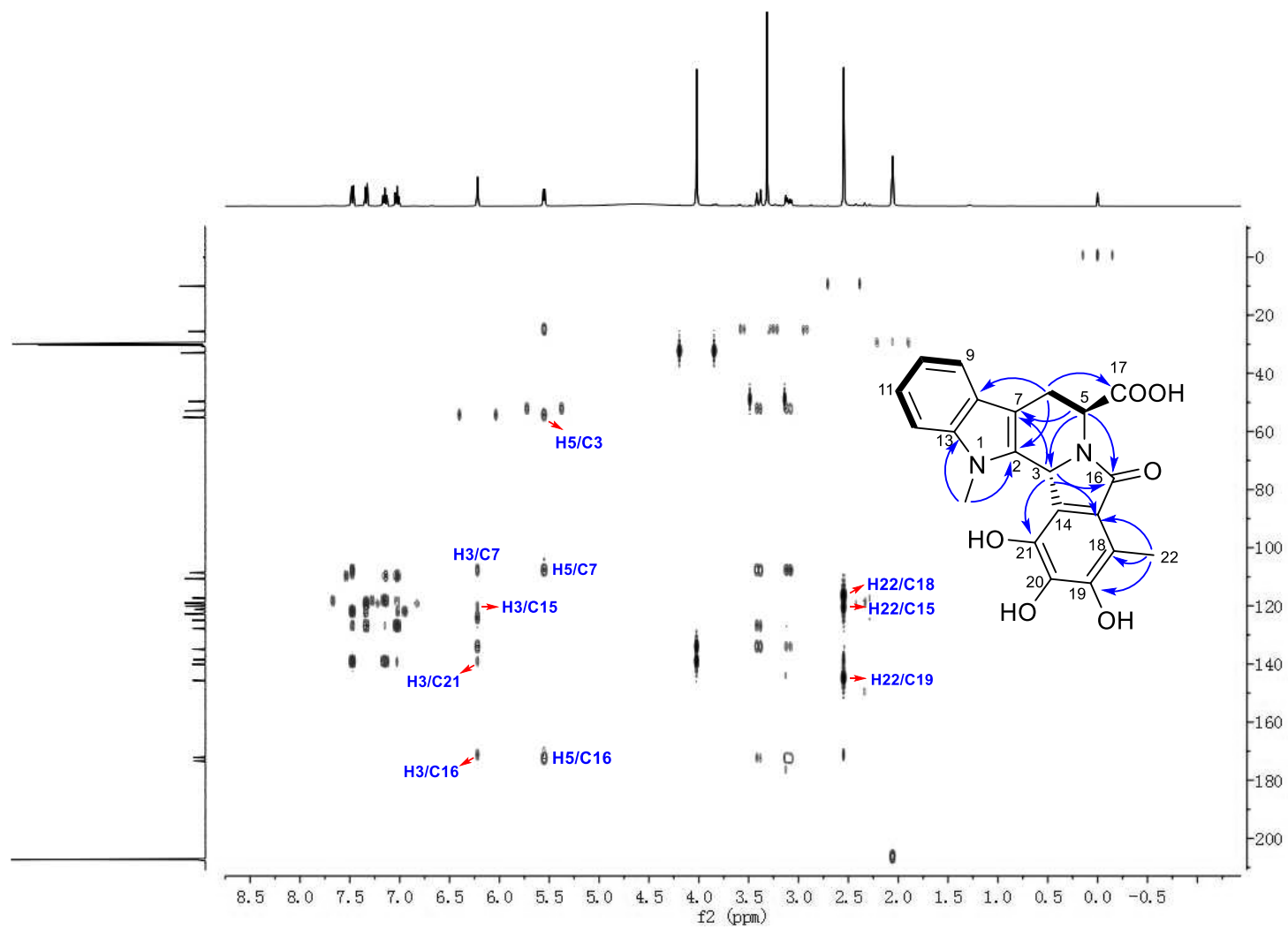


Figure S54. HMBC spectrum of chaetogline E (**5**) (acetone- d_6 , 400 MHz).

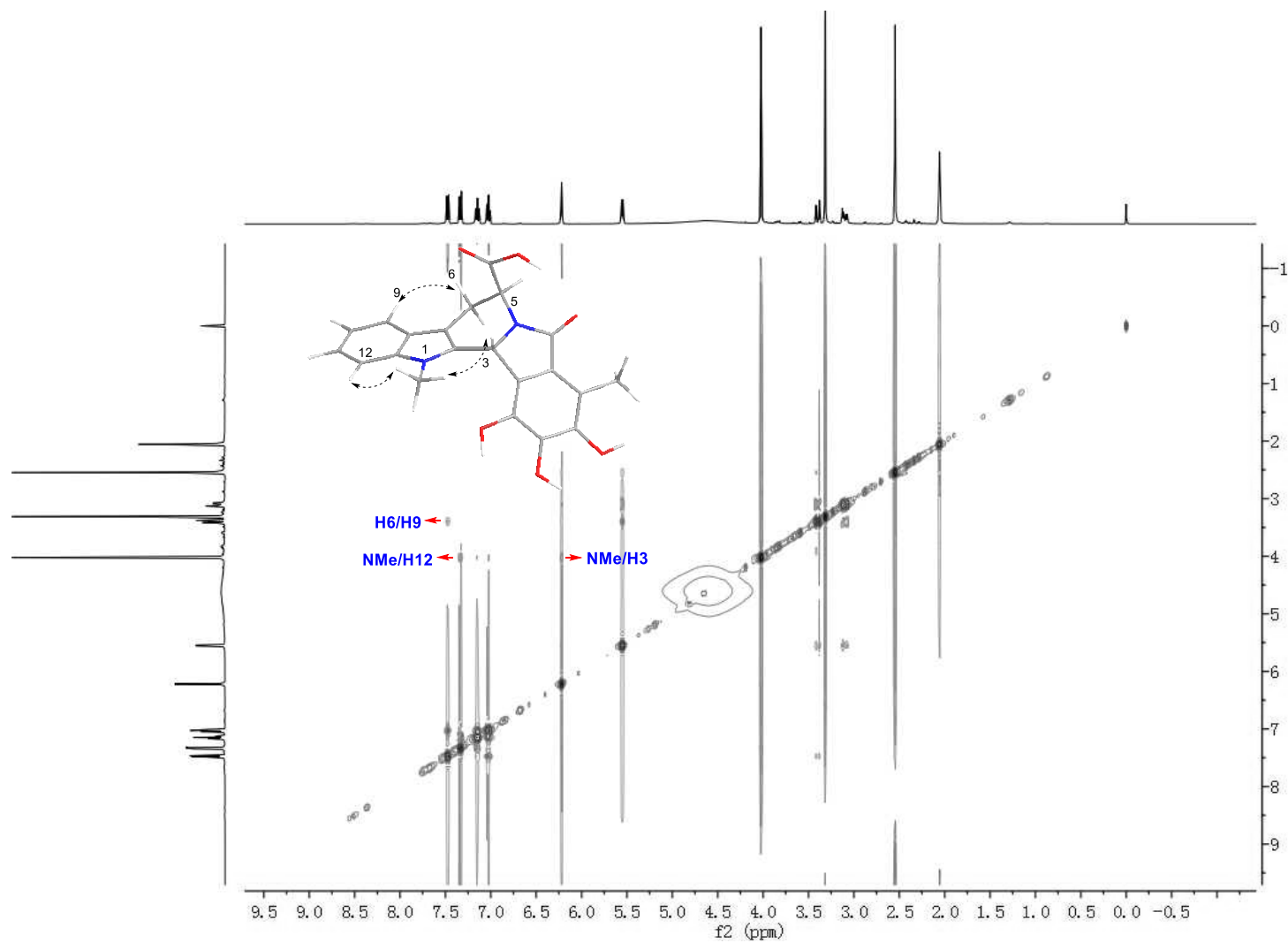


Figure S55. NOESY spectrum of chaetogline E (**5**) (acetone- d_6 , 400 MHz).

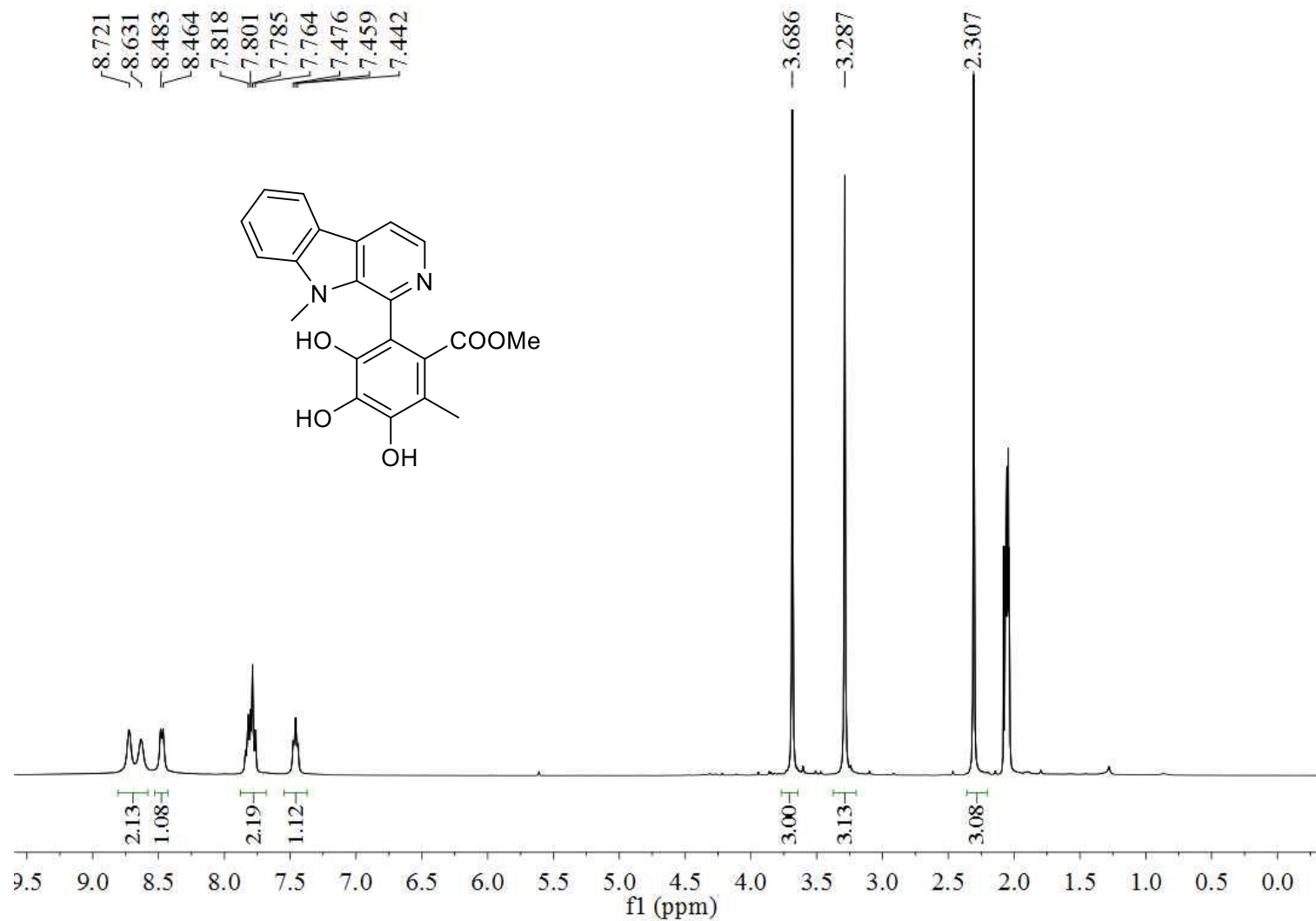


Figure S56. ¹H-NMR spectrum of chaetogline F (**6**) (acetone-*d*₆, 400 MHz).

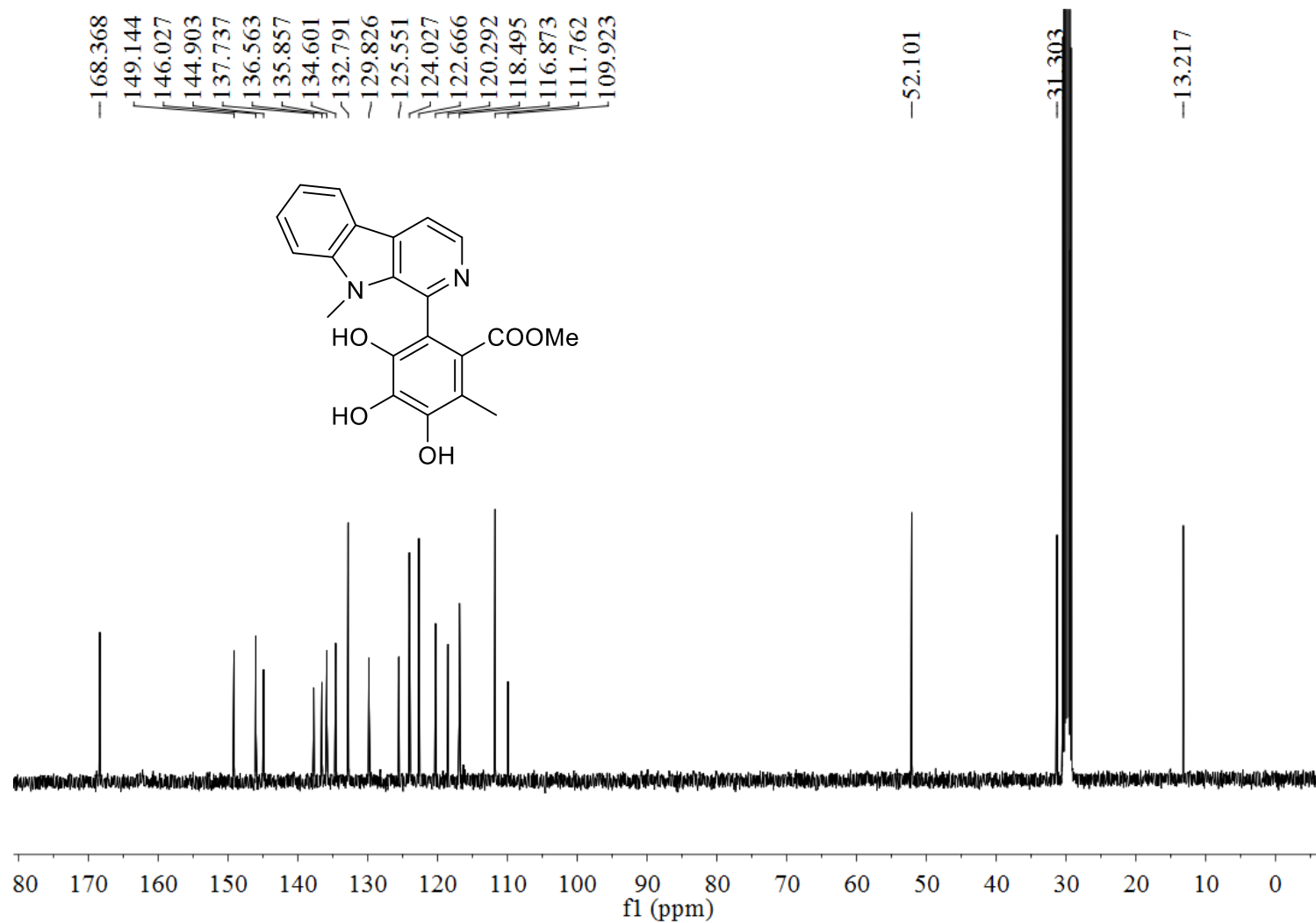


Figure S57. ^{13}C -NMR spectrum of chaetogline F (**6**) (acetone- d_6 , 400 MHz).

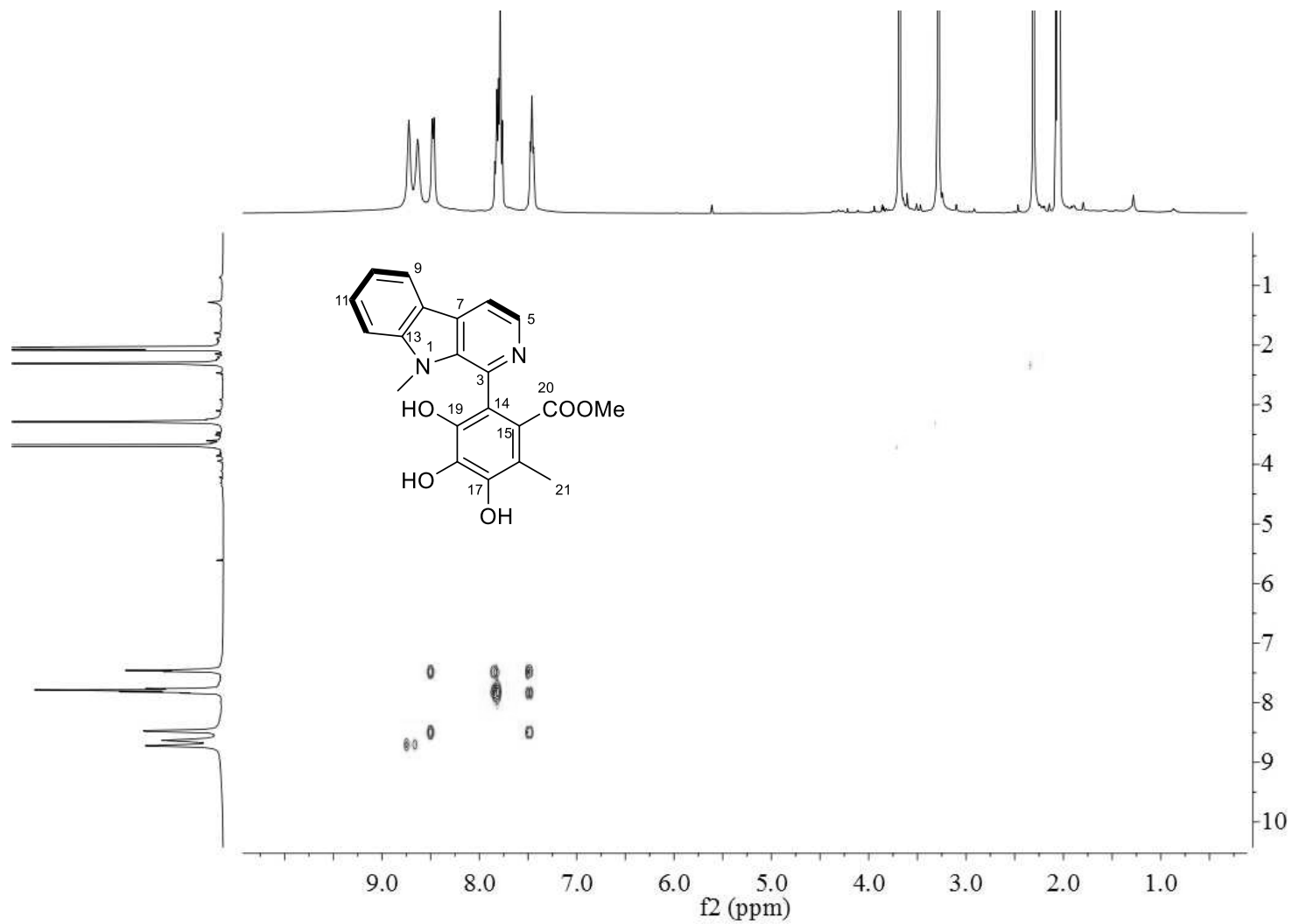


Figure S58. ^1H - ^1H COSY spectrum of chaetogline F (**6**) (acetone- d_6 , 400 MHz).

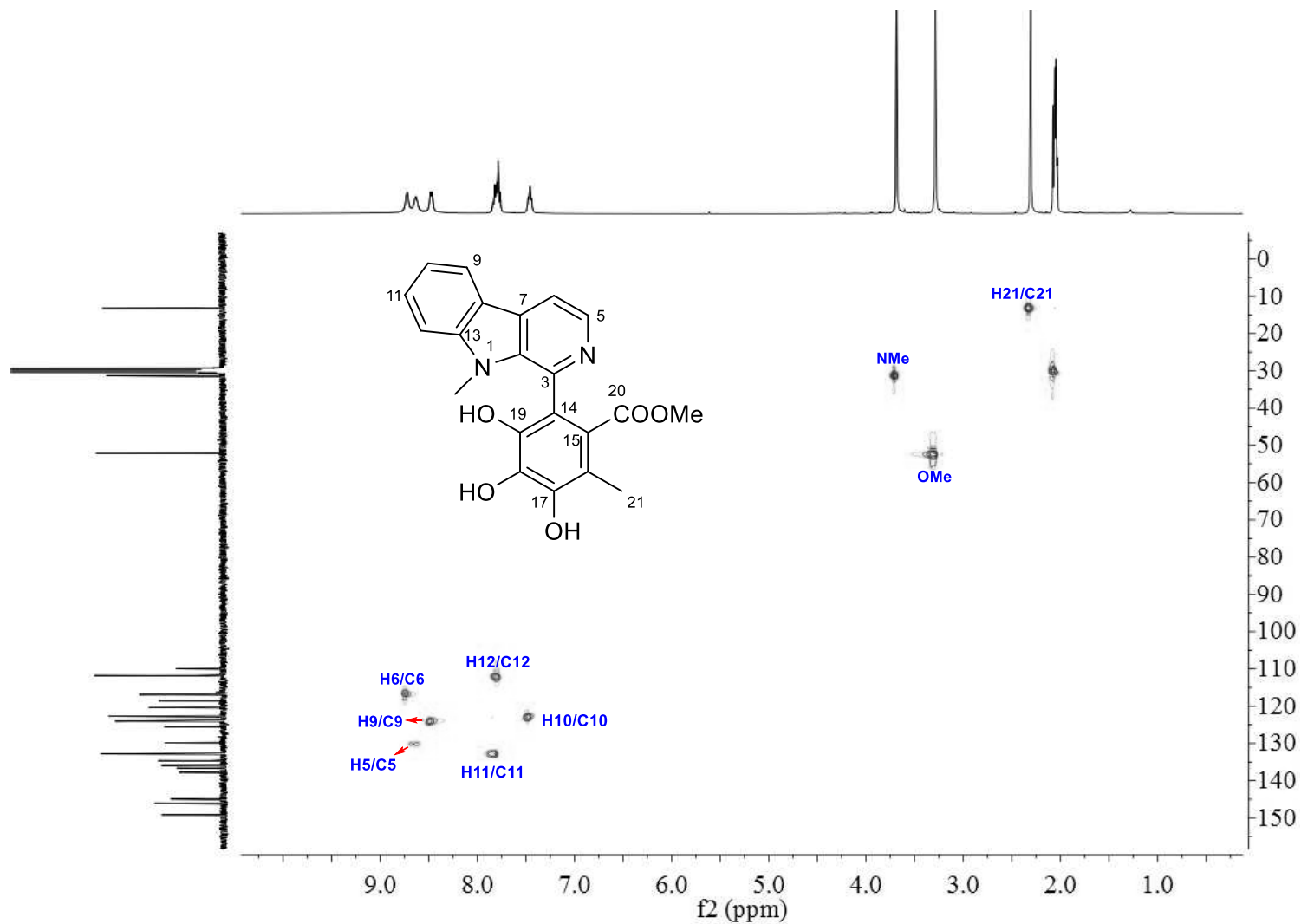


Figure S59. HSQC spectrum of chaetogline F (**6**) (acetone-*d*₆, 400 MHz).

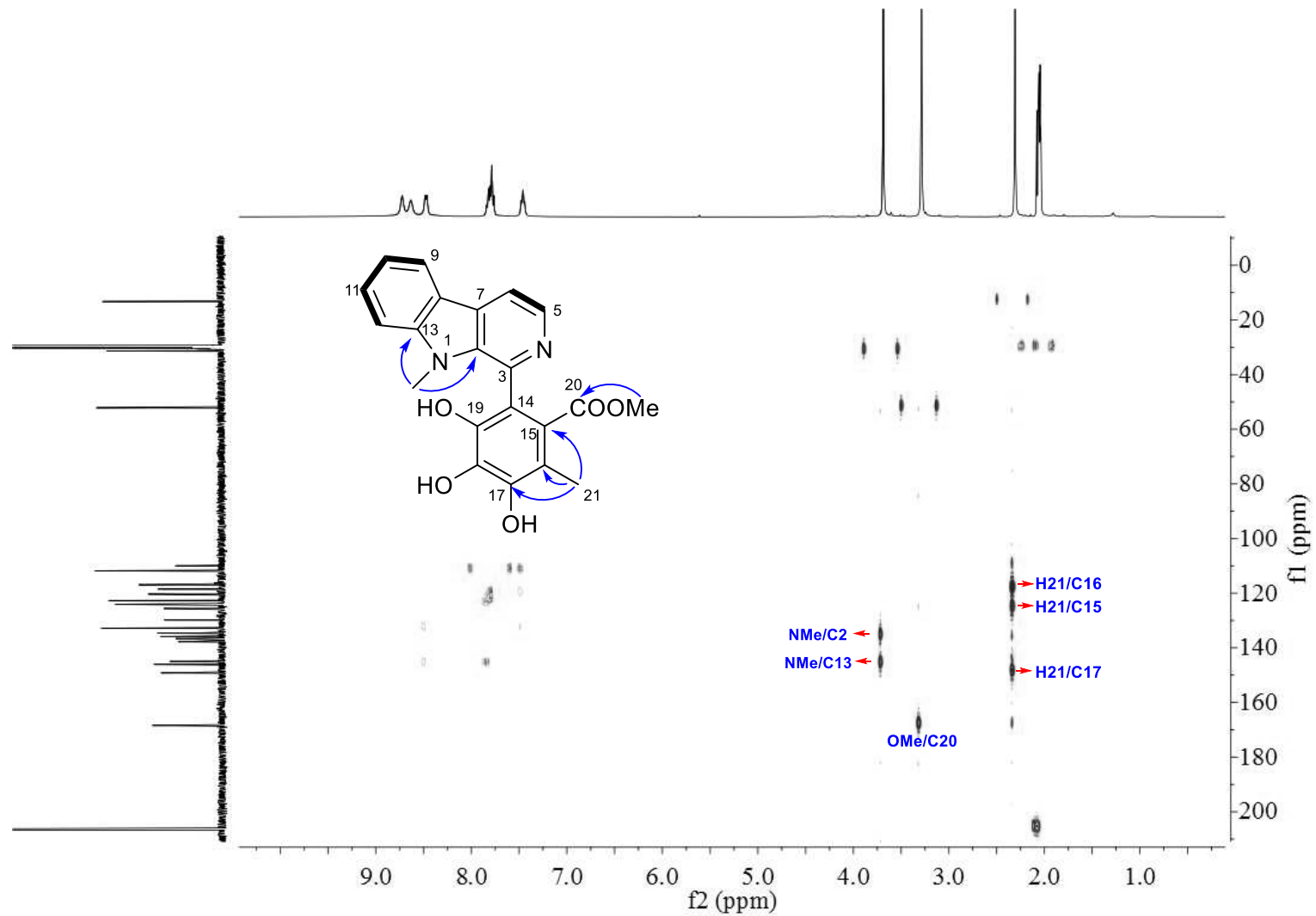


Figure S60. HMBC spectrum of chaetogline F (6) (acetone- d_6 , 400 MHz).

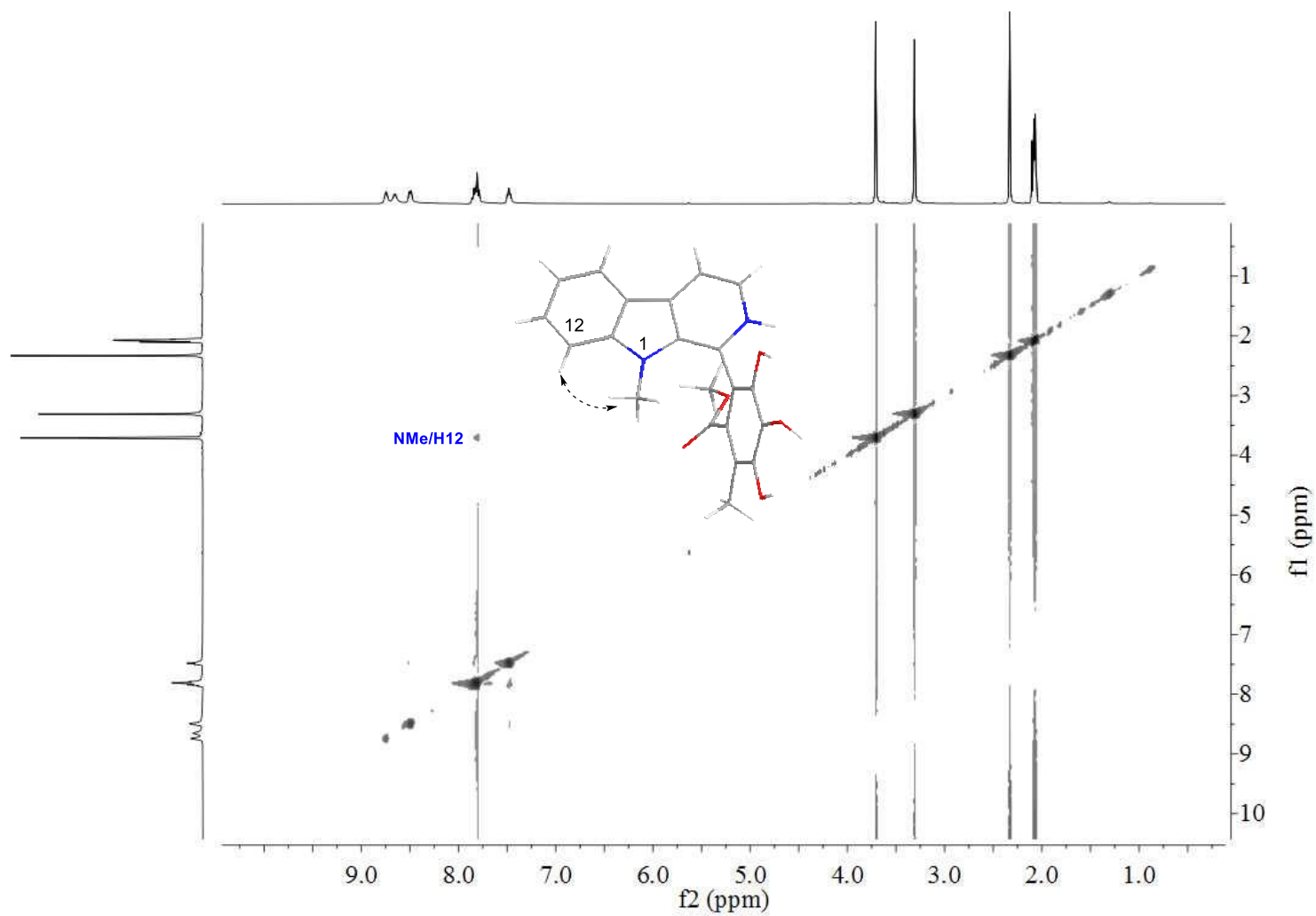


Figure S61. ROESY spectrum of chaetogline F (**6**) (acetone-*d*₆, 400 MHz).

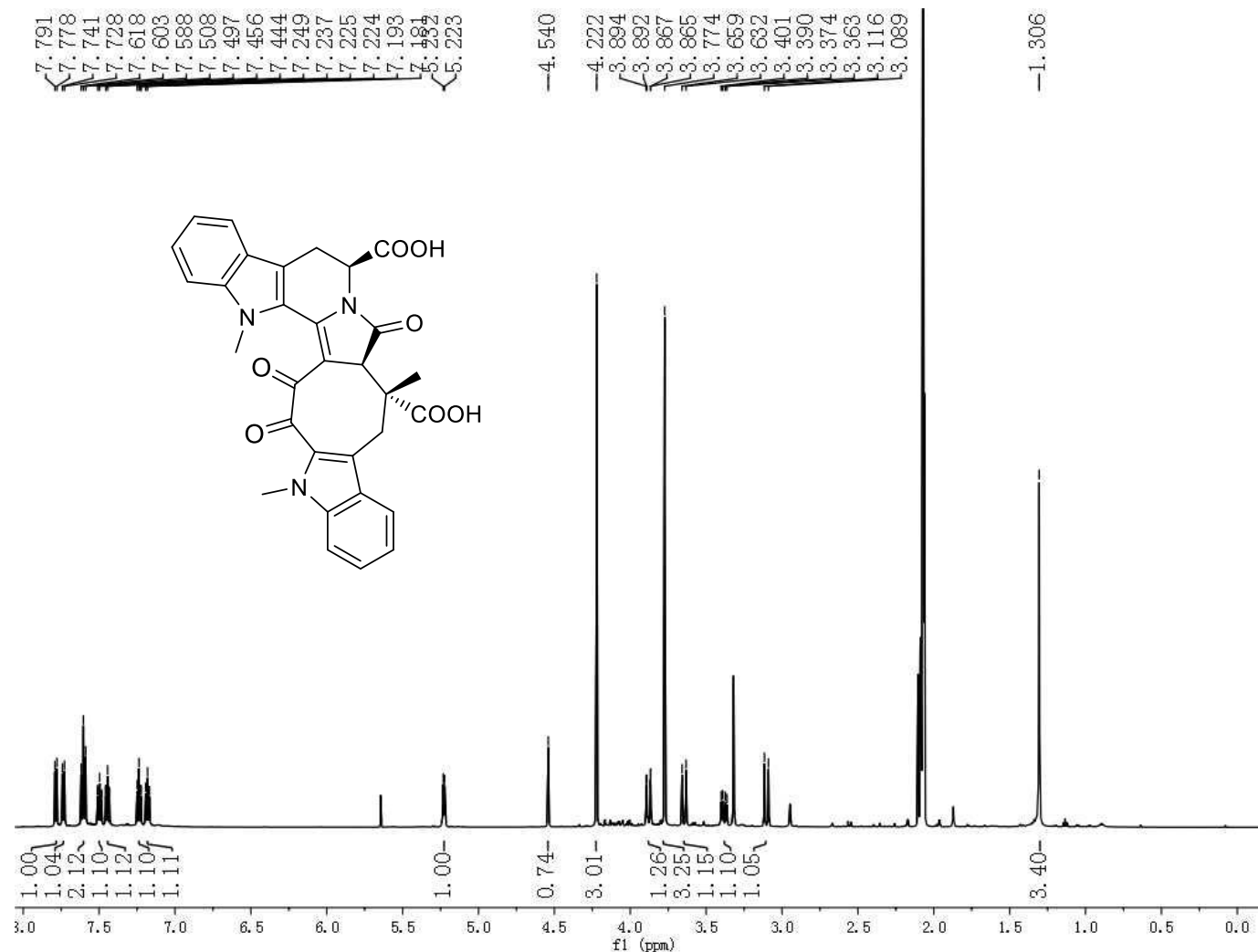


Figure S62. $^1\text{H-NMR}$ spectrum of chaetogline G (**7**) (acetone- d_6 , 600 MHz).

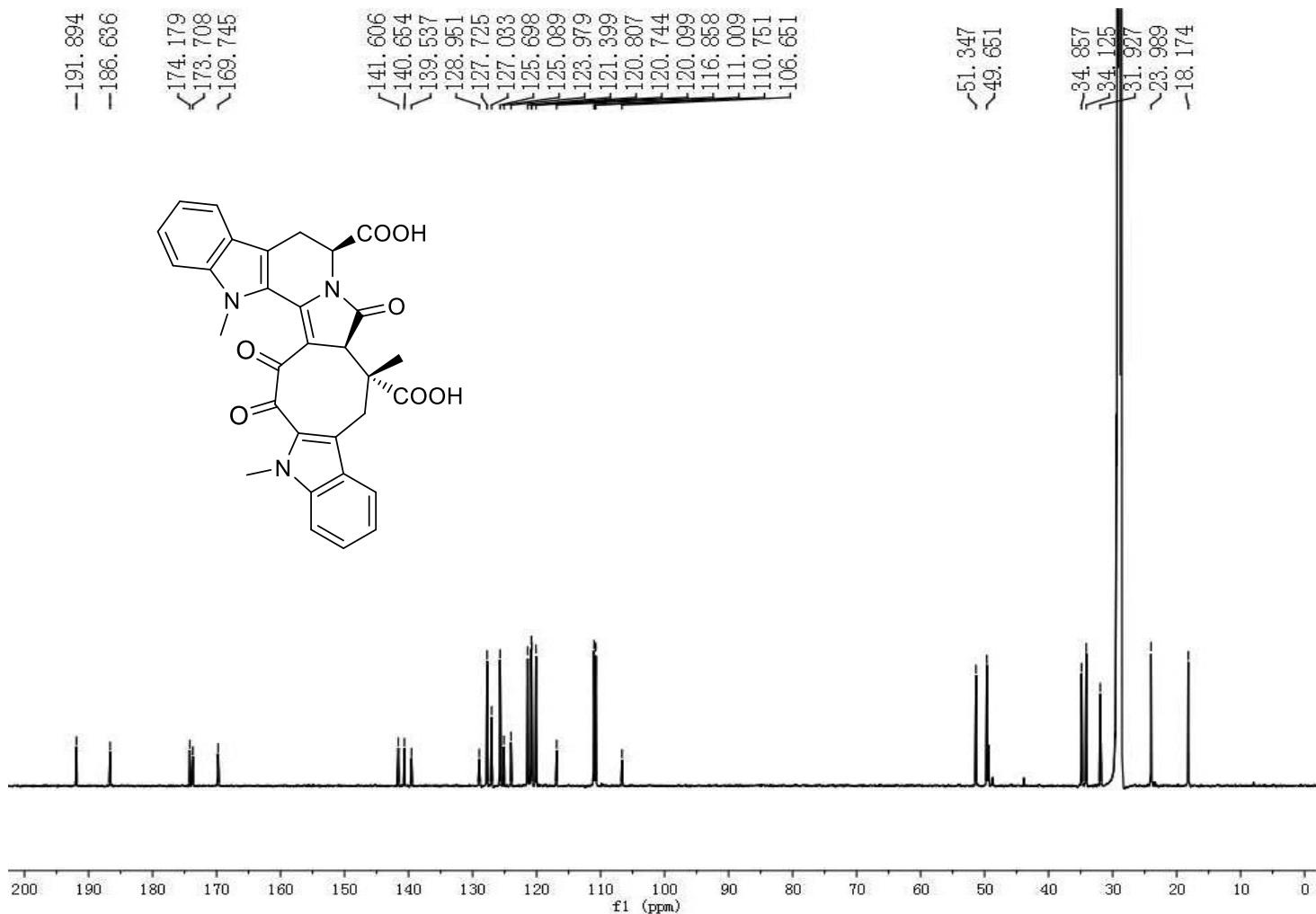


Figure S63. ¹³C-NMR spectrum of chaetogline G (**7**) (acetone-*d*₆, 600 MHz).

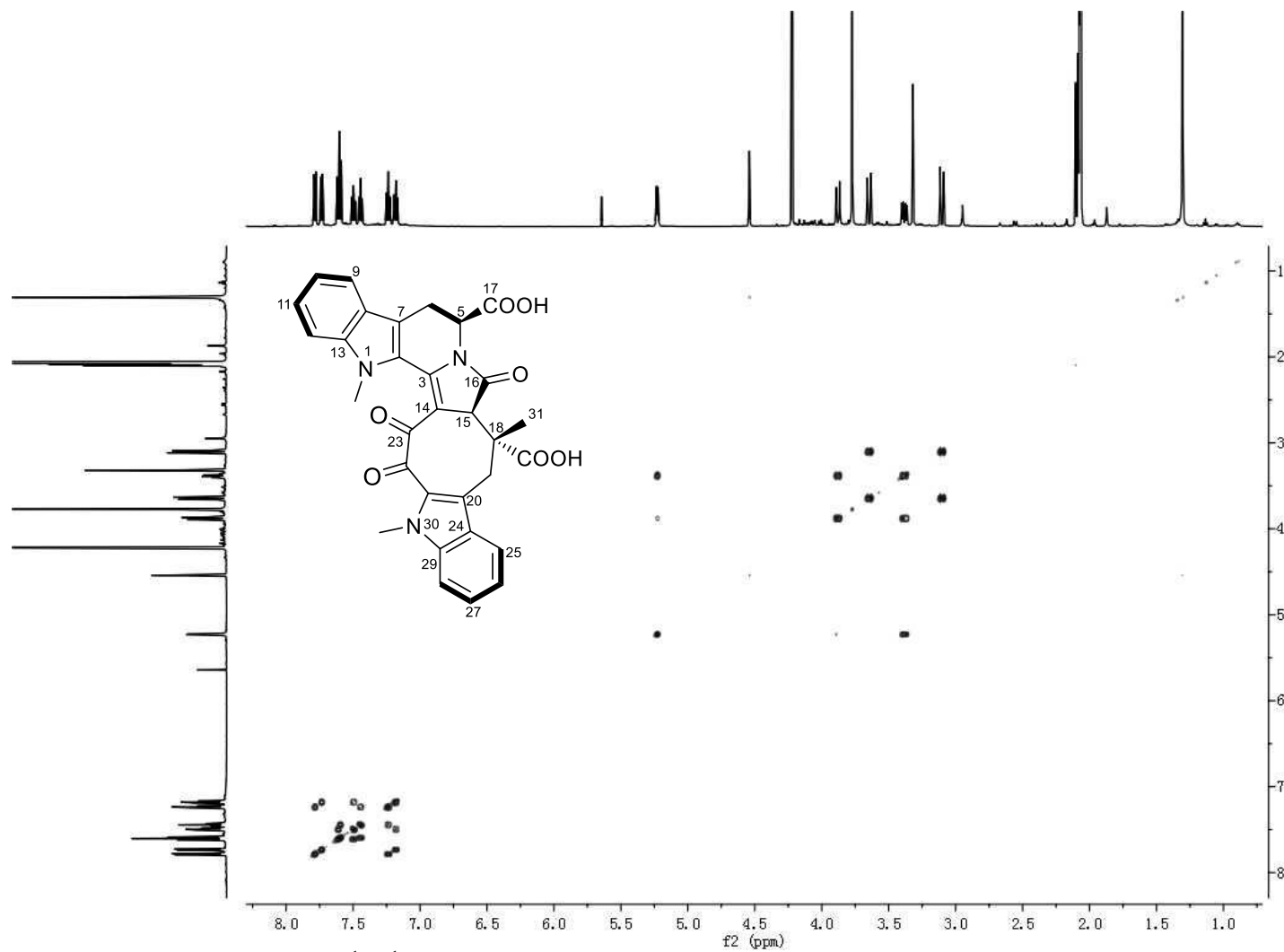


Figure S64. ^1H - ^1H COSY spectrum of chaetogline G (7) (acetone- d_6 , 600 MHz).

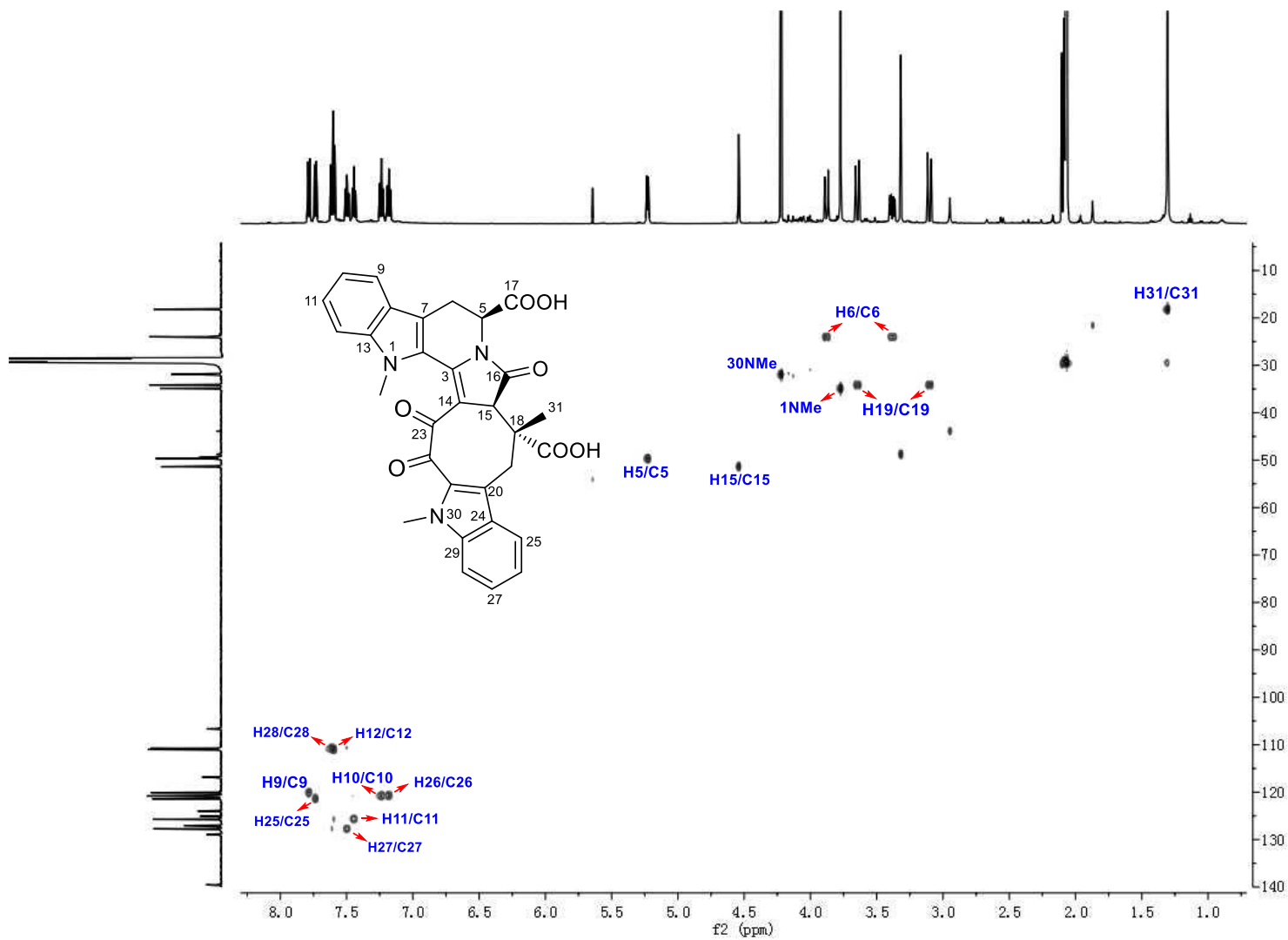


Figure S65. HSQC spectrum of chaetogline G (7) (acetone- d_6 , 600 MHz).

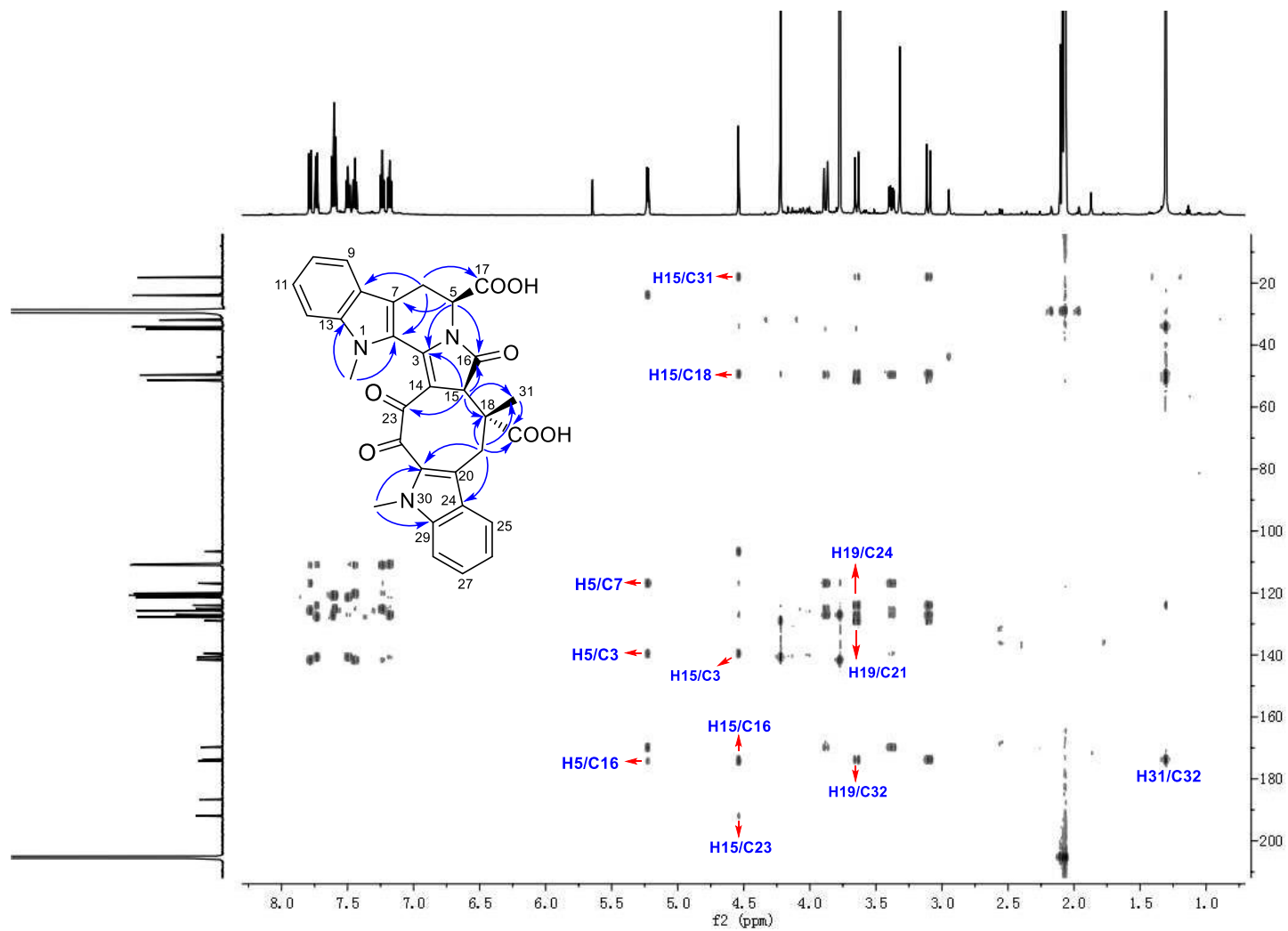
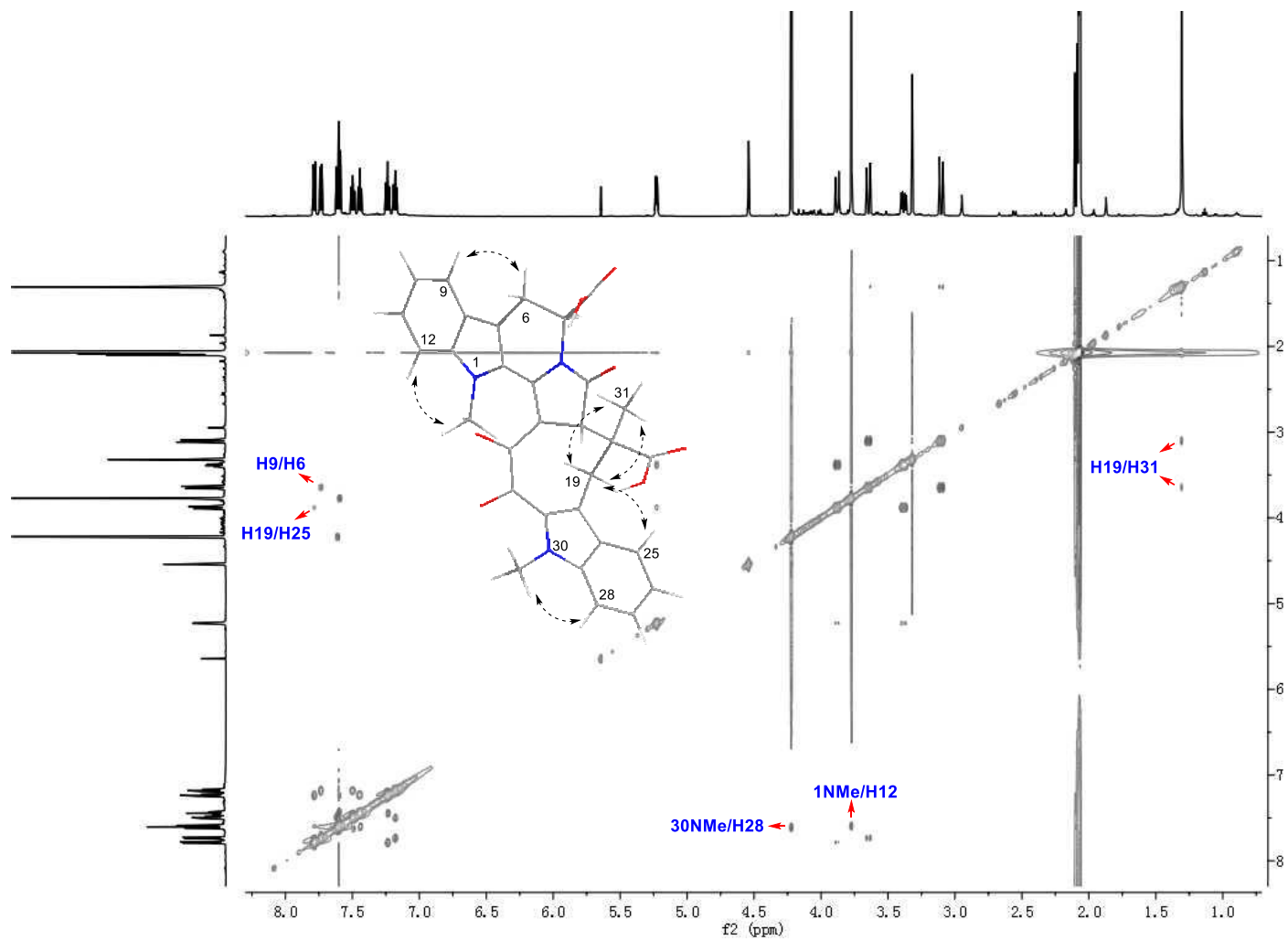
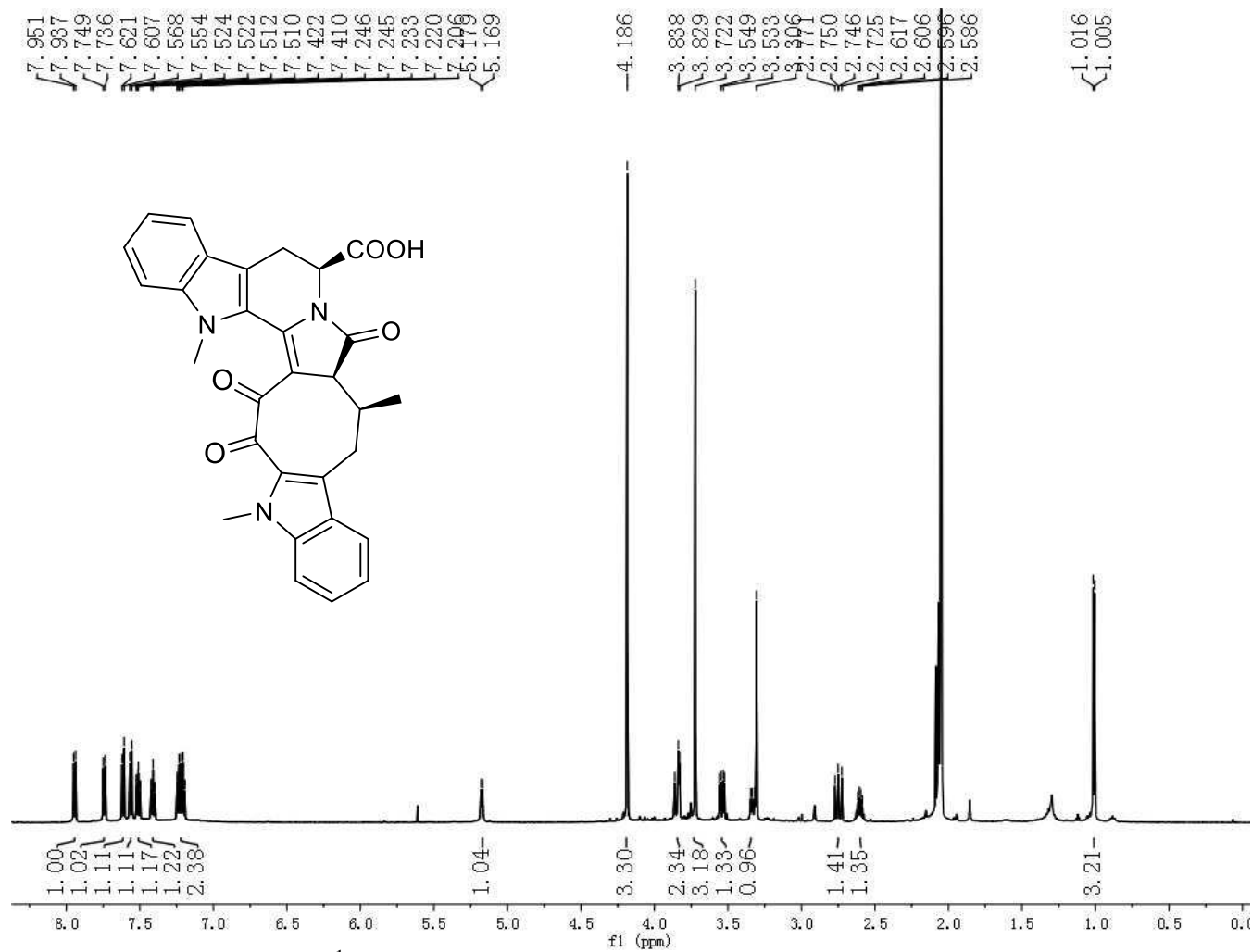


Figure S66. HMBC spectrum of chaetogline G (**7**) (acetone- d_6 , 600 MHz).





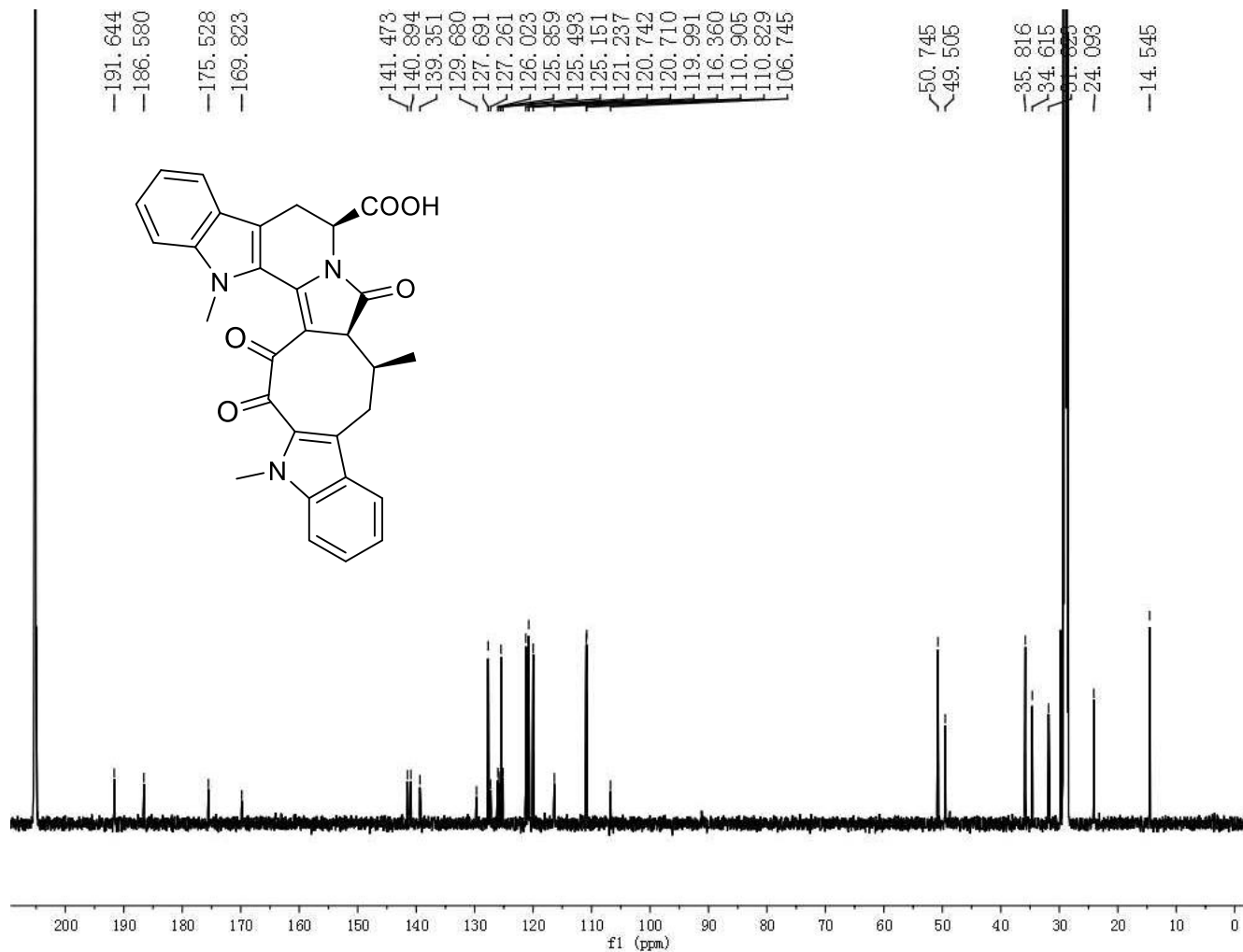


Figure S69. ^{13}C -NMR spectrum of chaetogline H (**8**) (acetone- d_6 , 600 MHz).

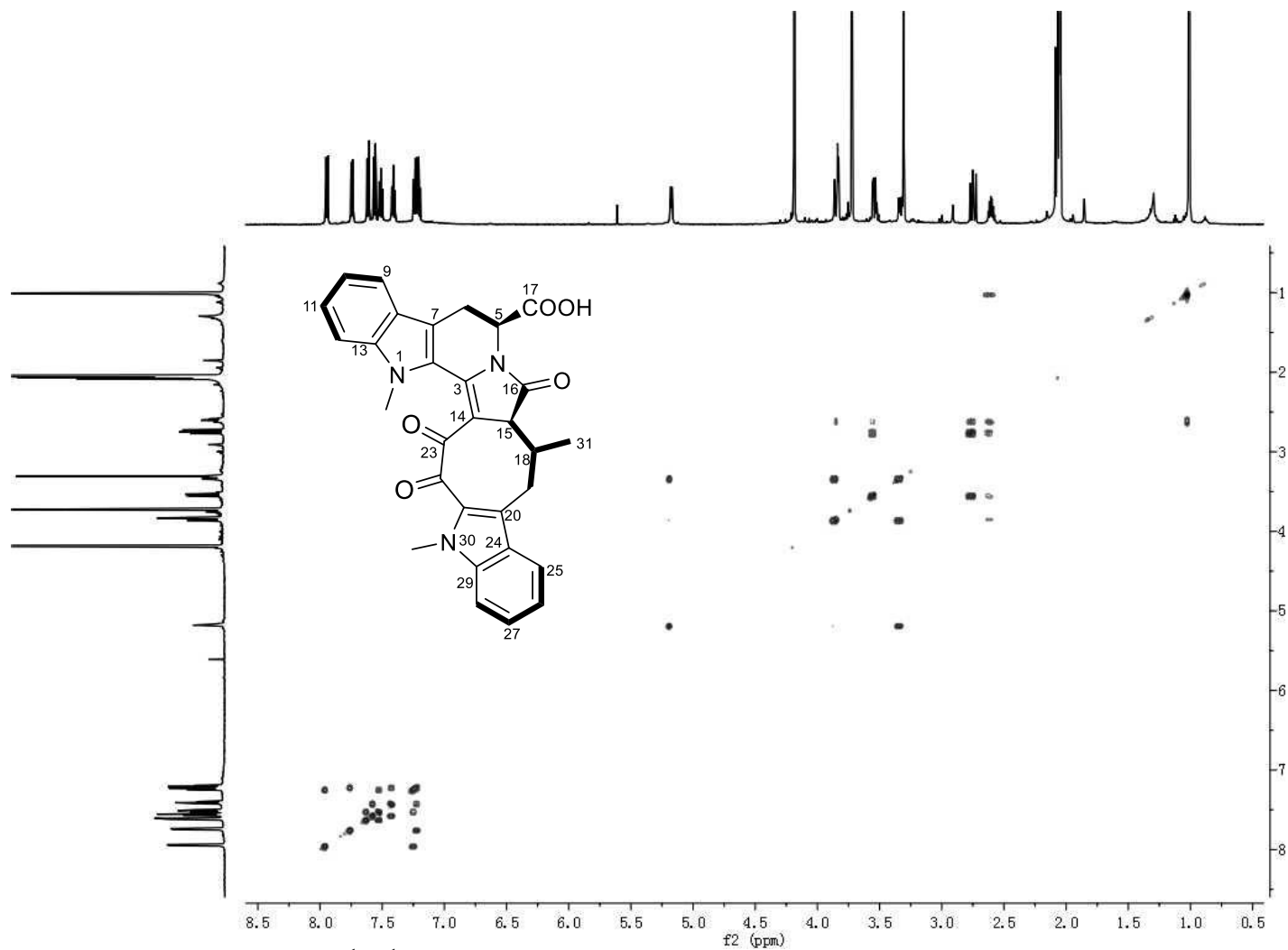


Figure S70. ^1H - ^1H COSY spectrum of chaetogline H (**8**) (acetone- d_6 , 600 MHz).

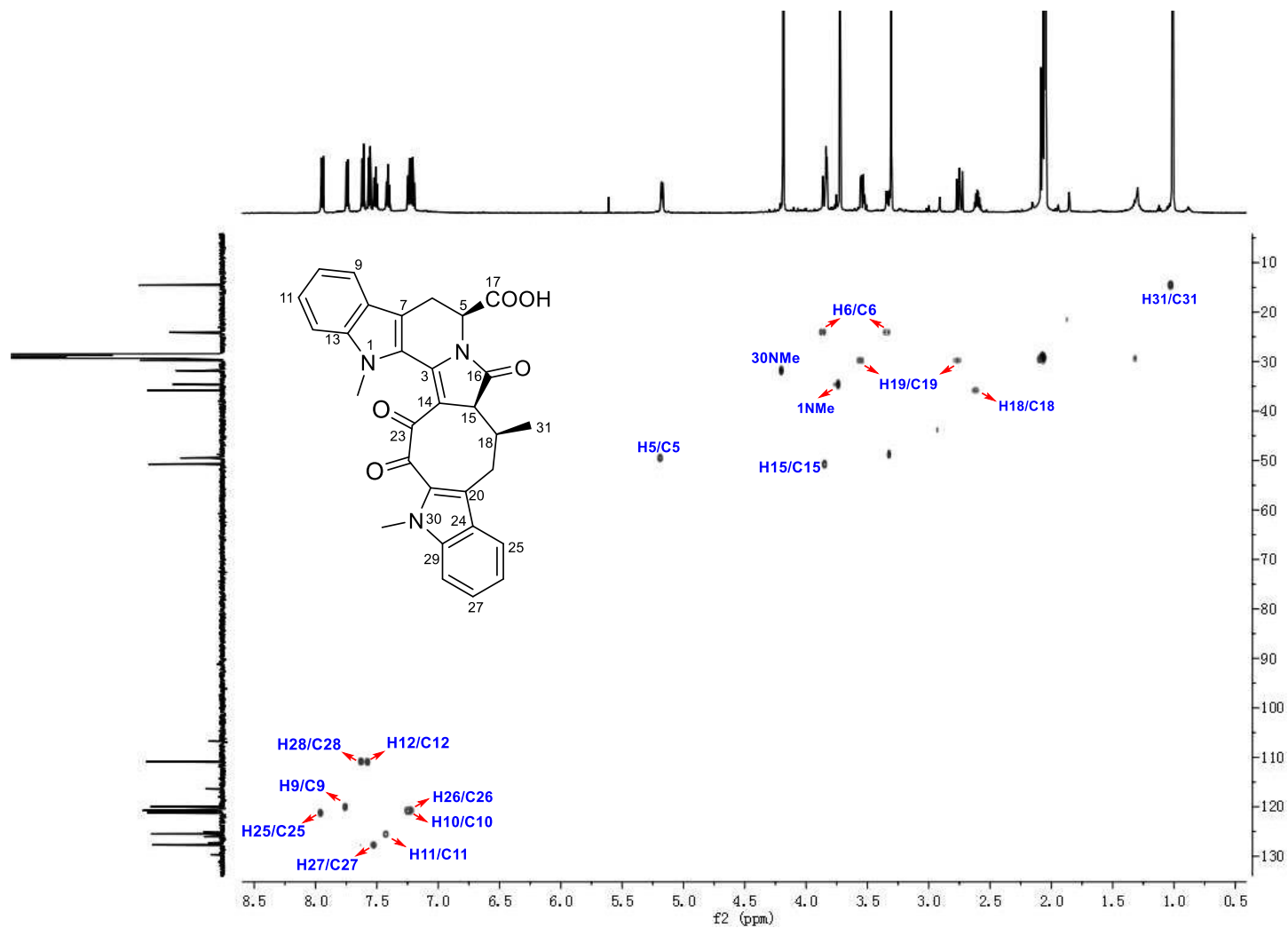


Figure S71. HSQC spectrum of chaetogline H (**8**) (acetone-*d*₆, 600 MHz).

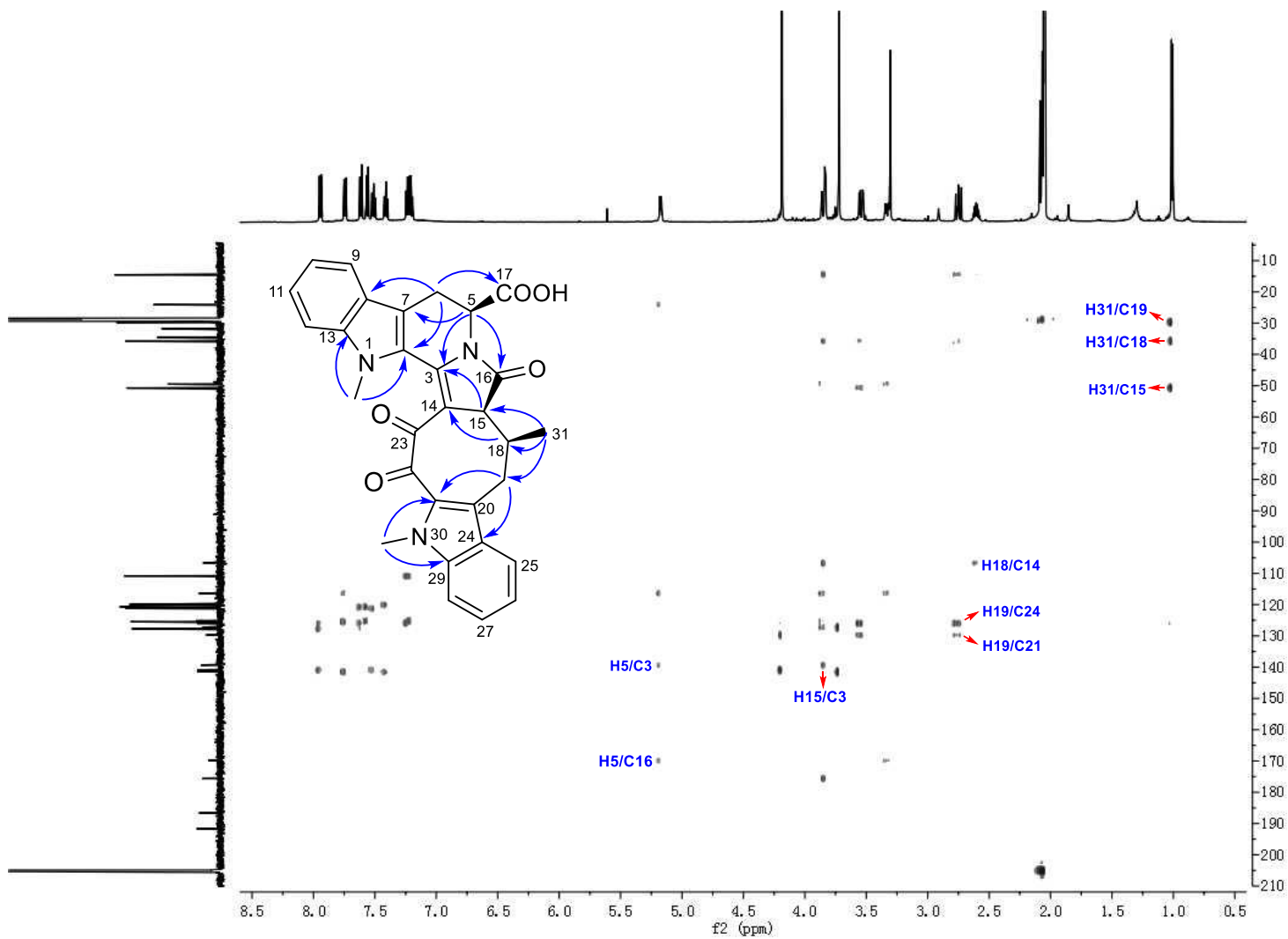


Figure S72. HMBC spectrum of chaetogline H (**8**) (acetone-*d*₆, 600 MHz).

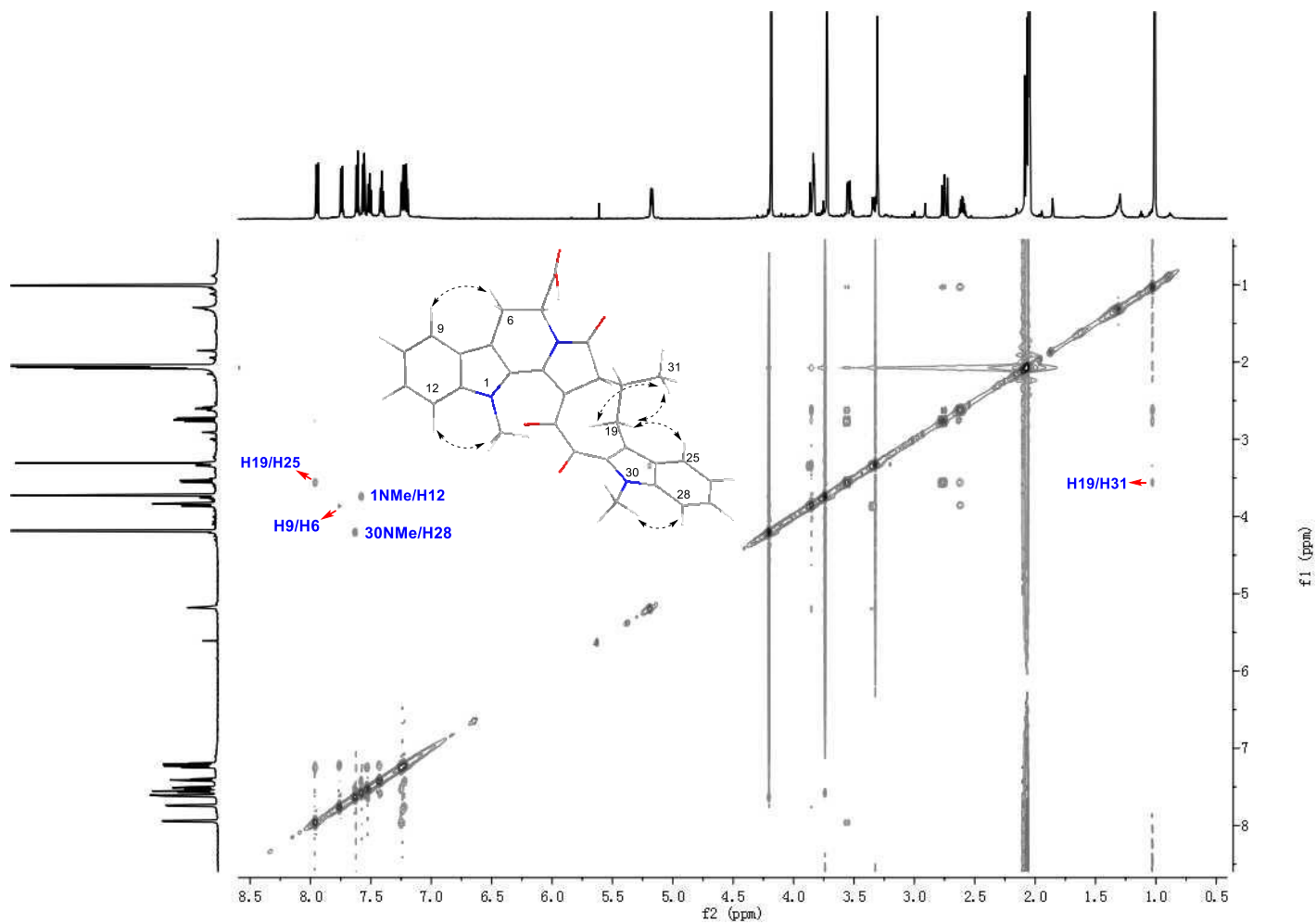


Figure S73. ROESY spectrum of chaetogline H (**8**) (acetone- d_6 , 600 MHz).

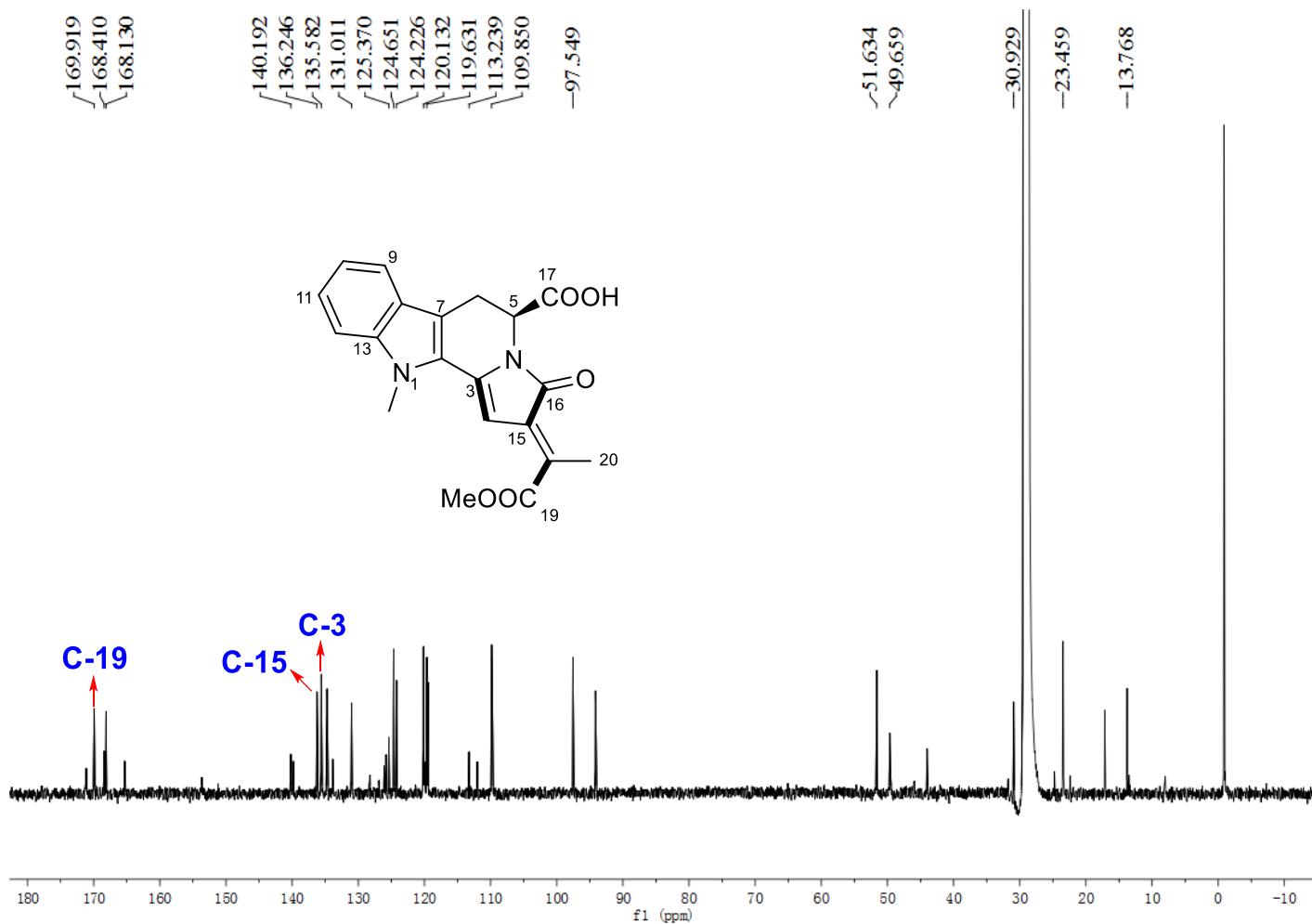


Figure S74. ^{13}C -NMR spectrum of **1a** generated by feeding sodium $[1-^{13}\text{C}]$ acetate (acetone- d_6 , 600 MHz).

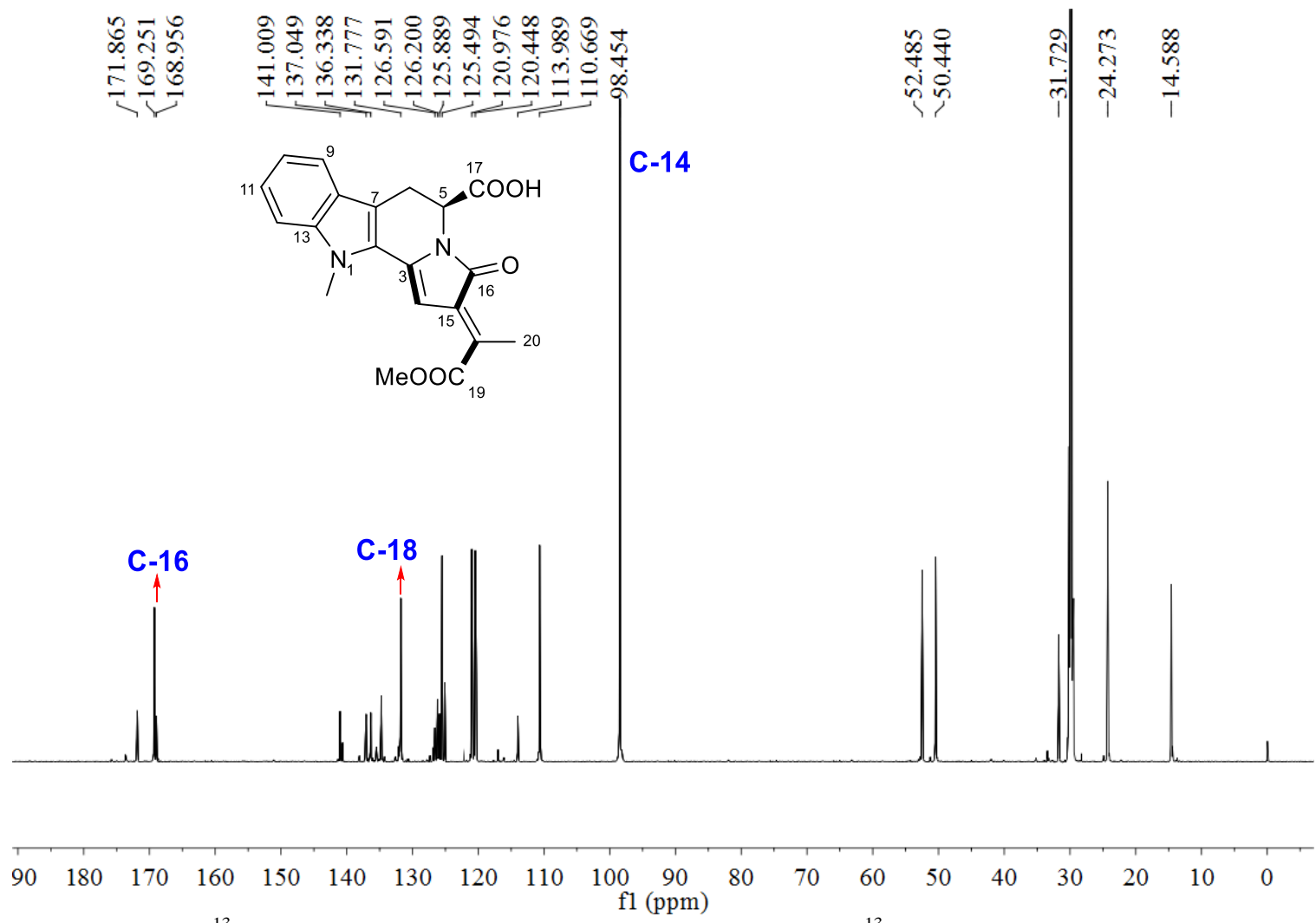


Figure S75. ¹³C-NMR spectrum of **1b** generated by feeding sodium [2-¹³C]acetate (acetone-*d*₆, 600 MHz).

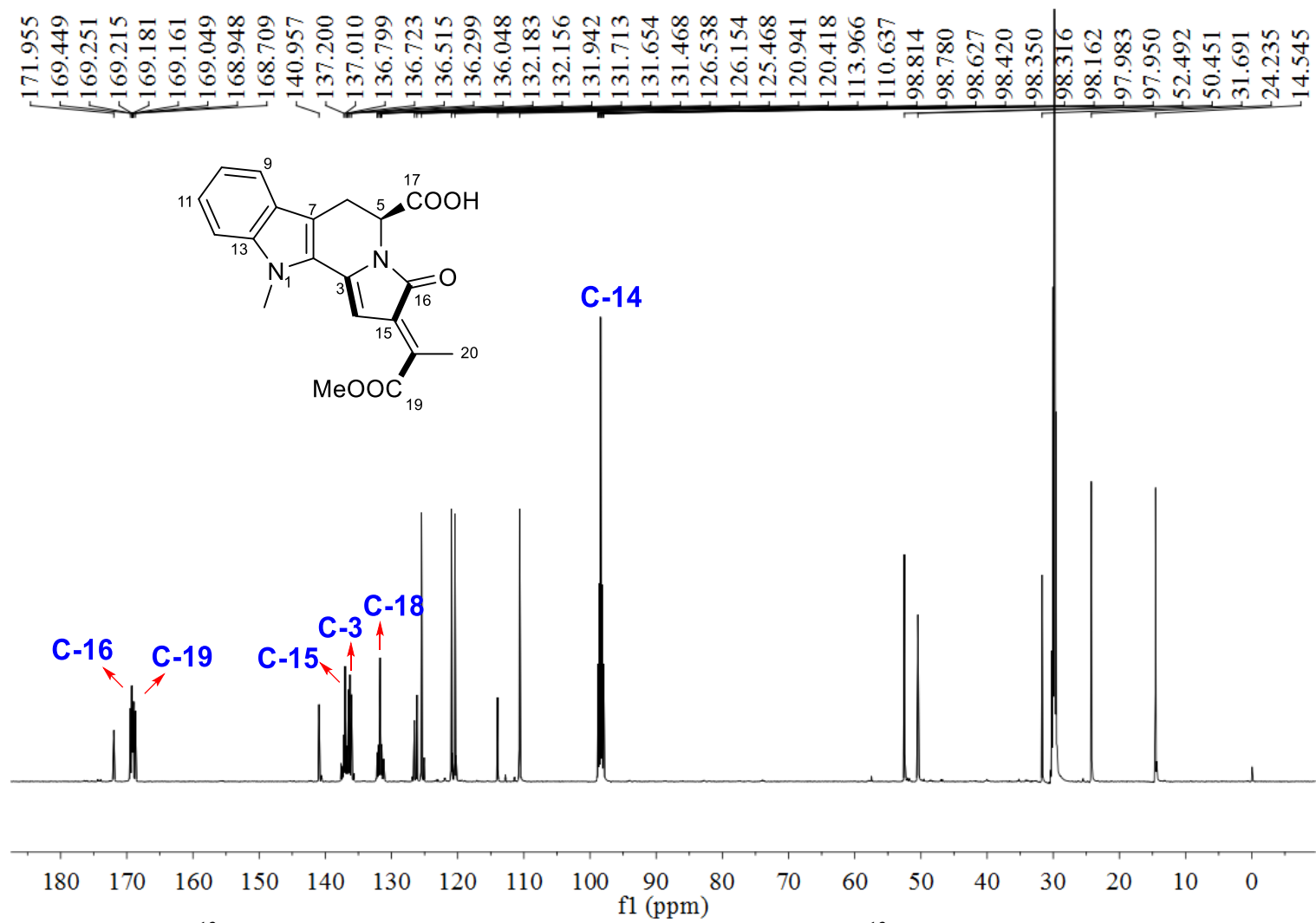


Figure S76. ¹³C-NMR spectrum of **1c** generated by feeding sodium [1,2-¹³C₂]acetate (acetone-*d*₆, 600 MHz).

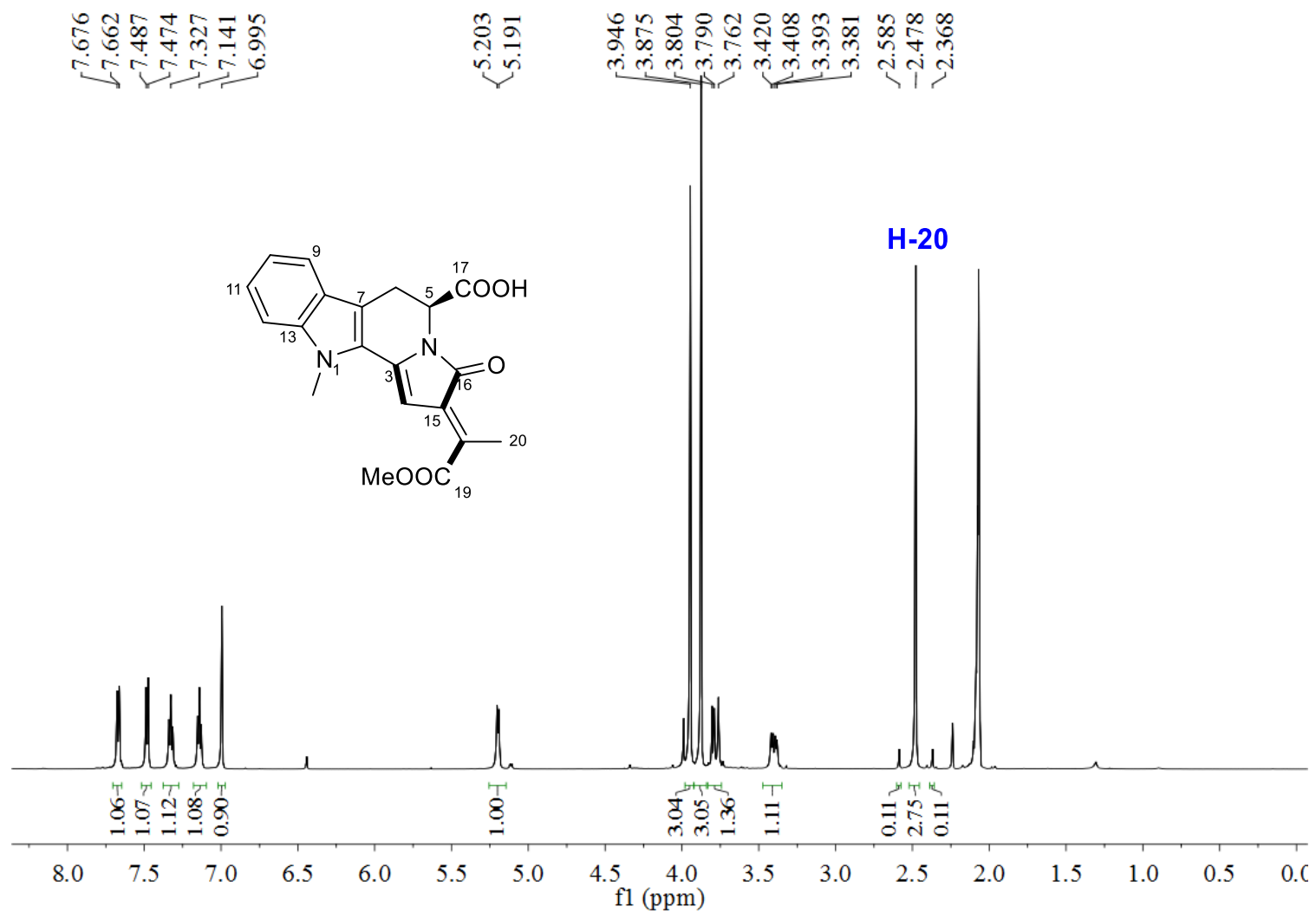


Figure S77. $^1\text{H-NMR}$ spectrum of **1d** generated by feeding [methyl- ^{13}C]-L-methionine (acetone- d_6 , 600 MHz).

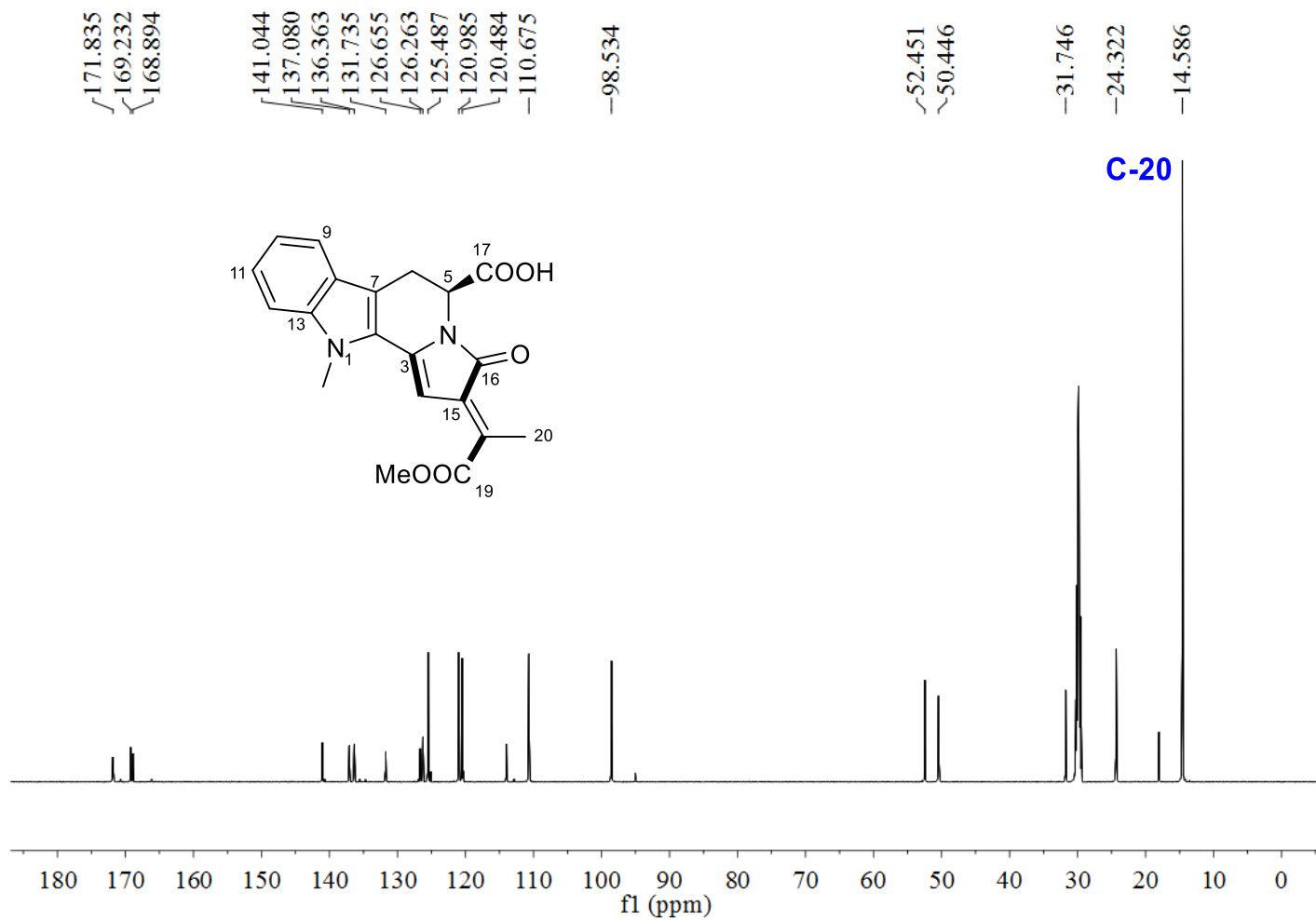


Figure S78. ¹³C-NMR spectrum of **1d** generated by feeding [methyl-¹³C]-L-methionine (acetone-*d*₆, 600 MHz).

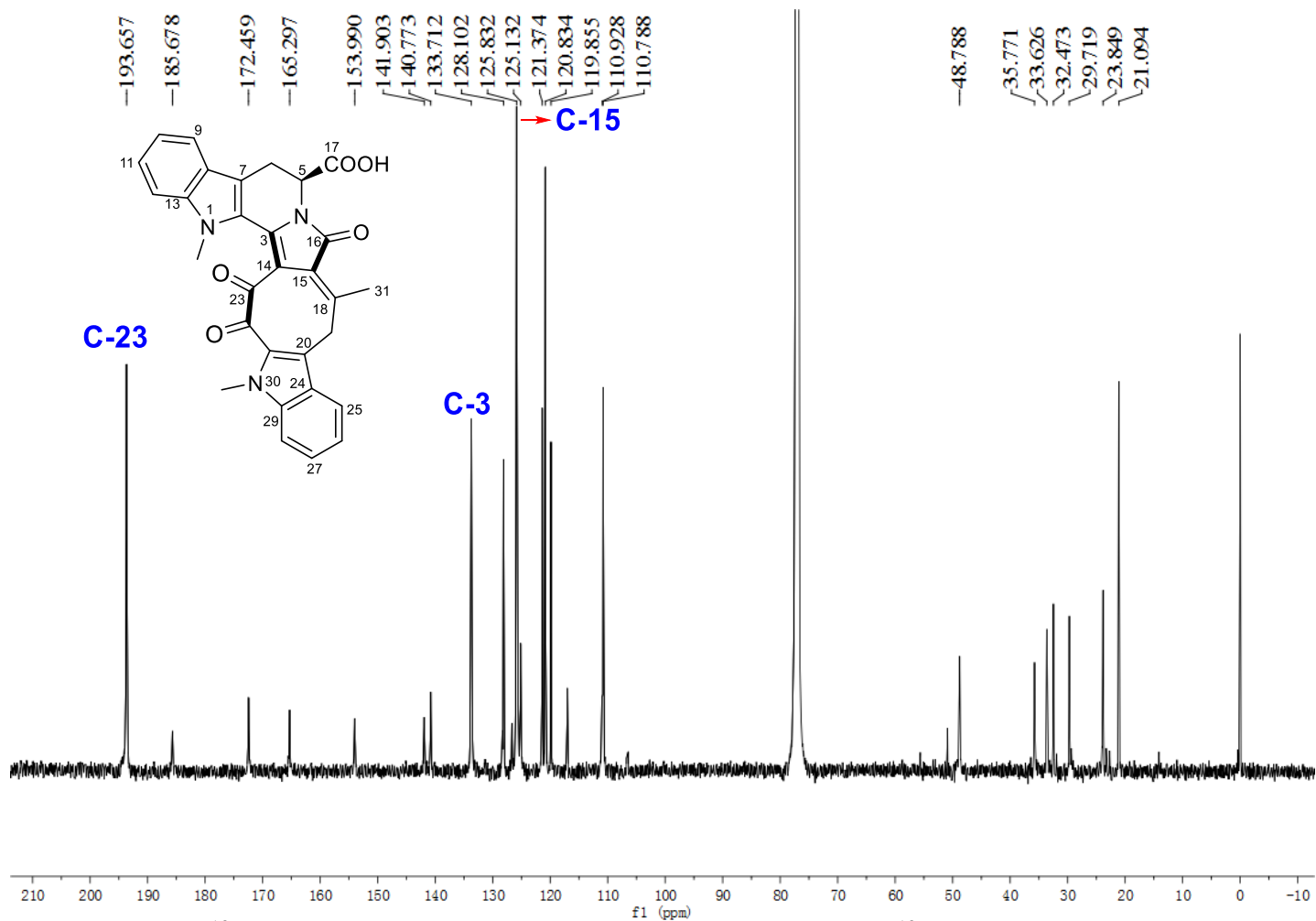


Figure S79. ¹³C-NMR spectrum of **2a** generated by feeding sodium [1-¹³C]acetate (CDCl₃, 600 MHz).

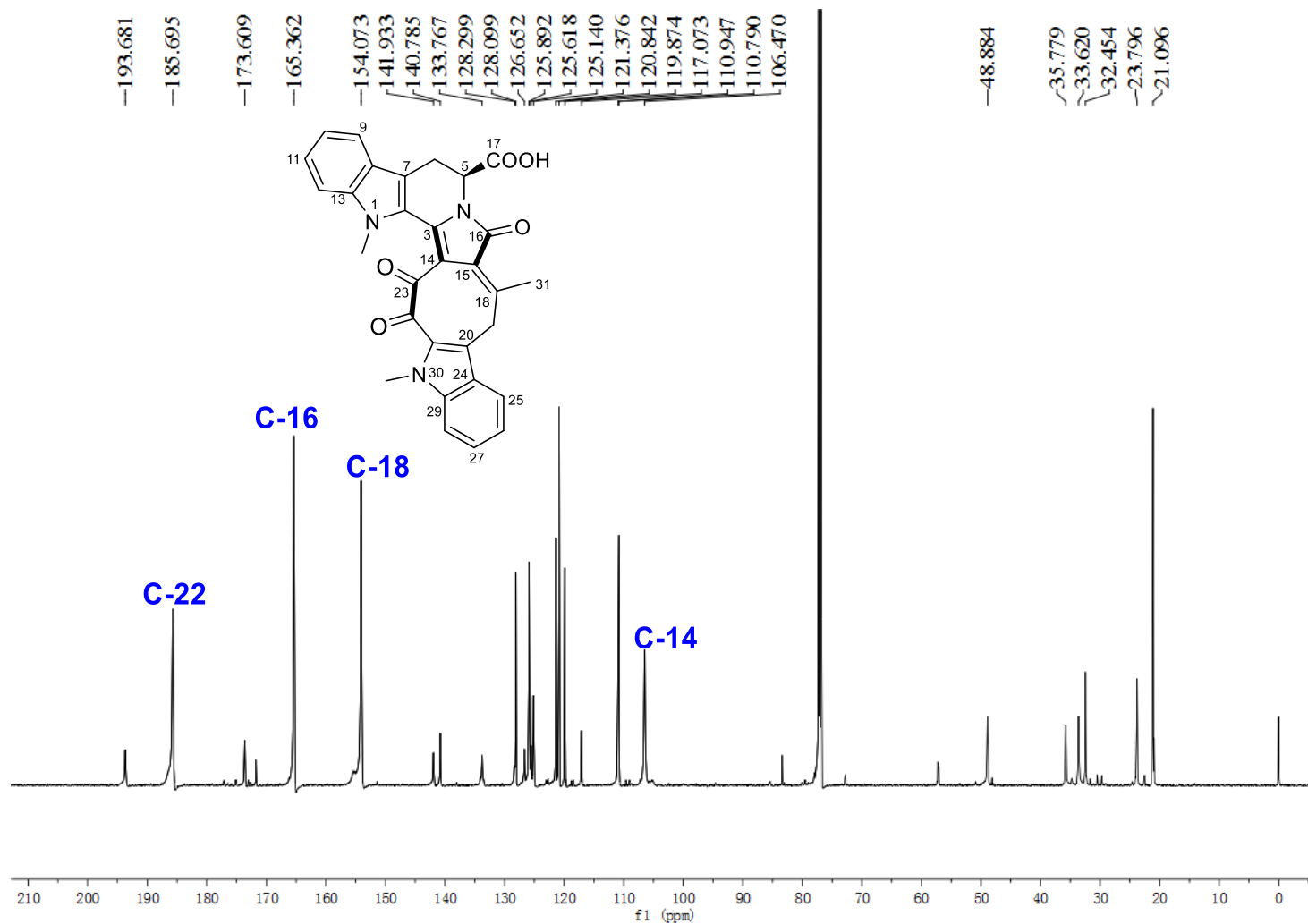


Figure S80. ^{13}C -NMR spectrum of **2b** generated by feeding sodium $[2\text{-}^{13}\text{C}]$ acetate (CDCl_3 , 600 MHz).

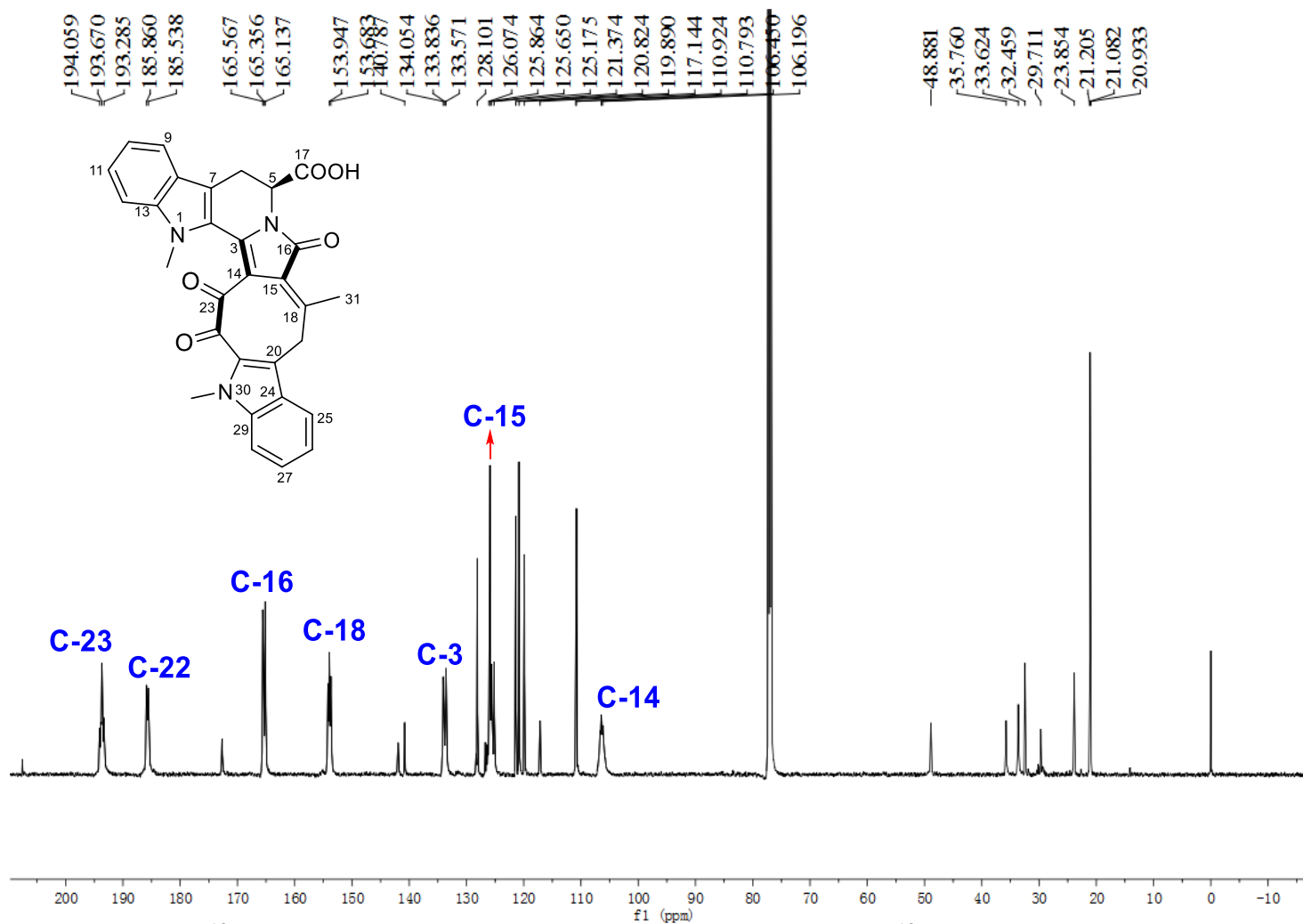


Figure S81. ^{13}C -NMR spectrum of **2c** generated by feeding sodium $[1,2\text{-}^{13}\text{C}_2]$ acetate (CDCl_3 , 600 MHz).

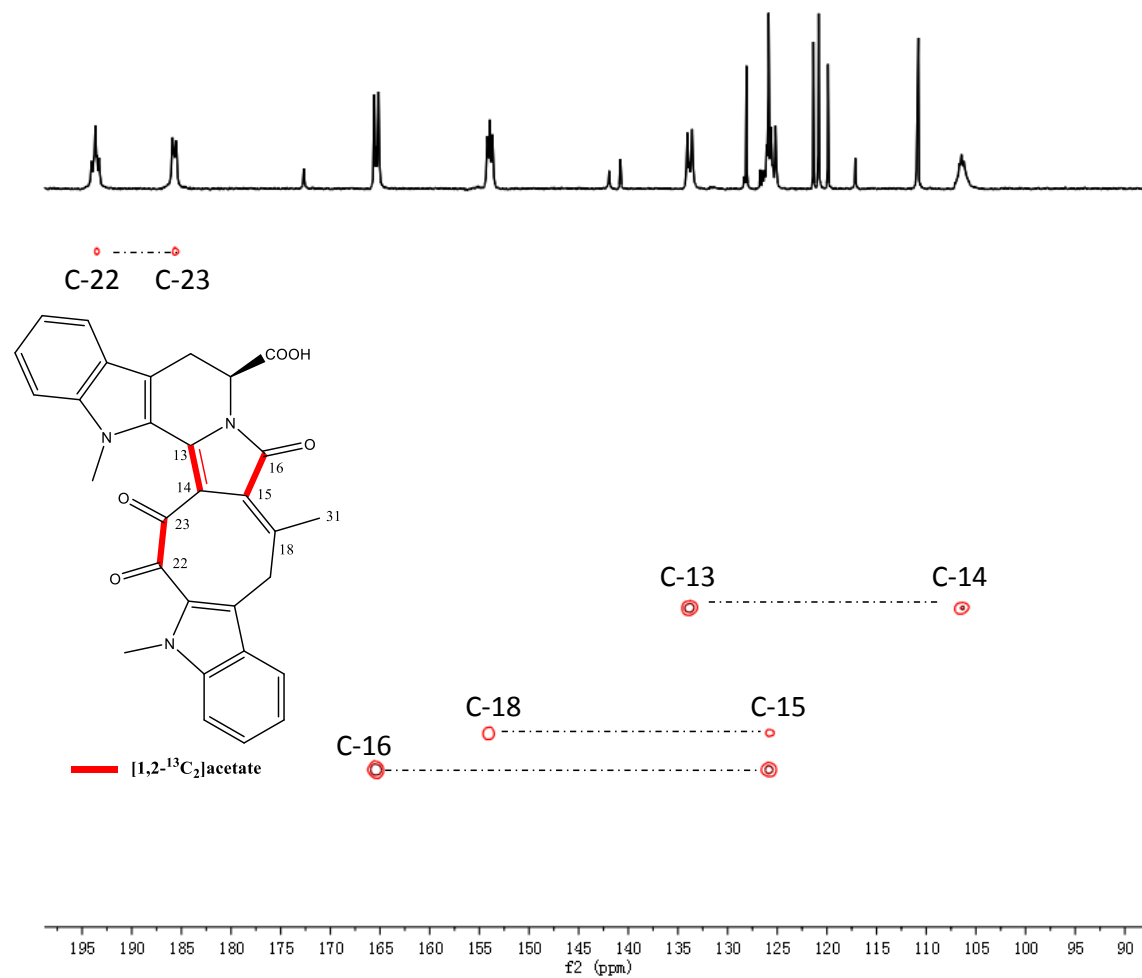


Figure S82. INADEQUATE spectrum of **2c** (CDCl_3 , 600 MHz).

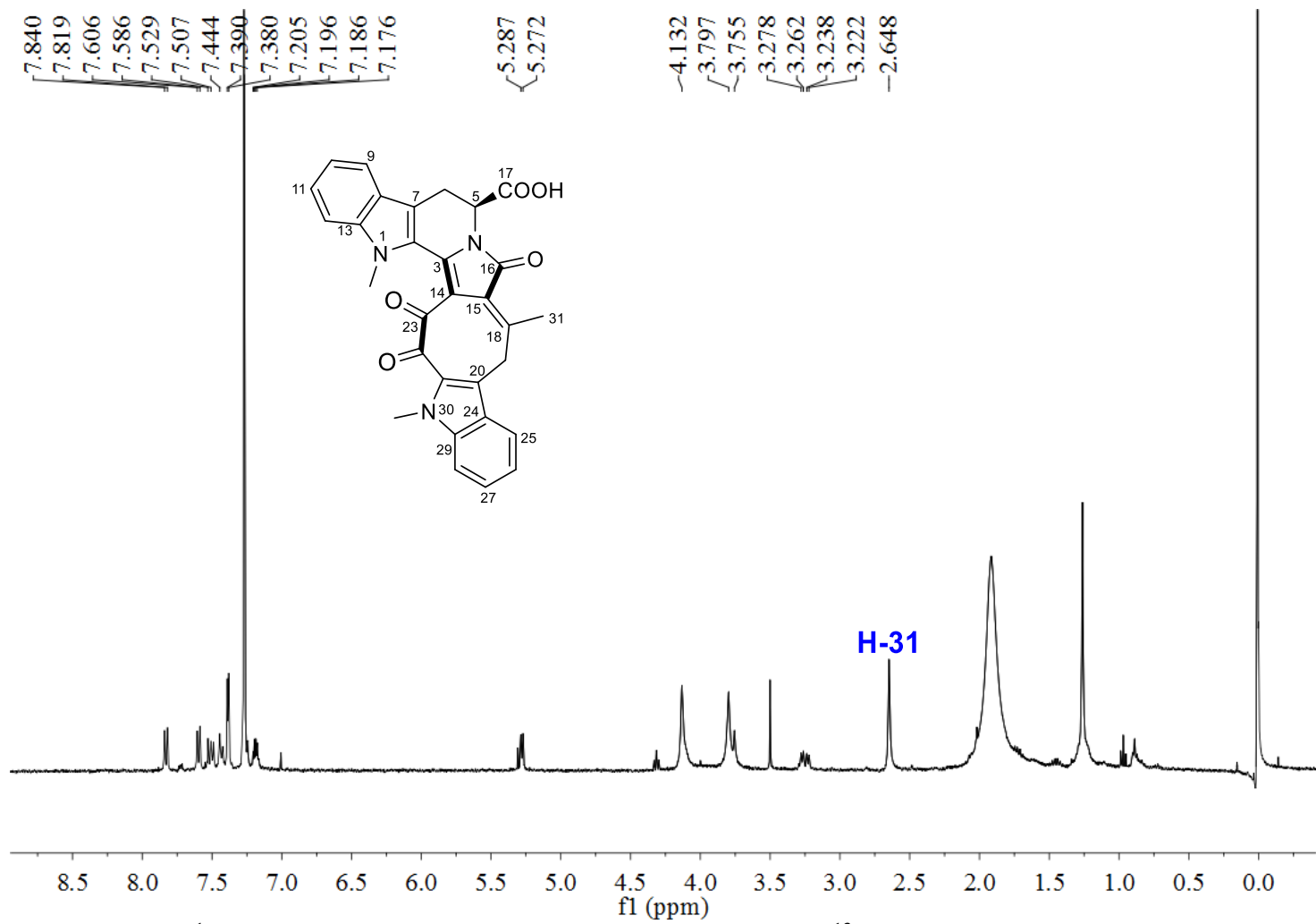


Figure S83. ¹H-NMR spectrum of **2d** generated by feeding [methyl-¹³C]-L-methionine (CDCl₃, 600 MHz).

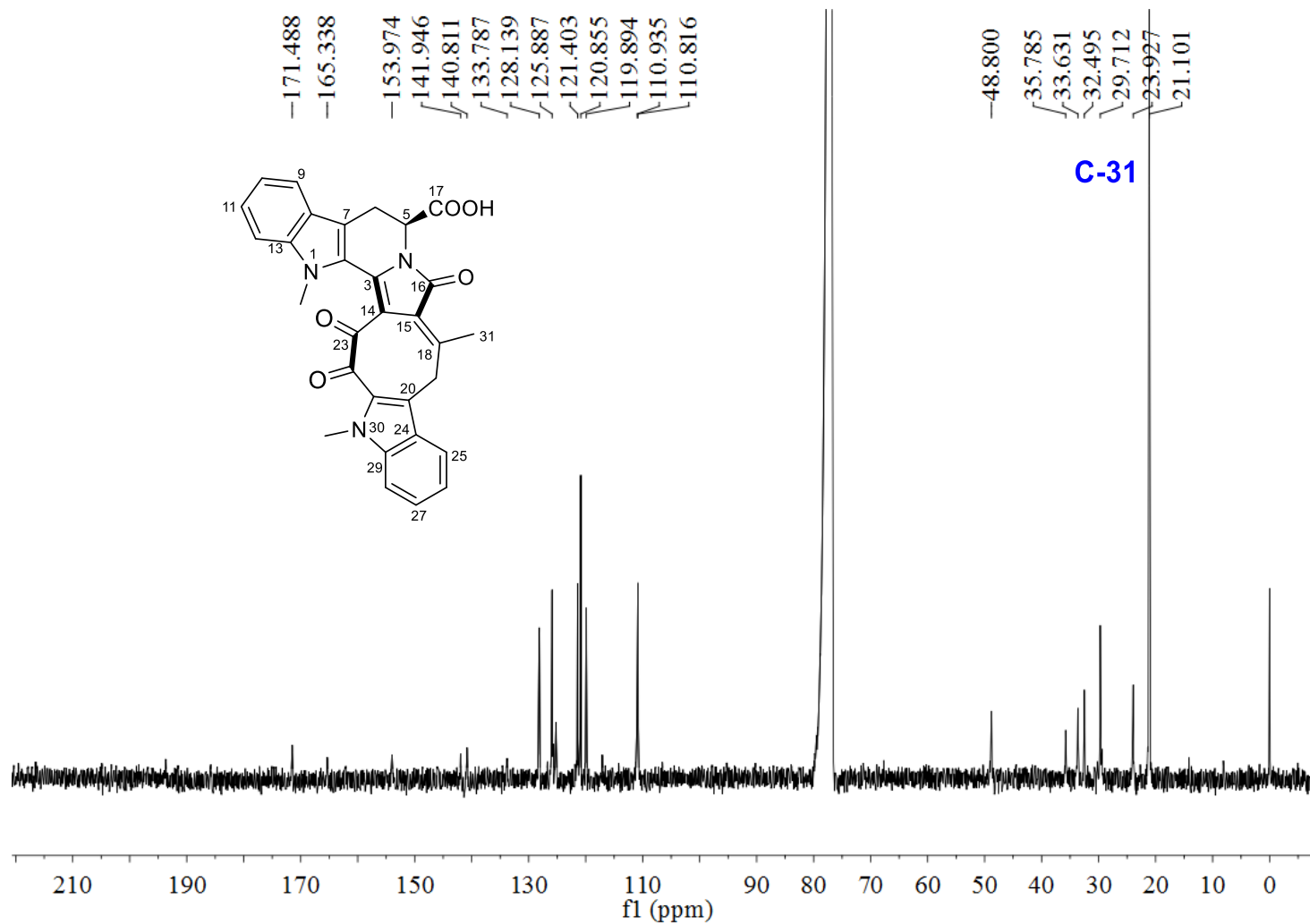


Figure S84. ¹³C-NMR spectrum of **2d** generated by feeding [methyl-¹³C]-L-methionine (CDCl₃, 600 MHz).

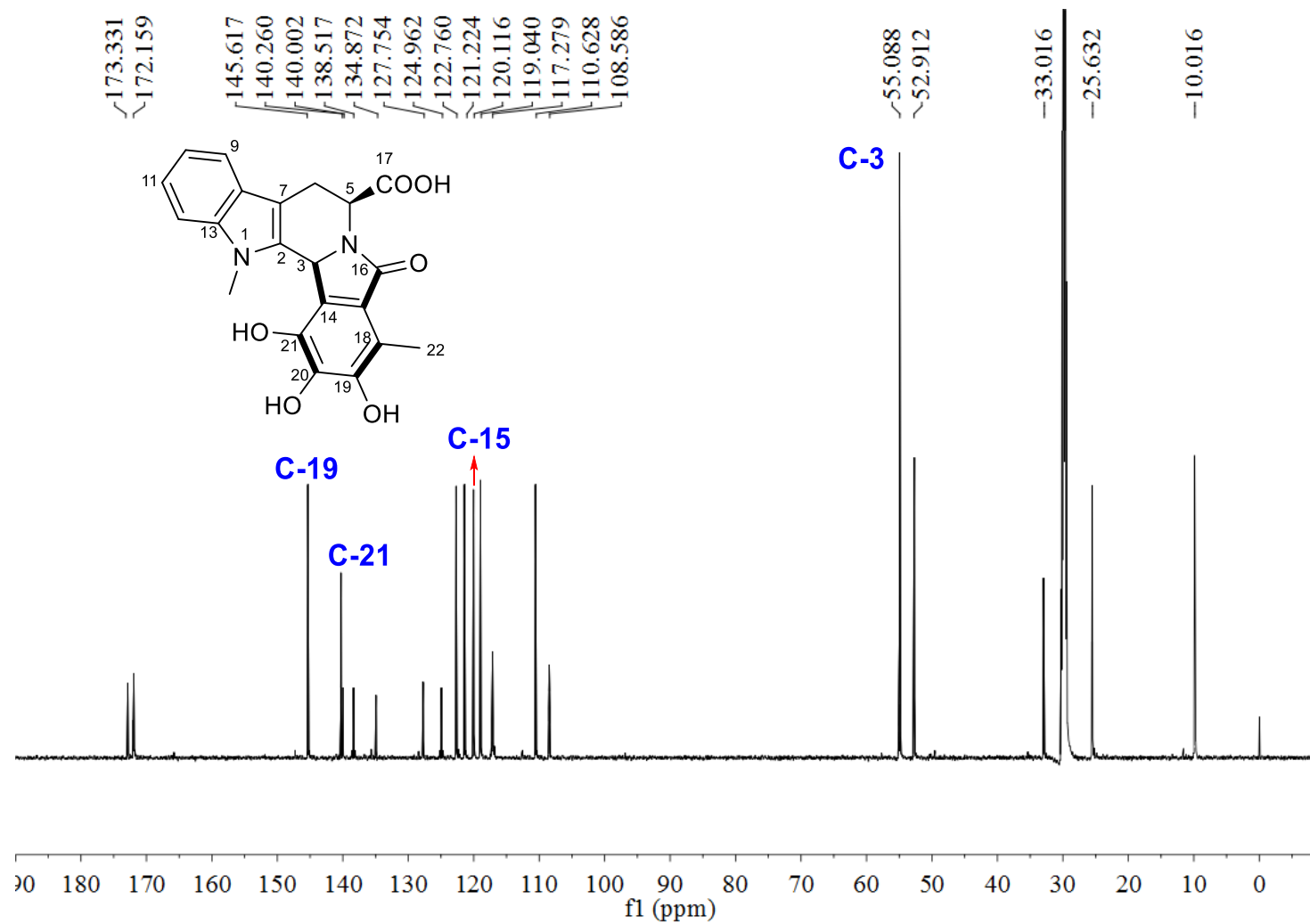


Figure S85. ^{13}C -NMR spectrum of **5a** generated by feeding sodium $[1-^{13}\text{C}]$ acetate (acetone- d_6 , 600 MHz).

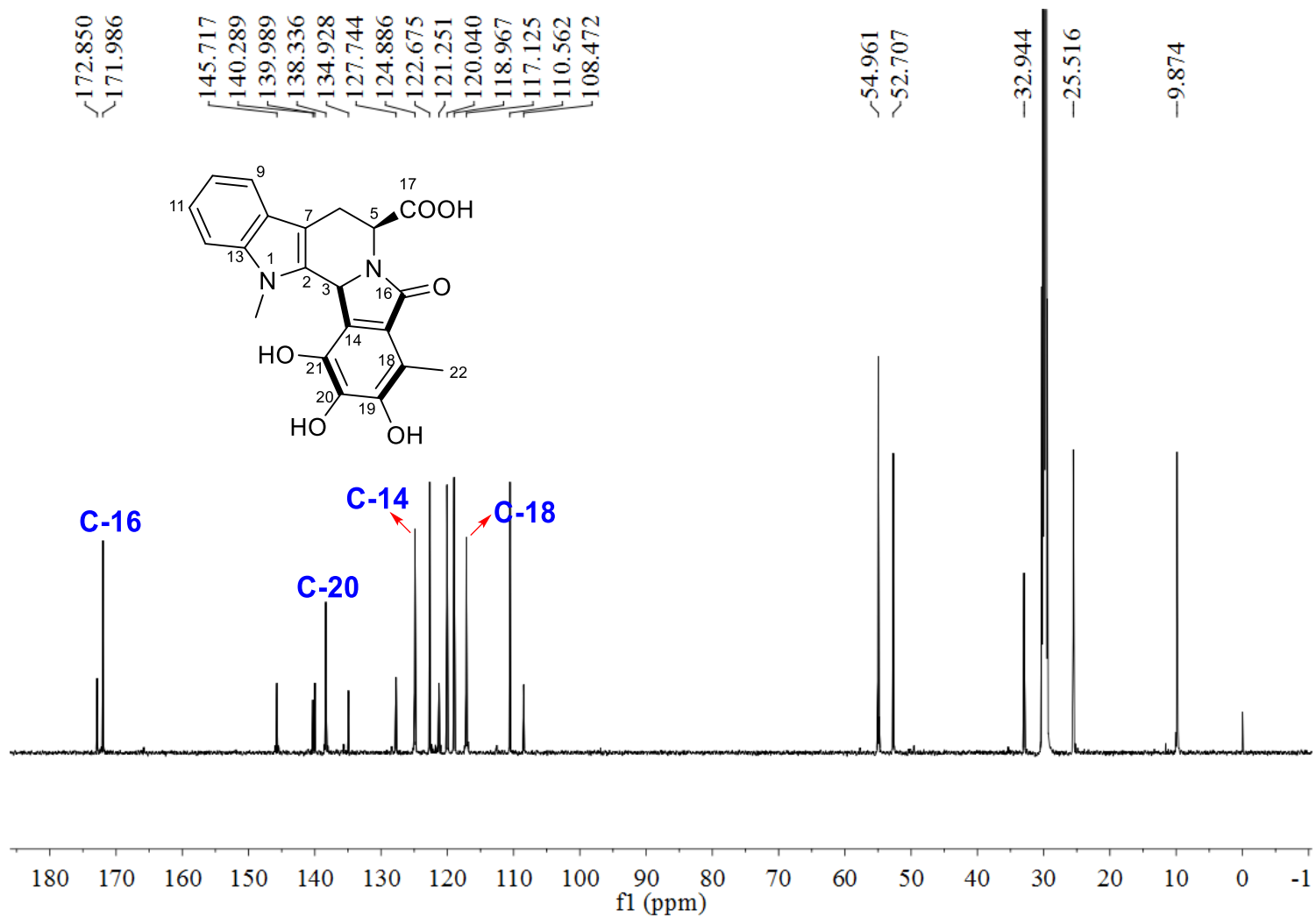


Figure S86. ¹³C-NMR spectrum of **5b** generated by feeding sodium [2-¹³C]acetate (acetone-*d*₆, 600 MHz).

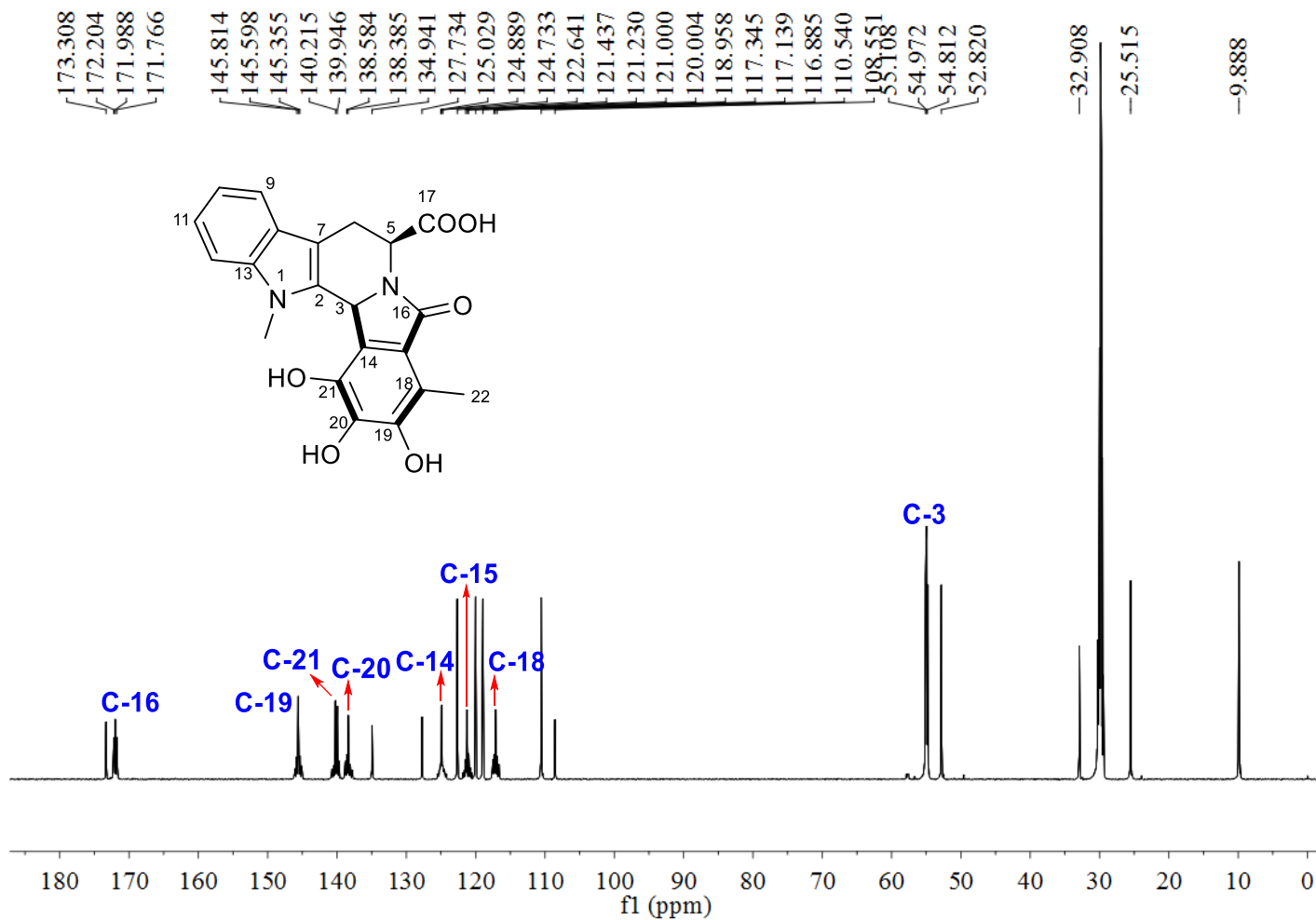


Figure S87. ^{13}C -NMR spectrum of **5c** generated by feeding sodium $[1,2-^{13}\text{C}_2]$ acetate (acetone- d_6 , 600 MHz).

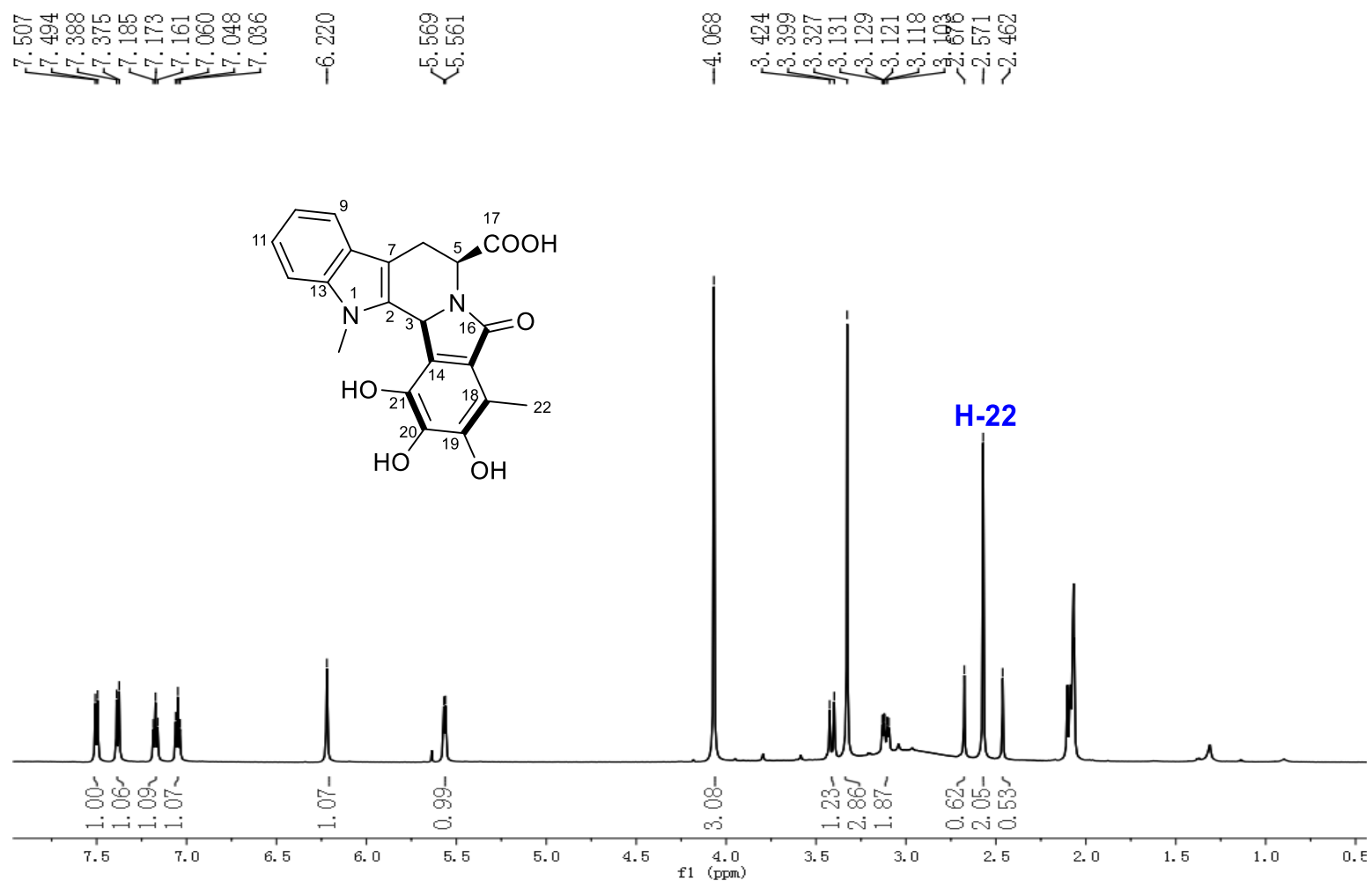


Figure S88. ¹H-NMR spectrum of **5d** generated by feeding [methyl-¹³C]-L-methionine (acetone-*d*₆, 600 MHz).

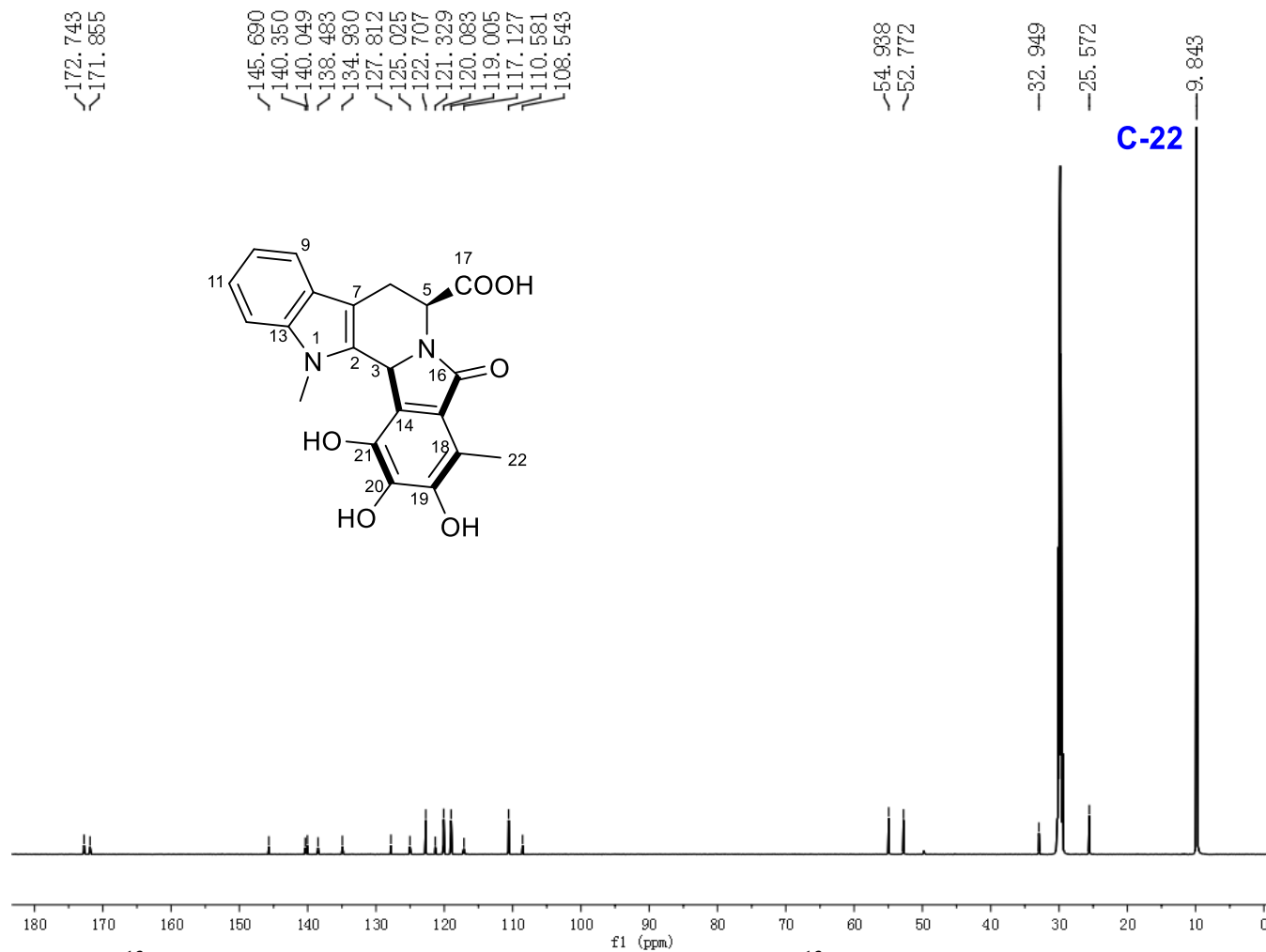


Figure S89. ^{13}C -NMR spectrum of **5d** generated by feeding [methyl- ^{13}C]-L-methionine (acetone- d_6 , 600 MHz).

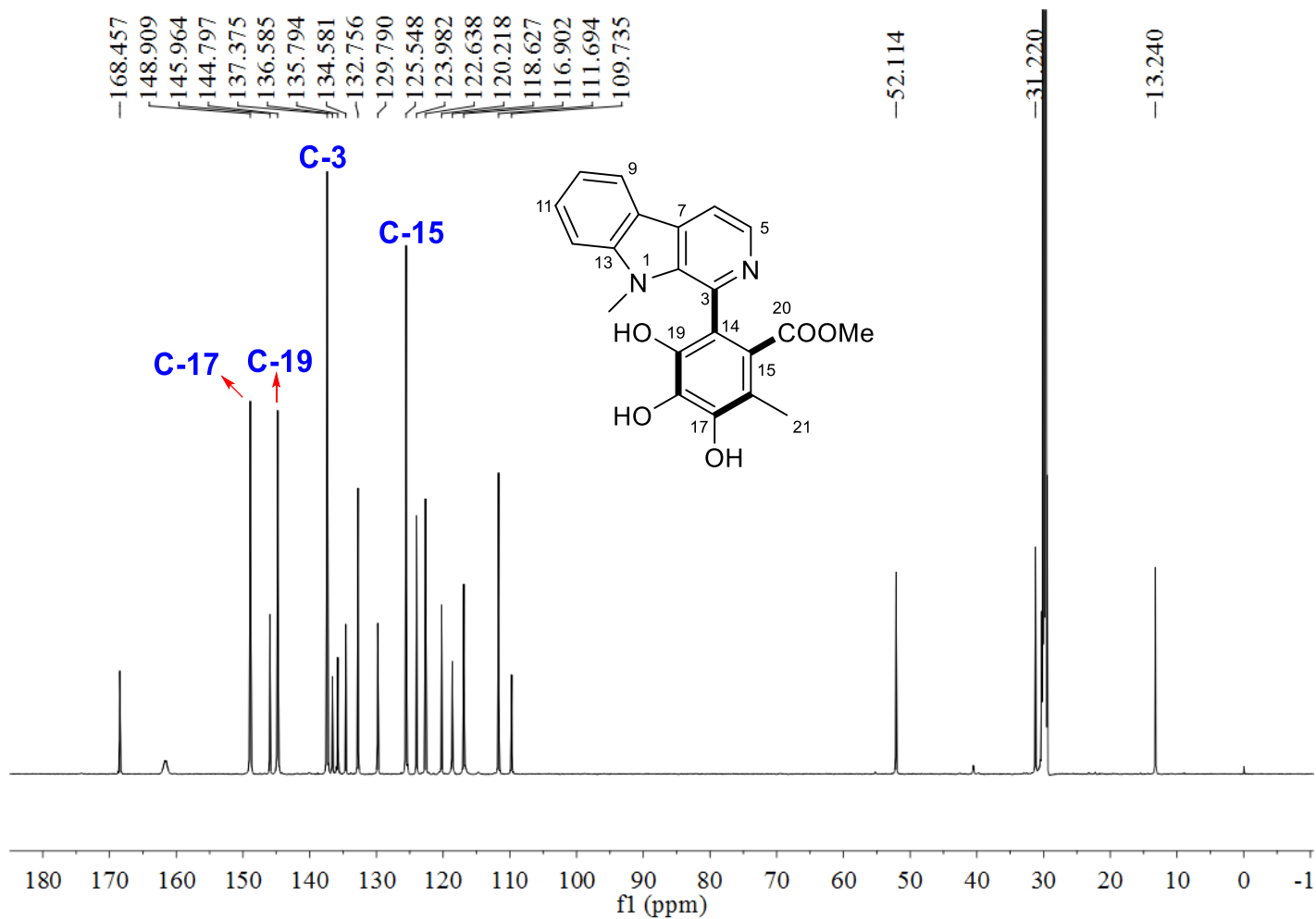


Figure S90. ^{13}C -NMR spectrum of **6a** generated by feeding sodium $[1-^{13}\text{C}]$ acetate (acetone- d_6 , 600 MHz).

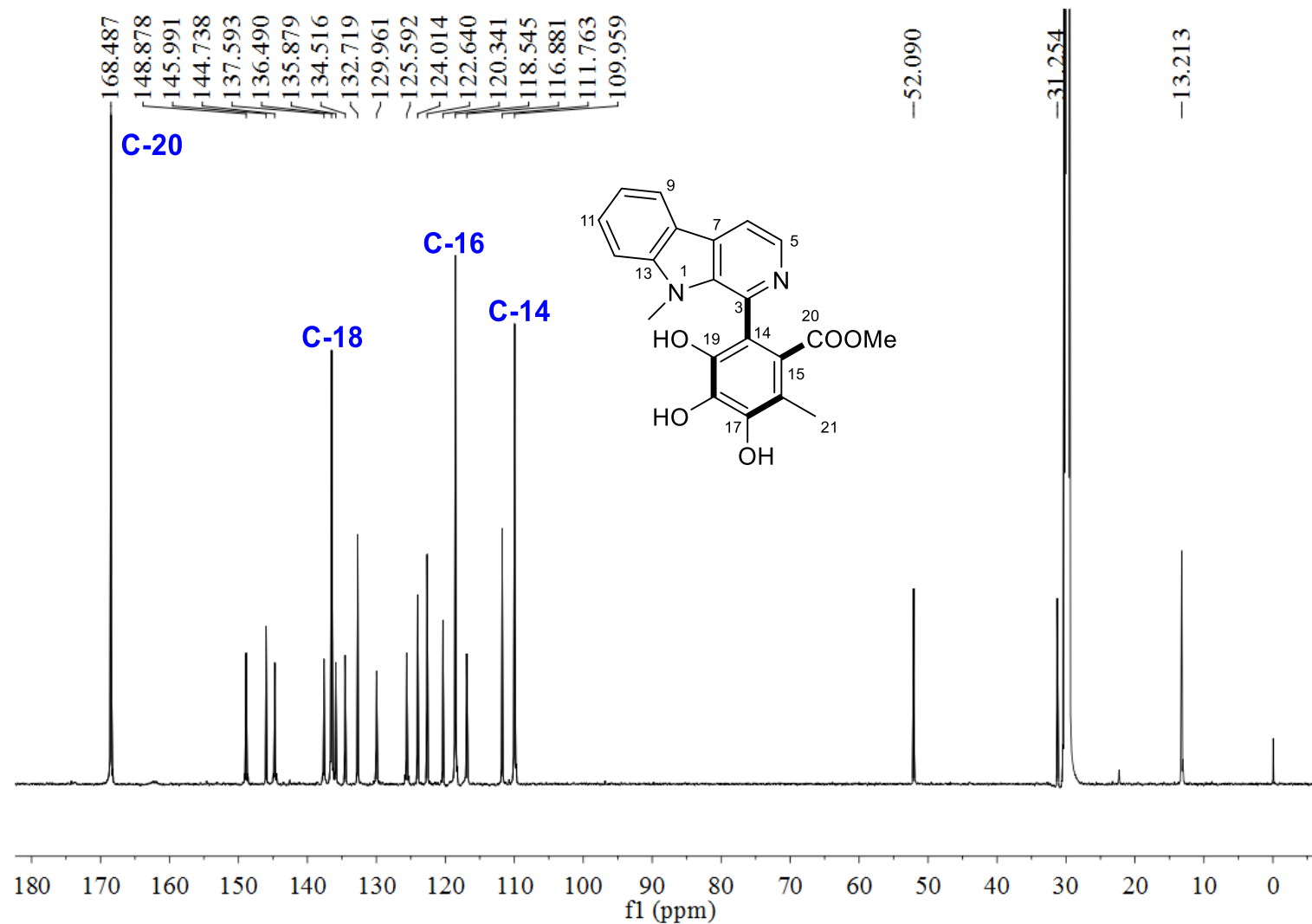


Figure S91. ^{13}C -NMR spectrum of **6b** generated by feeding sodium $[2-^{13}\text{C}]$ acetate (acetone- d_6 , 600 MHz).

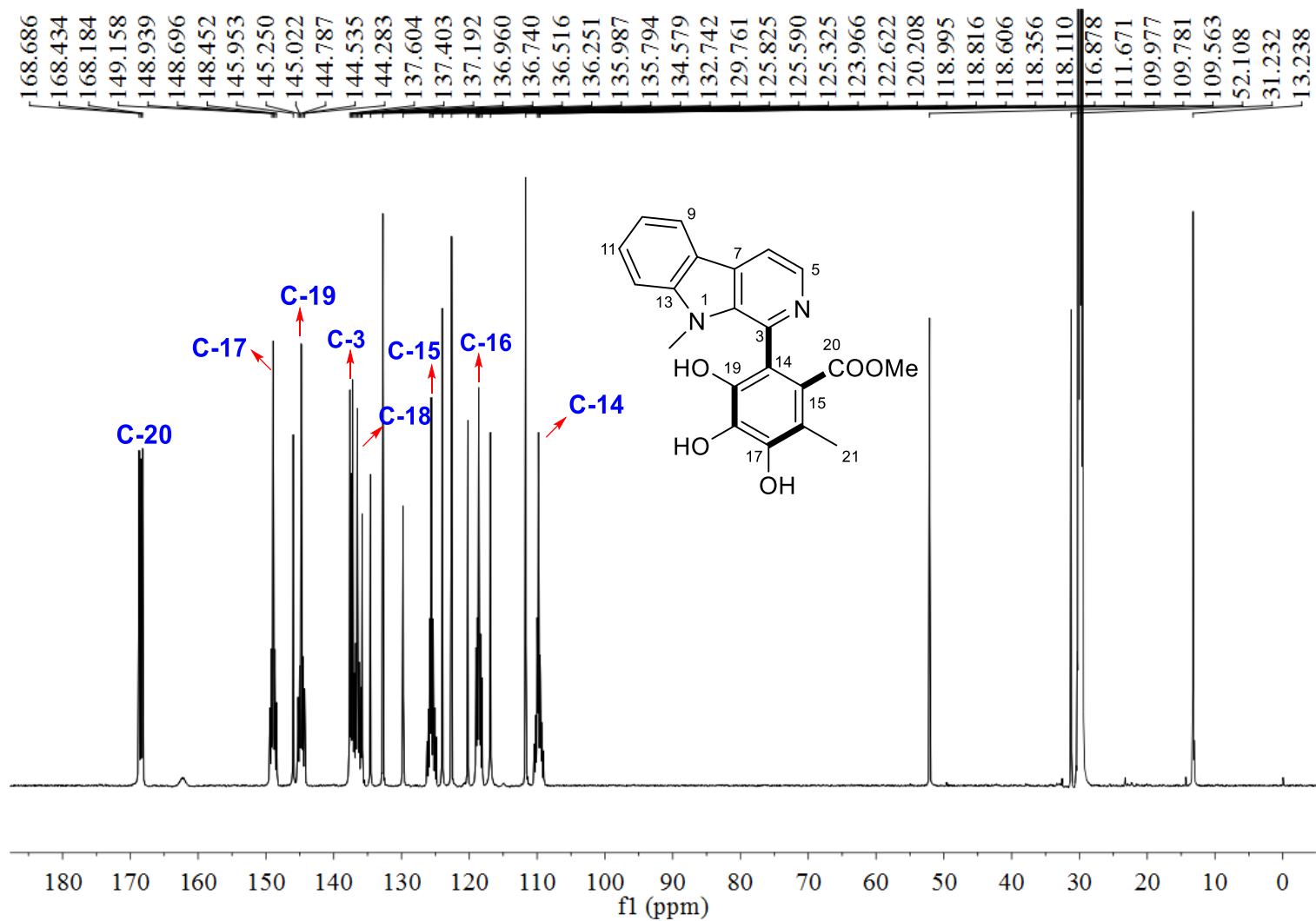


Figure S92. ^{13}C -NMR spectrum of **6c** generated by feeding sodium $[1,2-^{13}\text{C}_2]$ acetate (acetone- d_6 , 600 MHz).

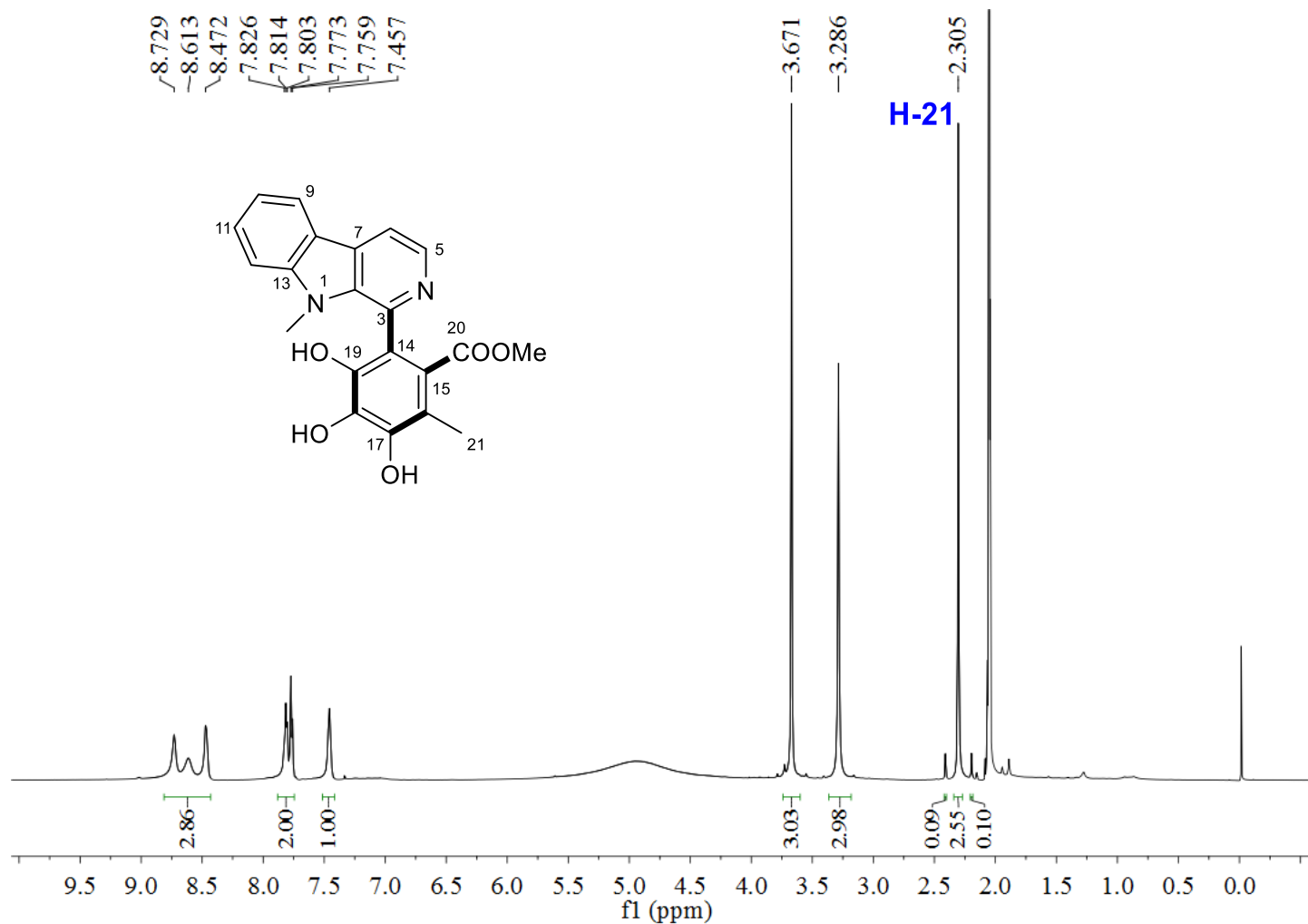


Figure S93. ¹H-NMR spectrum of **6d** generated by feeding [methyl-¹³C]-L-methionine (acetone-*d*₆, 600 MHz).

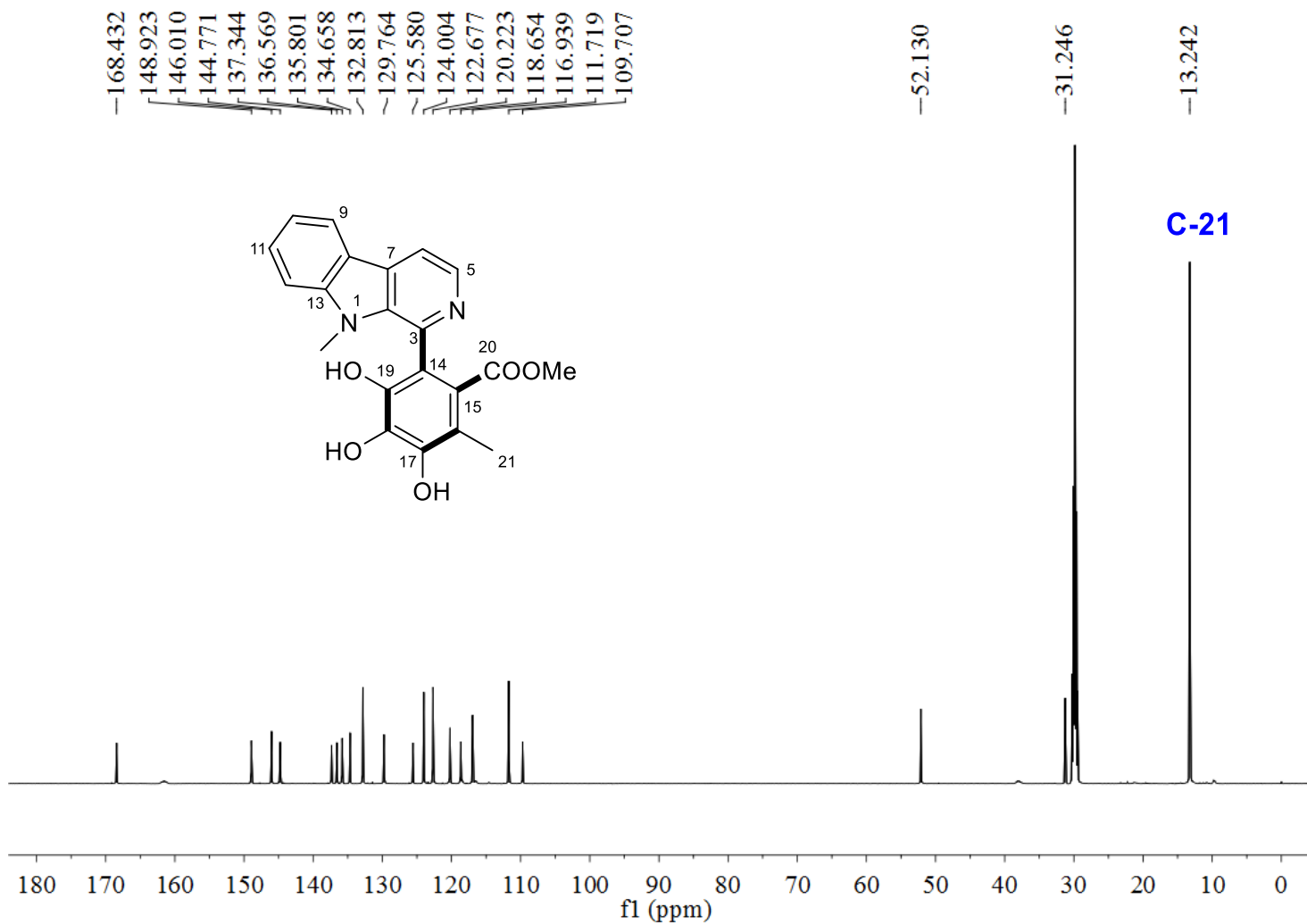


Figure S94. ¹³C-NMR spectrum of **6d** generated by feeding [methyl-¹³C]-L-methionine (acetone-*d*₆, 600 MHz).